

DEVELOPMENT OF BOLTED FLANGE DESIGN TOOL BASED ON FINITE  
ELEMENT ANALYSIS AND ARTIFICIAL NEURAL NETWORK

A THESIS SUBMITTED TO  
THE GRADUATE SCHOOL OF NATURAL AND APPLIED SCIENCES  
OF  
MIDDLE EAST TECHNICAL UNIVERSITY

BY

ALPER YILDIRIM

IN PARTIAL FULFILLMENT OF THE REQUIREMENTS  
FOR  
THE DEGREE OF MASTER OF SCIENCE  
IN  
AEROSPACE ENGINEERING

SEPTEMBER 2015



Approval of the thesis:

**DEVELOPMENT OF BOLTED FLANGE DESIGN TOOL BASED ON  
FINITE ELEMENT ANALYSIS AND ARTIFICIAL NEURAL NETWORK**

submitted by **ALPER YILDIRIM** in partial fulfillment of the requirements for the degree of **Master of Science in Aerospace Engineering Department, Middle East Technical University** by,

Prof. Dr. Gülbin Dural Ünver  
Dean, Graduate School of **Natural and Applied Sciences**

\_\_\_\_\_

Prof. Dr. Ozan Tekinalp  
Head of Department, **Aerospace Engineering**

\_\_\_\_\_

Prof. Dr. Altan Kayran  
Supervisor, **Aerospace Engineering Dept., METU**

\_\_\_\_\_

**Examining Committee Members:**

Asst. Prof. Dr. Ercan Gürses  
Aerospace Engineering Dept., METU

\_\_\_\_\_

Prof. Dr. Altan Kayran  
Aerospace Engineering Dept., METU

\_\_\_\_\_

Asst. Prof. Dr. Tuncay Yalçınkaya  
Aerospace Engineering Dept., METU

\_\_\_\_\_

Assoc.Prof. Dr. Demirkan Çöker  
Aerospace Engineering Dept., METU

\_\_\_\_\_

Asst. Prof. Dr. Cihan Tekoğlu  
Mechanical Engineering Dept., TOBB ETÜ

\_\_\_\_\_

Date: 03.09.2015

**I hereby declare that all information in this document has been obtained and presented in accordance with academic rules and ethical conduct. I also declare that, as required by these rules and conduct, I have fully cited and referenced all material and results that are not original to this work.**

Name, Last name: Alper YILDIRIM

Signature :

## **ABSTRACT**

### **DEVELOPMENT OF BOLTED FLANGE DESIGN TOOL BASED ON FINITE ELEMENT ANALYSIS AND ARTIFICIAL NEURAL NETWORK**

Yıldırım, Alper  
M. S., Department of Aerospace Engineering  
Supervisor: Prof. Dr. Altan Kayran

September 2015, 117 pages

In bolted flange connections, commonly utilized in aircraft engine designs, structural integrity and minimization of the weight are achieved by the optimum combination of the design parameters utilizing the outcome of many structural analyses. Bolt size, number of bolts, bolt locations, casing thickness, flange thickness, bolt preload, and axial external force are some of the critical design parameters in bolted flange connections. Theoretical analysis and finite element analysis (FEA) are two main approaches to perform the structural analysis of the bolted flange connection. Theoretical approaches require the simplification of the geometry and are generally over safe. In contrast, finite element analysis is more reliable but at the cost of high computational power. In this work, the methodology developed for the iterative analyses of bolted flange utilizes artificial neural network approximation of FEA database formed with more than ten thousands of non-linear analyses involving contact. In the design tool, the structural analysis database is created by combining parametric variables by each other. The number of intervals for each variable in the upper and lower range of the variables has been determined with the parameters correlation study in which the significance of parameters are evaluated. As a follow-up study, the design tool is compared with FEA and the theoretical approach of ESDU.

Keywords: Bolted Flange Connection, Artificial Neural Network, Parameters Correlation, Finite Element Analysis

## ÖZ

### **CİVATALI FLANŞ TASARIM ARACININ SONLU ELEMANLAR ANALİZİ VE YAPAY SİNİR AĞI İLE GELİŞTİRİLMESİ**

Yıldırım, Alper  
Yüksek Lisans, Havacılık ve Uzay Mühendisliği Bölümü  
Tez Yöneticisi: Prof. Dr. Altan Kayran

Eylül 2015, 117 sayfa

Uçak motoru tasarımlarda sıkça kullanılmakta olan civatalı flanş bağlantılarında yapısal bütünlüğün korunması ve ağırlığın azaltılması, yapısal analizlerin sonuçlarına dayanarak tasarım değişkenlerinin en uygun birleşimi seçilerek sağlanır. Civatalı flanş bağlantılarında, civata boyutu, civata sayısı, civata pozisyonu, kılıf kalınlığı, flanş kalınlığı, civata önyüklemesi ve eksenel dış kuvvet kritik tasarım değişkenleridir. Teorik analiz ve sonlu elemanlar analizi civatalı flanş bağlantılarının yapısal analizlerinde kullanılan iki temel analiz yöntemidir. Teorik yaklaşım geometrinin basitleştirilmesini gerektirir ve genellikle gereğinden fazla emniyetli sonuç verir. Öte yandan sonlu elemanlar analizi daha doğru sonuçlar verir, fakat daha uzun hesaplama süresi gerektirir. Bu çalışmada, civatalı flanş bağlantılarının tekrarlı analizlerine yönelik geliştirilmiş olan yöntem, on binden fazla doğrusal olmayan, kontak içeren sonlu elemanlar analiz sonucunun oluşturduğu yapay sinir ağını kullanır. Bu tasarım aracında, yapısal analizleri içeren veri tabanı, parametrik değişkenlerin birbirleri ile kombine edilmesiyle oluşur. Parametrik değişkenlerin her birinin girdi sayısı, parametre korelasyonu çalışması ile parametrelerin etkisi değerlendirilerek belirlenir. Bu çalışmanın devamında, geliştirilen tasarım aracı sonlu elemanlar analizi yöntemi ve ESDU teorik yaklaşımıyla karşılaştırılır.

Anahtar Kelimeler: Civatalı Flanş Bağlantısı, Yapay Sinir Ağı, Parametre Korelasyonu, Sonlu Elemanlar Analizi

**To my mother, father, sister, and lovely one**

## ACKNOWLEDGEMENTS

The author would like to express his sincere gratitude to his supervisor Prof. Dr. Altan Kayran for his advice, criticism, and excellent guidance throughout the study.

The author also thanks to Assist. Prof. Dr. Ercan Gürses and Assoc. Prof. Dr. Demirkan Çöker for their decent contributions to this study.

The author has been supported by ASELSAN A.S. from the beginning to the end of this period and feels thankful for all the contributions by ASELSAN A.S.

The author has been supported by The Scientific and Technological Research Council of Turkey (TÜBİTAK) as a scholarship student of the support program “BİDEB 2210-A Genel Yurt İçi Yüksek Lisans Burs Programı”. The author would like to take this occasion to deeply thank for this support.

There are many people who have significantly helped to this study so far; therefore, the author feels glad about the contribution of each one of them, whose names are not written here.

## TABLE OF CONTENTS

ABSTRACT.....	v
ÖZ.....	vii
ACKNOWLEDGEMENTS.....	x
TABLE OF CONTENTS.....	xi
LIST OF TABLES.....	xiii
LIST OF FIGURES.....	xv
LIST OF SYMBOLS AND ABBREVIATIONS.....	xix
CHAPTERS	
1. INTRODUCTION.....	1
2. SCOPE OF THE THESIS.....	13
3. FINITE ELEMENT ANALYSIS OF BOLTED FLANGE CONNECTION....	17
3.1 Analysis Geometry and Meshing.....	18
3.1.1 Bolted Flange Connection Assembly.....	18
3.1.2 Bolt-Nut Geometry.....	24
3.1.3 Flange Geometry.....	28
3.1.4 Washer Geometry.....	30
3.1.5 Mesh Quality.....	31
3.2 Material and Contact Details.....	31
3.3 Load and Boundary Conditions.....	33
3.4 Analysis Properties.....	34
3.5 Finite Element Solution of the Bolted Flange Connection.....	35
3.6 Case Studies.....	43
3.6.1 Comparison of Mesh Sizes.....	44
3.6.2 Comparison of Meshes with Linear and Quadratic Elements.....	46
3.6.3 Comparison of Small Deflection and Large Deflection Analysis.....	47
3.6.4 Comparison of Effective Bolt and Nut Diameter on the Results.....	48

4. PARAMETERS CORRELATION STUDY .....	49
4.1 Theory .....	49
4.2 Method.....	51
4.3 Results of Parameters Correlations .....	57
5. ARTIFICIAL NEURAL NETWORK APPROXIMATION .....	65
5.1 Theory .....	65
5.2 The Artificial Neural Network Generation Process .....	68
5.3 Results of the Artificial Neural Network .....	72
6. RESULTS AND EVALUATION.....	75
6.1 Comparison with Finite Element Analysis.....	76
6.2 Comparison with Theoretical Approach .....	80
7. CONCLUSION AND FUTURE WORKS .....	93
7.1 Conclusion.....	93
7.2 Future Works.....	95
REFERENCES .....	97
APPENDICES	
A. INSTRUCTIONS TO PREPARE ARTIFICIAL NEURAL NETWORK FOR THE BOLTED FLANGE DESIGN TOOL .....	101
B. THE ARTIFICIAL NEURAL NETWORK SETUP SCRIPT.....	113
C. SUPPLEMENTARY CHARTS.....	117

## LIST OF TABLES

### TABLES

Table 3.1 The nominal values of the parameters in the analysis model .....	22
Table 3.2 Material properties used in the analysis model [7] .....	32
Table 3.3 Materials of the components in analysis model .....	32
Table 3.4 Contact details of the analysis model according to Figure 3.16 .....	33
Table 3.5 The corresponding tensile stress area values for each bolt type .....	43
Table 3.6 The comparison of five different mesh sizes in analyses.....	46
Table 3.7 The effect of mid-side nodes on the analysis results .....	47
Table 3.8 The comparison of the large deflection behavior and the small deflection behavior in the analysis model .....	48
Table 3.9 The comparison of the effect of effective bolt diameter size on the results.....	48
Table 4.1 Sample problem data of Spearman's rank correlation .....	51
Table 4.2 The nominal values, upper and lower limits of all input parameters.....	56
Table 4.3 Bolt pretension and axial force values for each analysis set.....	57
Table 4.4 The correlation matrix of parametric set-1 .....	60
Table 4.5 The input values for the input parameters to be used in the main parametric study .....	63
Table 4.6 The correlation values for the remaining parametric sets as well as the main parametric set in reference to Table 4.3.....	64
Table 6.1 Test set-1, (the samples are selected from the training points).....	76
Table 6.2 The results of test set-1, (the samples are selected from the training points).....	77
Table 6.3 Test set-2, (the samples are in between the training points) .....	78

Table 6.4 The results of test set-2, (the samples are in between the training points)	79
Table 6.5 Test set-3, (extrapolation, the painted cells indicate the values outside the training limits) .....	79
Table 6.6 The results of test set-3 (extrapolation).....	80
Table 6.7 The results of the sample problems with and without separation solved by theoretical approach, FEA, and the developed tool.....	91
Table A.1 Limits of the input parameters for parametric analyses and ANN training.....	109
Table A.2 The parametric input values for each variable in the parametric analyses.....	109

## LIST OF FIGURES

### FIGURES

Figure 1.1 A bolted flange connection sample.....	2
Figure 1.2 A regular linear tetrahedral element with four nodes .....	4
Figure 1.3 A regular quadratic tetrahedral element with ten nodes .....	4
Figure 1.4 A regular linear hexahedral element with eight nodes .....	5
Figure 1.5 A regular quadratic hexahedral element with twenty nodes.....	5
Figure 2.1 Flowchart of the bolted flange design tool development procedure.....	15
Figure 3.1 Circular bolted flange connection geometry.....	19
Figure 3.2 Cross-sectional view of the bolted flange connection geometry with the components .....	19
Figure 3.3 Axisymmetric bolted flange sector model .....	20
Figure 3.4 The circular sector analysis model with the geometric parameters .....	21
Figure 3.5 Sectional analysis geometry of the circular bolted flange connection ...	23
Figure 3.6 Cross section view of the meshed geometry.....	23
Figure 3.7 The united analysis model of the bolt and the nut with the cylindrical outer geometries .....	25
Figure 3.8 The imaginary circles and the effective circle to calculate the effective diameter of the bolt head and the nut .....	26
Figure 3.9 Edge sizing of bolt-nut body .....	27
Figure 3.10 The angle of flange section used in the analysis.....	28
Figure 3.11 The variable distance of bolt hole to center axis nominated as Radius C.....	28
Figure 3.12 The multizone source surfaces painted in red of the flange .....	29

Figure 3.13 The opposite multizone source surfaces painted in red of the flange ....	29
Figure 3.14 Edge sizing of the circular sector flange body with the mesh structure.	30
Figure 3.15 Edge sizing of the washer .....	31
Figure 3.16 Representations of the contacts on the cross-sectional bolted flange connection view.....	33
Figure 3.17 Load and boundary conditions; the fixed end on the right and the external force applied on the left.....	34
Figure 3.18 Load and boundary conditions: the designated lateral surfaces of the analysis geometry.....	34
Figure 3.19 Equivalent Von Mises stress distribution in flange-1 with the maximum stress of 142.47 MPa .....	36
Figure 3.20 Equivalent Von Mises stress distribution inside the bolt with the maximum stress of 450.89 MPa (81X scaled, deformed body view) .....	37
Figure 3.21 Z-axis (axial) normal stress distribution map in flange-1 cross section under bolt pretension and axial external tensile force (undeformed body view) .....	38
Figure 3.22 Radial-axis (x) normal stress distribution map in flange-1 under bolt pretension and axial external tensile force (undeformed body view) .....	38
Figure 3.23 Radial-axis (x) normal stress distribution map in flange-1 under bolt pretension and axial external tensile force, the opposite view of Figure 3.22 (undeformed body view) .....	39
Figure 3.24 Equivalent Von Mises stress collection points on an imaginary circle of 1.75d in the flange geometry.....	41
Figure 3.25 The contact status map for the contact between flange-1 and flange-2.	41
Figure 3.26 Equivalent Von Mises stress map for the contact surface between flange-1 and flange-2.....	42
Figure 3.27 Resultant force reaction of 5832.4 N that occurs inside the bolt body when crossed orthogonally by a plane .....	43

Figure 4.1 Flowchart of the parameters correlation study for a single parametric set.....	54
Figure 4.2 The geometric input parameters of the analysis model .....	56
Figure 4.3 Visual chart of the correlation matrix of parametric set-1.....	59
Figure 4.4 The sensitivities chart of parametric set-1 .....	61
Figure 5.1 The structure of a sample ANN with three input and two output parameters.....	66
Figure 5.2 The mathematical process in a simple neuron.....	68
Figure 5.3 The failed analysis row encircled by red frame in a parametric study page in ANSYS .....	69
Figure 5.4 The failed analysis row encircled by red frame in a MS Excel exported results spreadsheet.....	69
Figure 5.5 The neural network training structure with seven input parameters and two output parameters .....	70
Figure 5.6 The performance improvement of the ANN along with the training iterations.....	73
Figure 5.7 Termination of the ANN training due to validation check limit .....	73
Figure 5.8 The regression plot to evaluate the ANN performance (the vertical axis stands for the training output results and the horizontal axis is for target results) ...	74
Figure 6.1 The schematic drawing of the thin feet bolted flange connection by ESDU [4].....	81
Figure A.1 ANSYS Workbench project schematic window for static structural analysis.....	102
Figure A.2 Exporting the parametric study results .....	103
Figure A.3 Data import from a text file .....	104
Figure A.4 Data import wizard window and row separation.....	104
Figure A.5 Column separation options .....	105

Figure A.6 Data type selection and finalizing .....	106
Figure A.7 The initial form of the imported data .....	107
Figure A.8 The final version of the imported data .....	107
Figure A.9 Loading input for each of the 25 parametric sets.....	110
Figure A.10 Giving input and taking output after training ANN in Matlab workspace.....	112
Figure C.1 The chart for variation in effective area of plates for axisymmetrically loaded joints (taken from ESDU [4]) .....	117

## LIST OF SYMBOLS AND ABBREVIATIONS

### SYMBOLS

A	Bolt size
$a$	The distance from bolt center to outer flange surface, neuron output
ANN	Artificial neural network
B	The number of bolts
b	The distance from bolt center to inner flange surface, bias scalar
C	Bolt location distance form center
D	Casing thickness
$D_f$	Effective diameter of practical flange working area
d	Bolt thread nominal diameter
$d_{bh}$	Bolt head effective diameter
$d_{corner}$	The diameter of the circle touching hexagonal corners of bolt or nut
$d_{edge}$	The diameter of the circle tangent to hexagonal edges of bolt or nut
$d_{eff}$	Effective bolt head-nut diameter
$d_{min}$	Bolt thread minor diameter
$d_{th}'$	Bolt effective thread portion diameter
$d_w$	Washer outer diameter
E	Flange thickness
$E_b$	Young's modulus of bolt
$E_f$	Young's modulus of flanges
$E_w$	Young's modulus of flanges
FE	Finite element
FEA	Finite element analysis
FEM	Finite element method
$F(w)$	Performance function
i	Neuron input
$k_b'$	Effective bolt stiffness
$k_f'$	Effective bolt stiffness

$k_{fb1}$	The stiffness of the flange-1 acting with the bolt group
$k_{fb2}$	The stiffness of the flange-2 acting with the bolt group
$k_{sh}$	Bolt shank stiffness
$k_{th}$	Bolt thread stiffness
$k_w$	Washer stiffness
$l_f'$	Equivalent total flange thickness
$l_{sh}$	Bolt shank length
$l_{sh}'$	Bolt effective shank length
$l_{th}$	Bolt thread length
$l_{th}'$	Bolt effective thread length
$P_b$	Total bolt force
$P_{bx}$	Bolt reaction force in x-axis
$P_{by}$	Bolt reaction force in y-axis
$P_{bz}$	Bolt reaction force in z-axis
$P_{ext}$	Axial external force
$P_b$	Bolt pretension
$P_t$	Bolt pretension
$p$	pitch of the bolt thread
$R_{in}$	Inner radius of flanges
$R_{out}$	Outer radius of flanges
$t_{bh}$	Bolt head and nut thicknesses
$t_w$	Washer thickness
$x_{nu}$	Nut contribution coefficient
$x_{sh}$	Bolt head shank increase coefficient
$x_{th}$	Bolt thread diameter coefficient
$x_{pt}$	Bolt-nut thread engagement coefficient
$w$	Weight vector
$e$	Error vector
$\lambda$	Lagrangian multiplier term
$\mu$	Penalty term

## **CHAPTER 1**

### **INTRODUCTION**

Developing an optimized structural design without compromising safety is often an iterative and time-intensive job in a critical structure with multiple parts. Hence, it requires efficient analysis techniques as stated by Demirkan et al. [1].

Bolted flange connection is a structure to connect two or more different parts in an assembly [2]. Figure 1.1 presents a circular bolted flange connection. In bolted flange connections, which are commonly utilized in aircraft engine designs, it is important to achieve structural integrity and also to minimize the weight. The forces and moments induced in an aircraft engine are transferred to other parts of the structure through the bolted flange connections. On the other hand, an overly safe bolted flange connection design leads to a heavier and less efficient aircraft engine. Since bolted flange connections have a direct impact on the safety of the design [3] by serving as load transfer mechanisms, structural analysis of the bolted flange connection should be carried out with high attention in the detailed design stage. It takes hours or even days to complete the analysis iterations as the number of degrees of freedom and the nonlinearity level increase in the finite element analysis of the bolted flange connection due to the contact definitions. Therefore, the standard finite element analysis exercise causes to slow down the design process considerably. The need for a bolted flange connection design tool that can reduce the engine weight in small amount of computational time by generating quick, accurate analysis results is in a way inevitable.

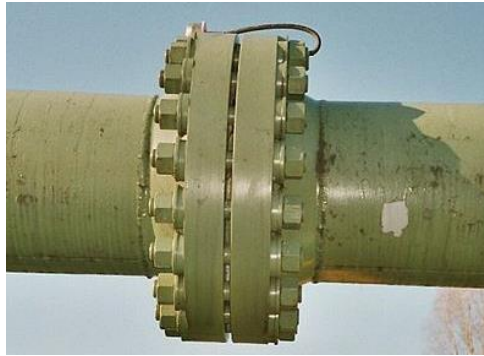


Figure 1.1 A bolted flange connection sample

The number of bolts, bolt locations, bolt size, casing thickness, flange thickness, bolt preload and axial external force are some of the critical design parameters affecting the safety of the bolted flange connection. In such a design, several trials, supported by structural analysis, are required to determine the optimum combination of the critical design parameters. Engineering analysis can be made by two approaches: classical methods and numerical methods. In the classical methods, analytical or approximate solutions of the derived equations are used while the numerical methods include techniques such as finite element method. Theoretical analysis and finite element method (FEM) analysis are two main approaches to perform structural analysis of bolted flange connections. Application of theoretical/analytical approaches, such as ESDU [4], ASME [5] standards, etc., require simplifying assumptions about the geometry and the load transfer mechanism and such approaches are difficult to apply for specific geometries. According to Coro [6], the theoretical approach of structural analysis of the bolted flange connection based on beam theory often results in overly safe results. However, theoretical approaches are fast in arriving at the optimum design. In contrast, FEM analysis requires almost no simplification of the geometry and is more reliable when properly modeled, but at the cost of high computational power [6].

In this study, the main objective is to develop a new bolted flange design tool based on the power of the FEM solution and the nonlinear approximation capability of artificial neural network (ANN). The expectation from the design tool is to give very quick structural analysis results for the bolted flange connections for medium size

aircraft engines without compromising the reliability. It should be noted that FEM analysis requires longer model preparation and analysis times. For this purpose, structural FE analysis in ANSYS Static Structural tool [7], parameters correlation study in ANSYS DesignXplorer tool, and artificial neural network training in MATLAB Neural Network tool [8] are used in combination to develop an ANN based bolted flange design tool.

Linear behavior assumption in analysis is applicable to quite limited cases in real world applications. On the contrary, the nature presents countless phenomena with different types of nonlinearities. In the present study, several structural analysis should be conducted including the nonlinear effects in order to simulate the deformation mechanisms for the bolted flange connection. The nonlinear structural analysis needs considerable amount of computational power since the process is iterative with progressive modification as stated by Deng and Ghosn [9]. In a structural analysis, one can mention three fundamental nonlinearity sources: material nonlinearity, geometric nonlinearity, and boundary nonlinearity. The material nonlinearities can be divided into three; time independent elastic-plastic behavior under load beyond yield point, time dependent creep behavior under load with high temperature, and the viscoelastic/viscoplastic behavior [10]. Large deflections or some critical deformation shapes can cause geometric nonlinearities in solid structures [10]. Nonlinearities due to boundary conditions are generally due to contact and friction [10].

Finite element problem solution can be achieved with the implementation of different meshes on the geometry in consideration. One of the most critical factors affecting the analysis results in FEM is the choice of element types to be used in the mesh structure. In this study, 3D solid hexahedral elements are used because the geometry is suitable to be filled with high quality hexahedral elements and meshing with hexahedral elements give trustworthy results as it is explained later. A regular linear tetrahedral element has four nodes and four triangular surfaces as seen in Figure 1.2, whereas the quadratic version of the same element is made up of ten nodes with the inclusion of mid side nodes, as shown in Figure 1.3. A regular hexahedral element,

also known as brick element, is presented in both Figure 1.4 with linear formulation and in Figure 1.5 with quadratic formulation. The linear structural hexahedral element is formed by eight nodes at the corners and designated as SOLID185 in ANSYS [11]. Each node in this finite element model (SOLID185) has three degrees of freedom, x, y, and z translations. The quadratic form of the same element contains 20 nodes having again three degree of freedom and are named as SOLID186 in ANSYS [11].

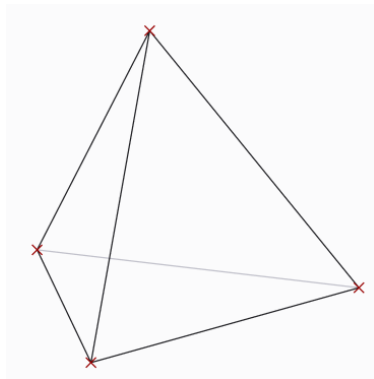


Figure 1.2 A regular linear tetrahedral element with four nodes

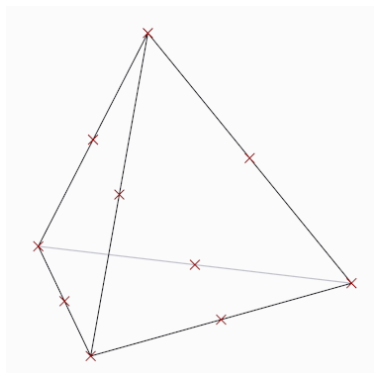


Figure 1.3 A regular quadratic tetrahedral element with ten nodes

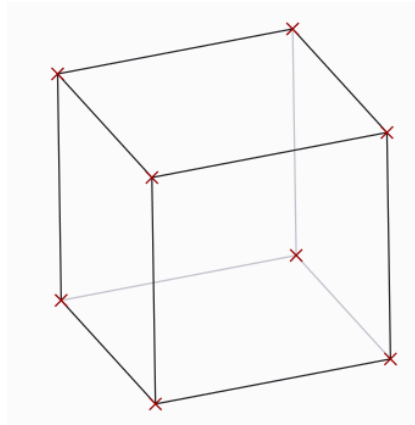


Figure 1.4 A regular linear hexahedral element with eight nodes

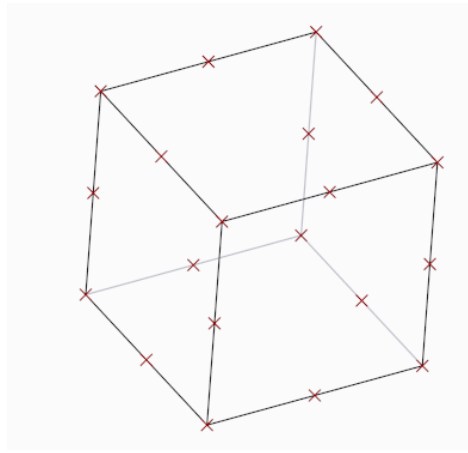


Figure 1.5 A regular quadratic hexahedral element with twenty nodes

Element type, order of the element, the number of numerical integration points, and the number of degrees of freedom are the factors affecting computational time in a structural FEA. Replacement of tetrahedral meshes with hexahedral ones of the same edge sizes decreases the number of elements used for the same structure. Since similar accuracy in the same geometry is achieved with higher number of tetrahedral elements, the analysis with tetrahedrons causes more CPU time due to having more integration points [11]. However, employment of mesh with high quality (perfect cube like shape) hexahedral elements gets more difficult if the analysis geometry has a complex shape. In such circumstances, implementation of the hexahedral elements requires special attention. The automatic mesher tool of the commercial FEA software

used (ANSYS) tends to fill the complex geometries with tetrahedral elements in most cases unless the special meshing arrangements are specified apriori. On the other hand, proper hexahedral mesh with smooth distribution in rectangular-prismatic like geometries may be helpful in terms of obtaining almost perfect-cube hexahedral elements. Moreover, the coherent analysis results between the separate analyses in the parametric analysis study can be achieved by the previously specified smooth mesh distribution. A research by Wang et al. [12] examines the comparison of tetrahedral and hexahedral elements in structural FEA. The study displays that good stress results are obtained without having very fine meshes by utilizing hexahedral elements in comparison to the use of tetrahedral elements. Linear tetrahedral elements are quite stiff and should be avoided in structural analysis, because the analysis results with linear tetrahedrons may lead to very inaccurate results [12]. Increasing the number of elements (finer mesh) cannot also solve the problem. Instead, quadratic tetrahedrons can give trustworthy results for the displacements and the stresses [12]. Quadratic hexahedral elements are very successful in almost all types of structural analysis, but at the cost of computational power [12]. Linear hexahedral elements also give sufficiently accurate results. ANSYS Help document [11] recommends the utilization of fine linear elements most of the time instead of using relatively coarse quadratic elements in order to attain better accuracy with less computational cost in nonlinear structural analyses. However, there are two critical points in using linear hexahedral elements in structural FEA. These elements are susceptible to large corner angles. The analyses may end up with misleading stress results if the corner inner angles approach to 180 degree rather than the right angle. The second point to be paid attention is the shear locking problem encountered in linear hexahedral elements. When shear locking occurs, the structure shows wrong displacement and stress results under dominant bending loads due to the poor approximation of the edges between the two nodes with linear shape functions as it is clearly seen in the case study by Wang et al. [12]. It is suggested to include extra shape functions or enhanced strain formulations to evade the shear locking problem under bending dominant loads if linear hexahedrons are to be used [12].

The utilization of 3D finite elements in comparison to lower dimensions such as 1D or 2D, the increase in the degrees of freedom, and the higher order of elements in FEM result in complex equations in formation of element matrices during FEM solutions. Moreover, mapping operation and inversion of Jacobian matrix are the other sources increasing the complexity levels. Solving these equations by algebraic manipulations is almost impossible. Therefore, numerical integration techniques are used to evaluate equations in which the integrals are calculated by summation [13]. The numerical integration is also known as “quadrature”. Gauss integration (Gauss quadrature) is the most often used method in creation of element matrices by defining sampling points and assigning weights to approximate integrals [14]. The number of sampling points in Gauss quadrature determines the capability of approximating the order of integral. In order to give accurate results for higher order integral, the numerical integration points should be increased. If the number of integration points is sufficient to approximate the higher order terms in stiffness equations of elements, it is called “full integration”. On the other hand, if less integration points are used, the higher order terms are excluded and this numerical integration is known as “reduced integration”. However, the increase in the number of integration points does not change the accuracy level after a certain point for a specific order of integrand. In ANSYS Workbench, linear hexahedral elements with eight nodes use eight-point Gauss integration rule in full integration [11]. On the other hand, quadratic hexahedral elements formed by twenty nodes utilize fourteen-node Gauss integration rule in full integration [11]. The increase of the number of integration points in an element causes the increase of computational time in analysis. Utilization of full integration can cause shear locking problem with over stiff elements and takes longer time in comparison with reduced integration. On the other hand, reduced integration eliminates locking problem and gives solution in less amount of time. However, reduced integration can cause hourglass mode problem and the accuracy should be checked in this case.

Finite element analysis of multiple parts in the form of assemblies involves the utilization of contacts. The knowledge about the contact formulation is valuable in order to model the interaction between the contacting parts in a realistic way.

According to Cook et al. [15], the abrupt stiffness changes and the contact area variations are the sources of nonlinearity in the problems with contacts. If the contact stiffness is too low, overclosure (intersection) between two parts may occur. On the other hand, too stiff contact causes probable convergence failures [15]. Contact algorithms utilize special “contact elements” with special functions for detecting contacts, preventing-limiting the penetration, and controlling the contact stiffness [15]. The contact algorithms work on the principles of the slave nodes located on the contacting surface of one part and the master nodes located on the other part. As stated by the report [16]], checking the position of the slave nodes and detecting the penetration of the master surface are the steps to explore the contact. Subsequently, the slave nodes are relocated by pushing them back with respect to the master surface [16]]. The critical parameters of the contact including the contact point, the penetration level, and the pushback direction are controlled by the contact algorithms. In most cases, the solution requires iterative approximations. The selection of the master and slave surfaces is crucial in the solution process. If contacting surfaces are made up of the same material, then the surface with coarser mesh should be chosen as the master in order to prevent the undetected penetrations [16]]. Contact formulations are derived by imposing constraint equations on the finite element solution via minimization of potential energy. The commercial FEA software ANSYS [11] offers four different contact formulations, pure penalty, normal Lagrange, multipoint constraint, and augmented Lagrange. Multipoint constraint algorithm is applicable for the cases with “no separation” or “bonded” contact types to tie surfaces with each other [11]. In this study, there are no such type contacts used. The accuracy of penalty (pure penalty) algorithm depends on the correct selection of the penalty term,  $\mu$ , which is also known as the contact stiffness. In this method, as the value of  $\mu$  goes to infinity, the algorithm satisfies the contact conditions exactly [17]. However, since such a value cannot be stored in the solution matrices of the FEA, a finite value of penalty term has to be selected. Thus, penalty algorithm is an approximate solution [17]. Although selecting large penalty values increases the solution accuracy, it also causes numerically ill-conditioned problem such that the output error is highly sensitive to the input error. On the other hand, penalty algorithm is easy to implement in problems

by only modifying the stiffness terms, and it also exhibits good convergence property [11, 17]. In normal Lagrange algorithm, the Lagrange multiplier method is used, in which the multiplier,  $\lambda$ , is also known as the contact force [11]. The negative aspect of this method is the increase in the dimension of the solution matrix. Another disadvantage is the fact that the solution matrix comprises zero-diagonal element(s) so special technique is necessary to reorder and solve the equations. The main advantage of this method is the ability of satisfying the exact contact conditions [17]. In the augmented Lagrange algorithm, the negative aspects of the penalty and the Lagrange methods are aimed to be resolved. Consequently, augmented Lagrange method is formulated by employing both the penalty term  $\mu$  and the multiplier term  $\lambda$  in order to reduce the high dependency on  $\mu$  in the penalty method and discard the increase of the solution matrix dimension as in the case of Lagrange multiplier method [17]. In this method, an infinite  $\mu$  is not required and  $\lambda$  can be controlled within the desired tolerance [17]. In other words, the formulation is less sensitive to the correct selection of  $\mu$  in contrast to the penalty method. In this respect, the accuracy of the nodal displacements is also controlled. The disadvantage of the augmented Lagrange method is the necessity of iterative solution [17]. In this study, the contact algorithm is augmented-Lagrange method with the default coefficients controlled by ANSYS.

Parametric finite element (FE) analysis is a common method utilized in design practice of critical structural elements to obtain reliable design. Parametric study may require hundreds or thousands of FE analyses depending on how crucial the design is and how many input and output parameters exist to optimize the design. The completion of thousands of FE analyses takes significant amount of time for limited computational resources. Furthermore, all of the input parameters do not have the same effect on the selected output parameters (results) in a parametric study. One parameter may influence a specific output drastically whereas another one may hardly change the same output. Therefore, in the present study, sensitivity study on the effect of output on input parameters is carried out by utilizing parameters correlation study in ANSYS. Parameters correlation study works on the basis of deterministic model [11]. In contrast to the probabilistic models, no randomness is allowed in the

deterministic approach and one always gets the same output for a specific input. Therefore, parameters correlation study can present accurate results depending on the quantity and quality of the input. It is assessed that Spearman correlation is better in identifying non-linear, monotonic relationships such as bolted flange connections [11]. The principles of Spearman correlation will be explained in detail in the corresponding section.

The artificial neural network is a group of computational cells, called as neurons, in which each neuron has connections with all of the neurons located in the previous and next layers with different weights defined in the training [18]. ANN is an effective tool in approximating the non-linear relationships and the principles about ANN methodology will be discussed further in corresponding section. In the study by Muliana et al. [18], FE load displacement curves are generated with the help of ANN where they observed that the trained ANN model is successful in predicting the behavior of non-linear material property. Muliana et al. [18] also compared the performance of ANN approximation with separate FEM analysis results to verify the ANN performance. The study conducted by Muliana et al. proves the applicability ANN approximation over non-linear finite element analysis.

One of the essential reference source in the field of bolted flange connection is prepared by The Institution of Mechanical Engineers and established by ESDU [4]. This source discusses the problem of bolted flange under axial force by assuming the structure as a beam. The methodology starts with idealizing the bolted flange connection as an assembly of parallel springs formed by flange group and bolt group as explained by Shigley in more detail [19]. By evaluating the material properties and geometrical dimensions, the equivalent stiffnesses of both groups are calculated. Next, external load is considered whether separation occurs under bolt head. According to the result, prying effect is included or not in calculation of the corresponding bolt and flange loads [4].

ASME Boiler and Pressure Vessel Code Section VIII [5] is a solid ground in the literature with a very detailed theoretical approach to bolted flange connections. The code considers the flange design with several aspects and presents design suggestions and theoretical calculation methods and focuses especially on the complex flange structures with several types generally containing gasket with internal pressure. European standard on the flange calculation, EN 13445, considers ASME Code as a basis as stated by Schaaf, et al. in an ASME conference proceeding [20].

Coro [6], describes a new flange design methodology based on finite element analysis. Coro states that the finite element approach increases the level of precision in the analysis of flange joint when compared to the theoretical solutions dependent on the classical beam theory. The flange-design tool is mentioned to be a commercial product that can analyze different flange geometries with different loading cases in a parametric way. Although the author claims that flange-designer tool conducts structural analysis based on FEM, the article hardly explains the working principles or performance statistics. It should be noted that developed bolted flange tool explained in the study by Coro [6] is claimed to give accurate results in comparison with commercial FEA solution. The idea of utilizing FEM solution in a parametric methodology

Azim [21] carried out an analytical investigation on bolt tension of the bolted flange connection exposed to bending moments. The author examines the effects of parameters such as flange thickness, width of the flange and the number of bolts on the bolt tension by considering both the classical beam theory and FEM. Azim [21] concludes that the theoretical approach has a limited applicability for real cases and the error in the theoretical analysis increases as the input geometry differs from the standard condition. In other words, the theoretical approach in that study gives reliable results only for a limited range of the input. Therefore, it can be concluded that the theoretical analysis of bolted flange connection cannot be trusted all the time. Instead, analysis by FEM should be preferred in the analysis of such a critical structure.

In this study, a methodology has been developed for the iterative design and analysis of the bolted flange connection by utilizing artificial neural network approximation (ANN) of the database formed with thirteen thousand five hundred non-linear FE analyses involving contact under axial external load. “Function fitting” approach is used to train and then predict the complex, non-linear input output-behavior of the bolted flange connections using finite element analysis [22]. The main motivation of the study is to develop an ANN based bolted flange design tool for medium sized aircraft engines. The bolted flange design tool will be used in the preliminary design stage to assess the structural integrity of the bolted flanges very fast for various choices of the design parameters. Thus, long model preparation and analysis requirement of direct non-linear finite element based analysis will be eliminated and substantial reduction in design cycle time will be achieved. The flange design tool will also be used as the fast solver, which will replace the finite element solver, in conjunction with an optimizer to achieve weight reduction in the flange. Weight saving in any structural component of aircraft is one of the main goals in the design of aircraft.

## **CHAPTER 2**

### **SCOPE OF THE THESIS**

In this study, a methodology has been developed for the iterative design and analysis of bolted flange connections by utilizing artificial neural network approximation (ANN) of FEM analysis database formed with 13500 fine-meshed, non-linear structural analyses involving contact under axial external load.

Flowchart of the developed bolted flange design tool is presented in Figure 2.1. In chapter 3, determination of the analysis geometry and the input parameters is explained. There are seven input parameters, five of which are geometric parameters and the remaining two parameters are for load input. The analysis geometry is modeled in ANSYS DesignModeler [7] as 3-D computer aided drawing (CAD) file by considering the subsequent parametric study. In the next step, the analysis model is prepared in ANSYS-Static Structural module. In order to investigate the effects of input parameters on the output, parameters correlation study is conducted in ANSYS DesignXplorer tool [7] as described in chapter 4. According to the result of parameters correlation study, the input value intervals of the parameters within the upper and lower ranges of the parameters are determined. By running successive static structural FEM analysis, a database of 13500 analyses is formed by combining all the selected parametric design variables with each other. Subsequently, chapter 5 presents the artificial neural network training process with the finalized FEM analysis database to obtain a continuous solution domain within the upper and lower limits of the parameters.

In chapter 6 of the thesis, the developed bolted flange connection design tool is tested against different test cases to verify the performance of the design tool. The first test set is formed by ten test points which are exactly located on the initial training points of the design tool. In the second test set, there are ten test points which are not same

as the parameter design points, but selected inside the training points within the upper and lower limits of the parameters. The final test set consists of ten instances located outside the training limits. Furthermore, the performance of the developed tool is compared with the analytical approach of ESDU [4] for the same example problem. In the last chapter, whole study is summarized and the outcome is evaluated as well as stating the future work possibilities. Both case studies for testing shows that the developed bolted flange design can be used as a fast solver with very high accuracy within the training limits of the input parameters.

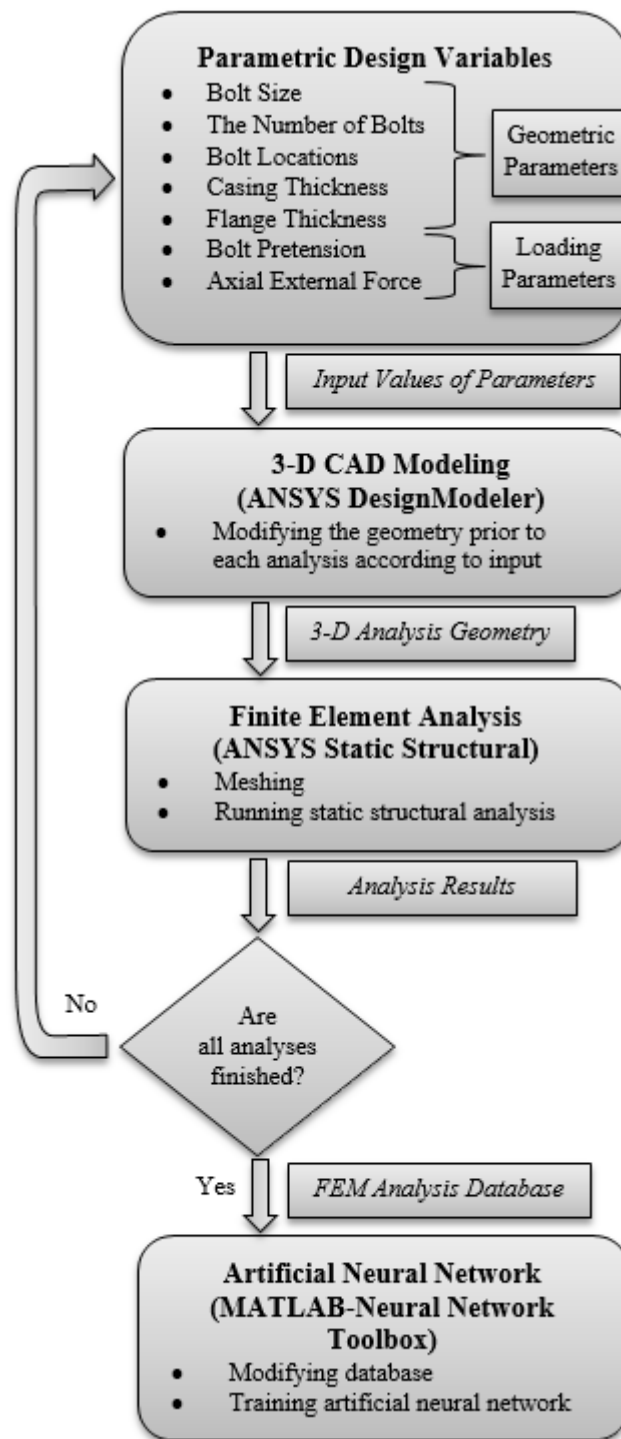


Figure 2.1 Flowchart of the bolted flange design tool development procedure



## CHAPTER 3

### FINITE ELEMENT ANALYSIS OF BOLTED FLANGE CONNECTION

Running structural finite element analysis (FEA) is a task with a trade-off between accurate results and computational power. Geometric and material non-linearities, existence of contacts between different parts, mesh size are some of the factors draining the computational sources.

In this study, finite element analysis (FEA) of bolted flange connection is carried out in an automated parametric study. To conduct thirteen thousand five hundred analyses in a parametric set with five geometric and two loading input parameters, the analysis model must be so arranged that parametric meshing operation should not fail to mesh the analysis geometry. Otherwise, the software cannot create the expected finite elements as defined by the initial settings so the analysis cannot converge to any result. The failed analyses cause data point losses, which are required for artificial neural network training.

ANSYS Workbench [7] is the finite element analysis software utilized in all the static structural analyses. DesignModeler toolbox [7] is employed for creation and modification of the analysis geometry.

The finite element analysis model is prepared by following certain steps. The 3D analysis assembly is modeled according to defined values of the geometric variables. The selected materials are assigned to corresponding parts in assembly. The contacts are defined between the parts of the analysis in Static Structural interface [7]. Meshing operation takes place according to the previously defined mesh method and sizing settings. After all required static structural analysis settings such as the number of solution steps or nonlinear solution options are specified, load and boundary

conditions are imposed on the analysis model. In the last step, the types of output results expected from the analysis are settled. Once all these steps are finalized, one can immediately run the analysis if it is single analysis. On the other hand, if the case is a parametric analysis study, the solution process of multiple analyses (design points) has to be commenced after the definition of the input parameter values for the desired number of design points.

### **3.1 Analysis Geometry and Meshing**

In this study, the area of interest is scoped out a medium scale bolted flange connection of an aircraft engine. The engine model with the nominal geometrical dimensions, the loading conditions, and the bolt pretension, have been previously specified prior to this study [23]. In the present study, the defined circular bolted flange connection is exposed to an axial external force. It is intended to optimize the modeling of the analysis geometry, meshing operation, and defining analysis details in order to run successfully the analyses of parametric sets in an automated way. The details are expressed in the corresponding sections.

#### **3.1.1 Bolted Flange Connection Assembly**

In line with the specified analysis model, a fully circular bolted flange connection structure is formed by two symmetrical flange extensions with nominal twenty four equally spaced bolt and nut pairs, and two identical washers for each bolt-nut pair (one being located between the bolt head and the flange-1, and the latter between the nut and the flange-2). The flange structure type is designated as inverted T-shape [6] in which the flanges are extended radially outward from casing. Figure 3.1 shows the complete geometry of the bolted flange connection to be analyzed in this study. Because the bolted flange connection geometry is circular with equally spaced bolt-nut pairs, the structure can be sliced into twenty four (equal to the number of bolts) identical sectors about the internal axis (z-axis in this study).

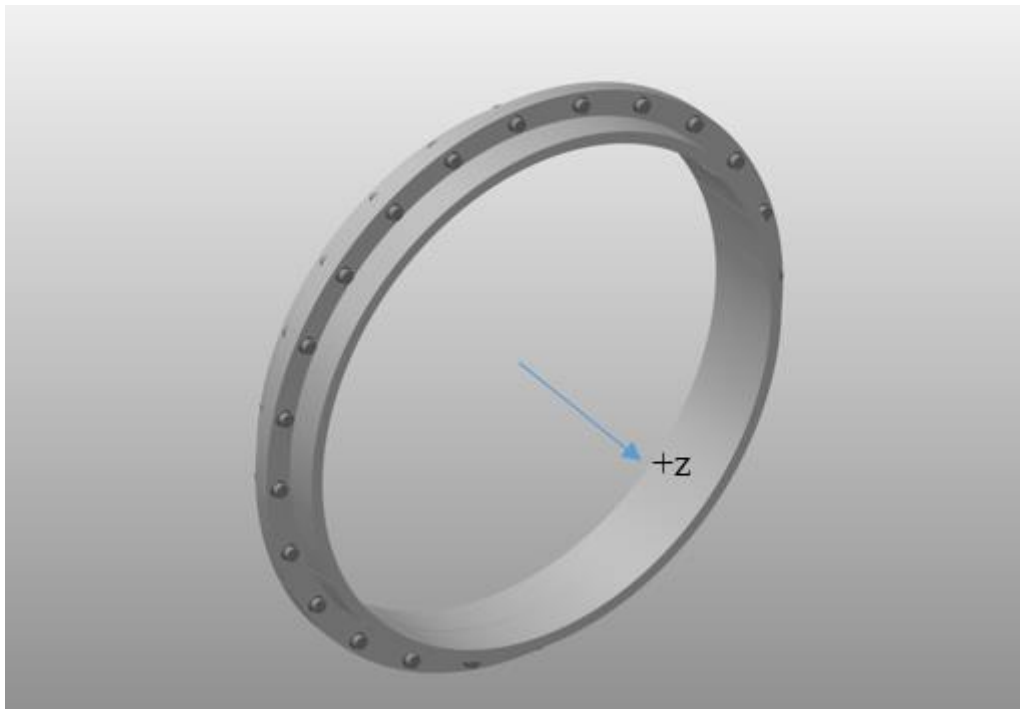


Figure 3.1 Circular bolted flange connection geometry

Figure 3.2 exhibits the components in the section view of the bolted flange connection assembly. It should be noted that there is no gasket or supplement materials between the flanges and the flanges are in direct contact with each other.

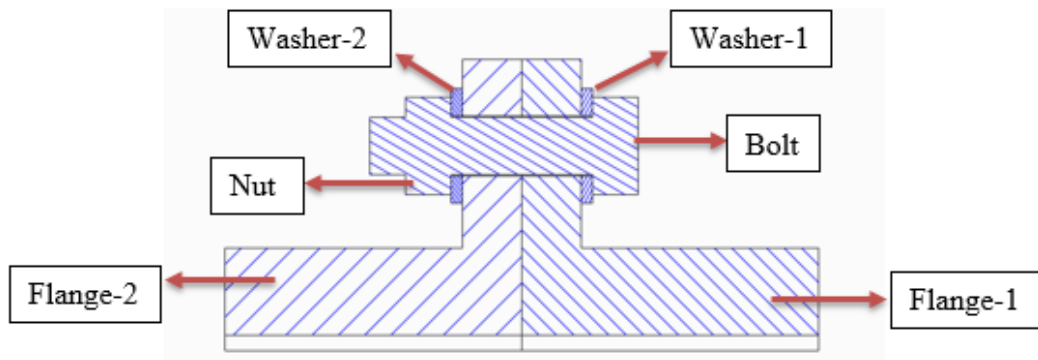


Figure 3.2 Cross-sectional view of the bolted flange connection geometry with the components

Due to the requirement of performing many non-linear finite element analyses involving contact with the prepared analysis model, it is essential to have an optimal model both in terms of accuracy of FE analyses results and efficient computational

power usage. Therefore, the bolted flange connection can be modeled as a circular sector containing one pair of bolt-nut, two washers, and the corresponding sectors of flange-1 and flange-2. Thus, the complete circumference is divided into the number of bolts as seen in Figure 3.3. Furthermore, using a circular sector analysis geometry gives the opportunity to eliminate so many contacts due to having many bolts and nuts in the analysis model. In this respect, the risk of probable convergence problem due to extra contacts is also minimized.

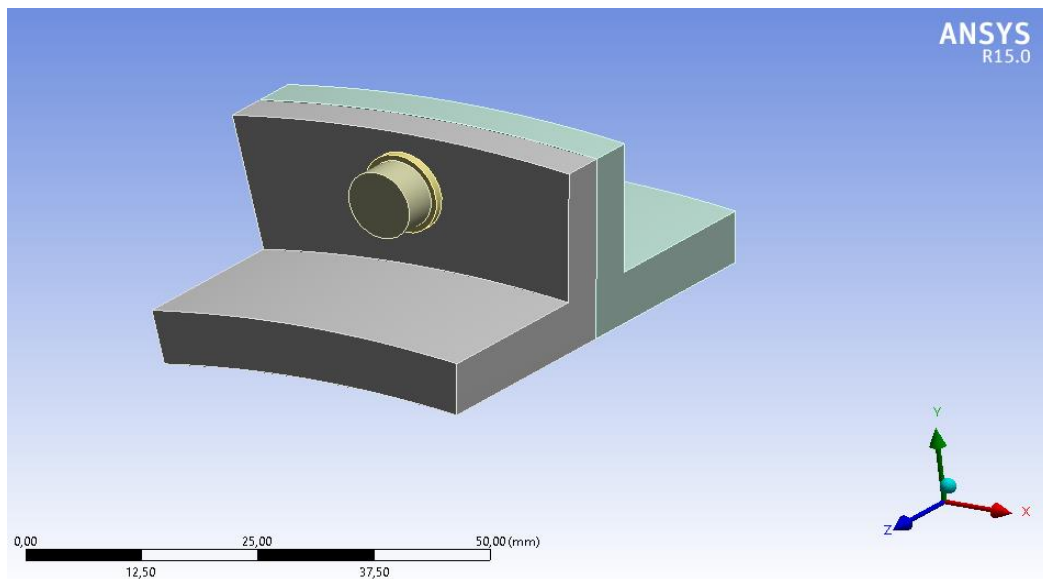


Figure 3.3 Axisymmetric bolted flange sector model

The analysis geometry of the medium scale bolted flange connection with the nominal dimensions of parameters are presented in Figure 3.4 and Table 3.1. As for the input parameters, there are five geometric and two loading parameters as shown in Table 3.1. It should be noted that the axial force indicates the corresponding loading portion for only a single bolt. Apart from the geometric parameters shown in Figure 3.4, there are two fixed dimensions that are specified apriori, these are the circular sector outer diameter (350 mm) and the circular sector inner diameter (303.8 mm). More details about the upper and lower limits of the design variables, and the parametric values of each variable are given in the “Parameters Correlation Study” section.

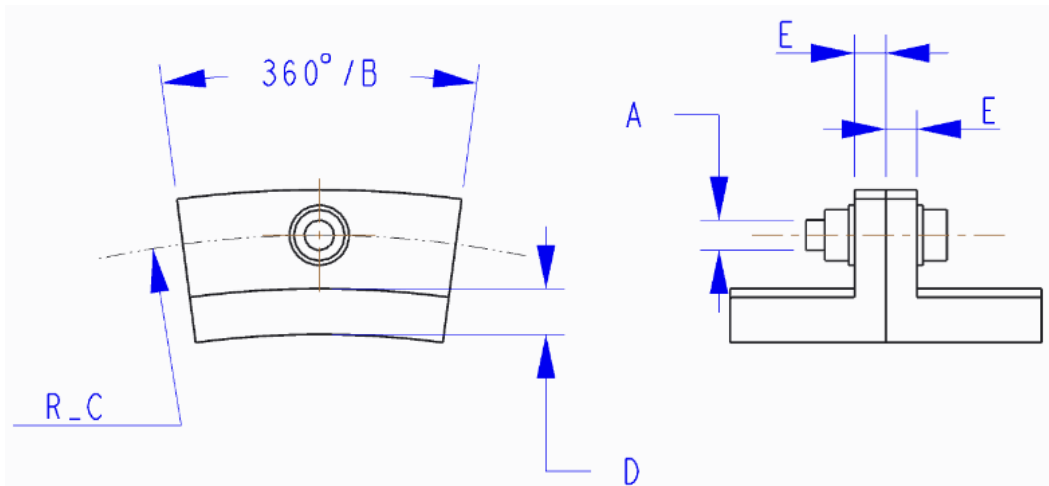


Figure 3.4 The circular sector analysis model with the geometric parameters

Table 3.1 The nominal values of the parameters in the analysis model

<b>GEOMETRIC PARAMETERS</b>		
<b>Input Variable</b>	<b>Explanation</b>	<b>Nominal Value</b>
<b>A</b>	<b>Bolt Size</b>	4.83 mm
<b>B</b>	<b>The Number of Bolts</b>	24 pcs
<b>C</b>	<b>Bolt Location</b>	167.75 mm
<b>D</b>	<b>Casing Thickness</b>	6.6 mm
<b>E</b>	<b>Flange Thickness</b>	5 mm
<b>Axial Force per Bolt</b>	-	1280 N
<b>Bolt Pretension</b>	-	5702 N

Several trial iterations are performed to reach the final form of the analysis model in order to create high-quality meshing for all analyses varying with the parametric changes. Figure 3.5 presents meshed structure of the finite element analysis model. The smooth mesh distribution inside the 3D solid parts is clearly observed in the cross sectional view of the analysis geometry given in Figure 3.6. In the finite element model, all of the parts are meshed with only hexahedral elements. A few elements containing mid-side nodes are used only in washers. The parts in analysis are meshed by taking advantages of advanced mesh techniques and the details of the meshing operation are discussed in the next sections.

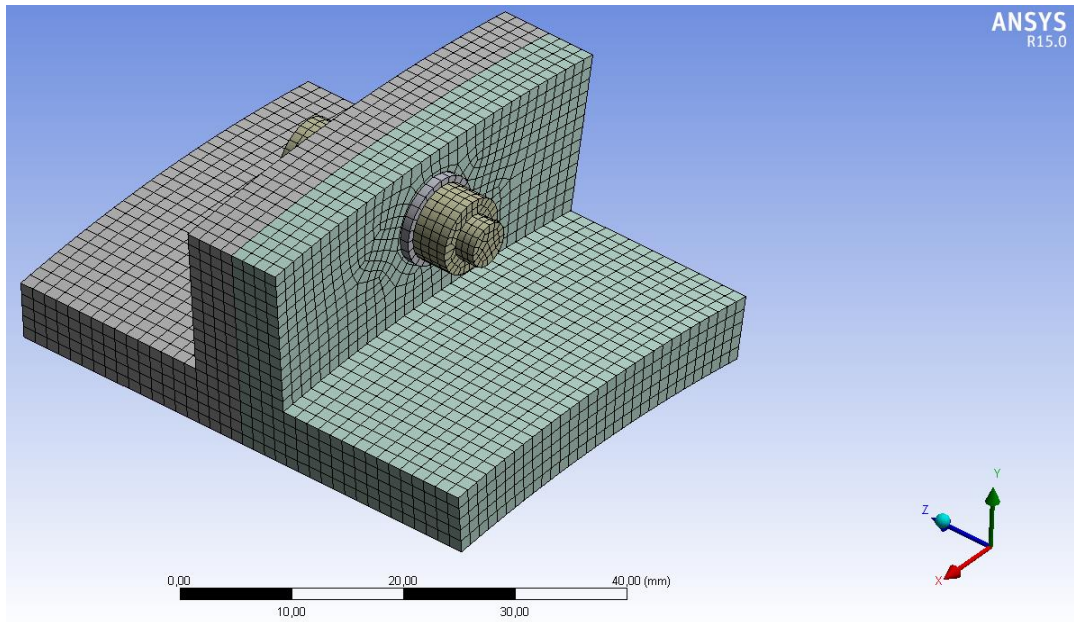


Figure 3.5 Sectional analysis geometry of the circular bolted flange connection

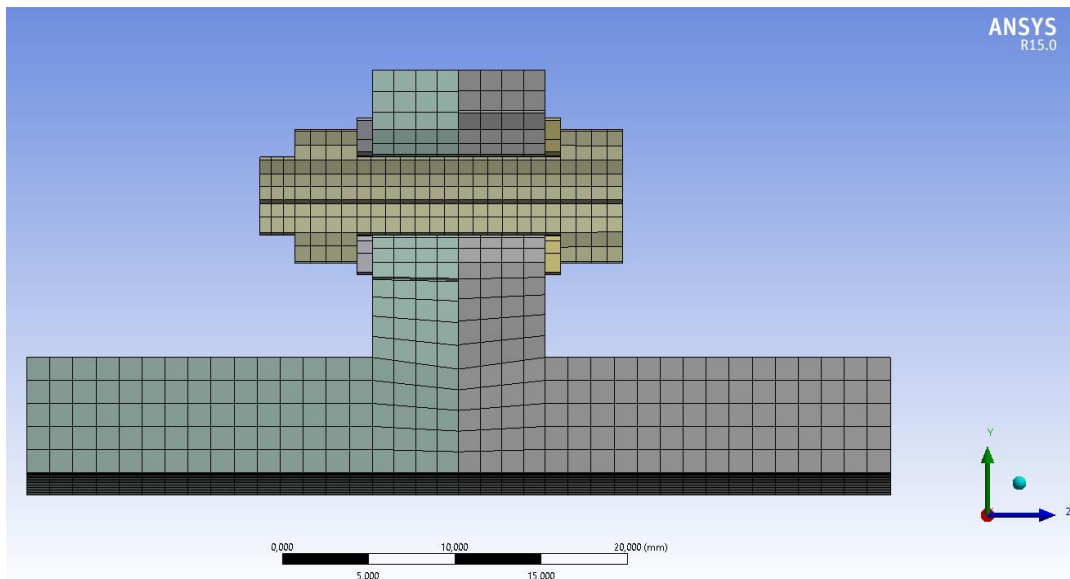


Figure 3.6 Cross section view of the meshed geometry

“Multizone” mesh method is one of the versatile tool used in meshing in order to achieve automatic decomposition of different geometric features in a single part in the meshing process [11]. If the multizone method is applied successfully to a body, the structure can be completely meshed with hexahedral elements. Multizone method

sometimes fails during meshing if the specified geometry is complicated to be resolved automatically. In such cases, the source and the target features have to be specified manually by the user so that the specified source and the target can be imprinted towards each other [11].

“Sizing” is a useful tool in meshing options to ensure that the automated analyses are conducted with meshes as fine as desired. In this study, two types of sizing are used. Edge sizing and body sizing are the options utilized to control mesh qualities to attain smoothly meshed parametric geometry. As one can easily predict, edge sizing option defines maximum element size on marked edges via either indicating the number of edge division or maximum element size. In the body sizing operation, a whole part is marked as the sizing target and the user specifies the maximum element size within the complete body. Sizing operations are expressed in detail for each part later on.

In the end of all analysis settings, the analysis model consists of 15608 nodes and 11302 hexahedral elements for the nominal values of all geometric input parameters.

### **3.1.2 Bolt-Nut Geometry**

Normally, the bolt head and the nut have hexagonal shapes with edges and corners which causes stress concentration. The contact interface between the bolt and the nut must successfully transfer relatively high loads occurring during the initial bolt pretension.

In this study, induced high local stresses due to the stress concentration effect in FEA of the bolted flange connection are not desired, since artificial neural network approximation might be trained with exaggerated results with high local stresses. As an alternative, the solution methods are so arranged that the results are gathered on special regions instead of taking single point with maximum stress. If the hexagonal bolt head and nut models are used, it would be necessary to chamfer the edges and corners as in the real designs. These chamfers lead to considerably finer meshes, which is unwanted side effect. Hence, as one can see in Figure 3.7, in the current

study, the outer bounds of the bolt head and the nut are taken as circular instead of hexagonal. The philosophy, here, is to exclude the stress concentrated regions and to ensure the smooth parametric meshing of the bolt and the nut while keeping the equivalent stiffness coefficients of the bolt head and the nut body the same as before. For this purpose, the article by ESDU [4] suggests to define an effective diameter in bolt head and nut such that the average of the diameter touching outer sharp corners and the largest diameter fitting inside the hexagon (tangent to the hexagonal edges) is taken as the effective diameter. It should be noted that the bolt head and the nut are assumed to have equal edge distances of the hexagon. As a result of all trial analyses, an even mesh distribution in the bolt-nut body is obtained in the latest analysis model.

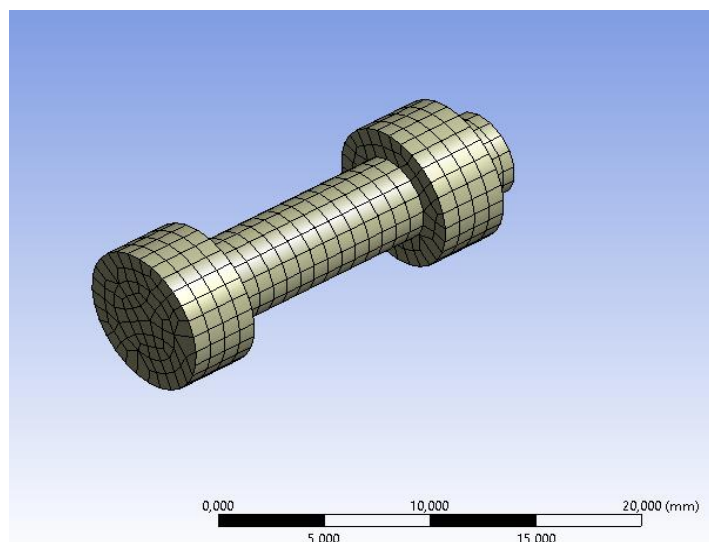


Figure 3.7 The united analysis model of the bolt and the nut with the cylindrical outer geometries

Bolt head and nut outer boundaries are in the form hexagonal shape under normal circumstances. During modeling of the bolt head and the nut as circles with effective diameter,  $d_{\text{eff}}$ , mean diameter of two circles are calculated as given in Equation 3.1. These two imaginary circles are shown in Figure 3.8. The first circle touches the corners of the hexagon whereas the smaller circle is tangent to the edges of the hexagon. It should be noted that the upper limit of bolt size to be used in the parametric analyses is M5 while the smallest bolt size is M4. Therefore,  $d_{\text{corner}}$  and  $d_{\text{edge}}$  values

are determined by referring to DIN 933-1987 [24, 25]. When one calculates the effective bolt diameters according to the reference bolt size tables [24, 25], the effective diameters are equal to 1.81d for M4 and 1.66d for M5 where “d” indicates the nominal bolt thread pitch diameter in mm. Since the nominal bolt thread size is specified as 4.83 mm (0.19 inch), the effective diameter is taken as 1.7d for all analyses in this study. The effect of taking 1.7d as the effective diameter on the analysis output is examined as a case study later. One should realize that the effective diameter changes as the bolt size value, d, alters in the analyses automatically. Likewise, the bolt head and nut thicknesses are taken as 0.8d [24, 25].

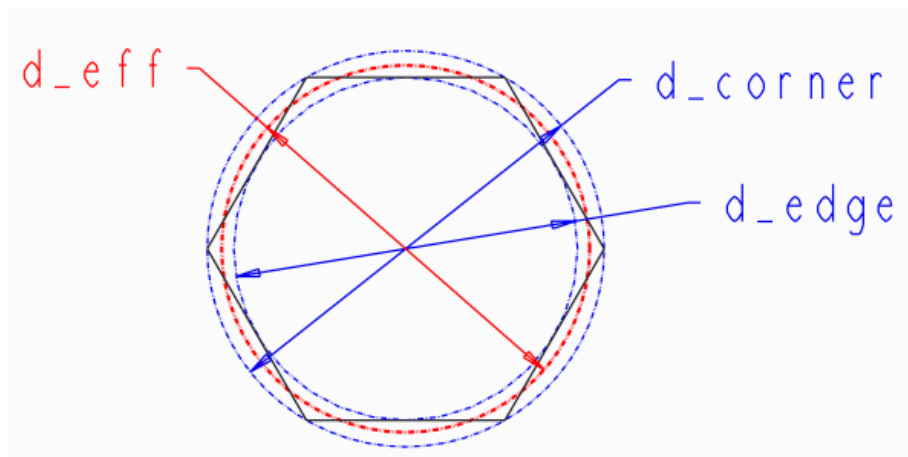


Figure 3.8 The imaginary circles and the effective circle to calculate the effective diameter of the bolt head and the nut

$$d_{eff} = \frac{d_{corner} + d_{edge}}{2} \quad (3.1)$$

In the beginning of the analysis study, the bolt and the nut had been modeled as the separate parts which are in contact. Bonded contact had been defined between the two parts in order to simulate the engaging threaded regions of the nut and the bolt. However, the initial analysis trials have revealed that there were problems in transmitting the force reactions from the bolt to the nut. In addition to the incorrect force reaction results, the existence of one more extra contact had caused extended analysis process time. Modeling of the bolt and the nut as a single, united structure is

seen to give the correct reaction forces and excludes the need for the bonded contact between the inner surface of the nut and the threaded section of the bolt. Both the bolt and the nut are made up of same material in this study. Hence, the united, single body modeling of the bolt and nut is a realistic engineering approach. The united bolt-nut model is given in Figure 3.7 as mentioned before.

To ensure the proper meshing of the bolt-nut body during the automated parametric analyses (bolt diameter is one of the geometric parameters), multizone mesh method is implemented in the bolt-nut body. As seen in Figure 3.7, the inner cylinder (bolt thread and shank portions together) is decomposed from the imaginary outer hollow cylinders of the bolt head and the nut. As a result, high quality hexagonal meshes are generated at a rate of one hundred percent without having any tetrahedral or triangular prism elements as desired.

Edge sizing and body sizing methods are also applied in order to preserve the mesh quality in parametric analyses. Four edges belonging to the bolt head and the nut shown in Figure 3.9 are divided into 15 equal segments while meshing. Furthermore, the maximum element size is limited with 4 mm.

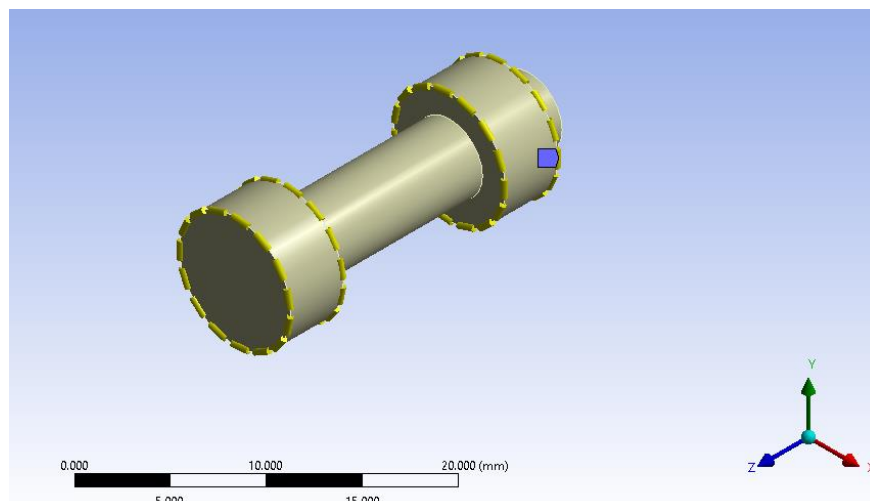


Figure 3.9 Edge sizing of bolt-nut body

### 3.1.3 Flange Geometry

The geometry of the circular sector flange is governed by the number of bolts assembled on the fully circular flange. The circular sector flange angle, shown in Figure 3.10, is equal to  $360^\circ$  divided by the number of bolts used. The nominal design geometry specified by TEI is formed by 24 bolts all around. Therefore, the sectional flange angle is  $15^\circ$ . This angle changes simultaneously as the number of bolts changes during the parametric study. The bolt hole located on the middle axis of the flange section has a diameter of  $1.1d$  in order to form clearance between the bolt and hole. In parametric study, the bolt hole center distance from the circular axis varies in each analysis as seen in Figure 3.11.

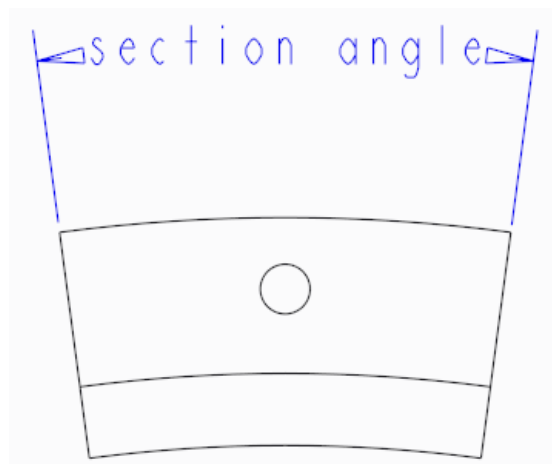


Figure 3.10 The angle of flange section used in the analysis

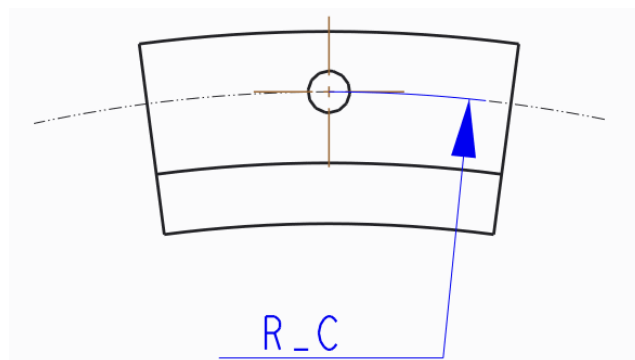


Figure 3.11 The variable distance of bolt hole to center axis nominated as Radius C

In order to obtain high quality finite elements, multizone method is applied to flanges to decompose the features into sub-parts as seen in Figures 3.12 and 3.13.

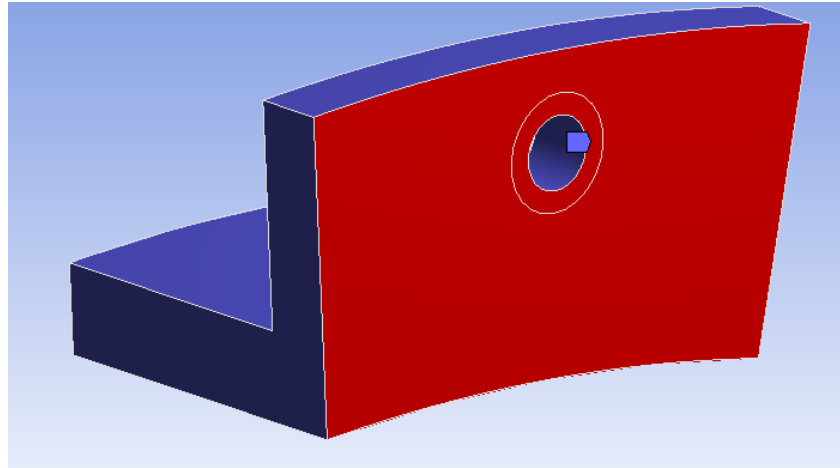


Figure 3.12 The multizone source surfaces painted in red of the flange

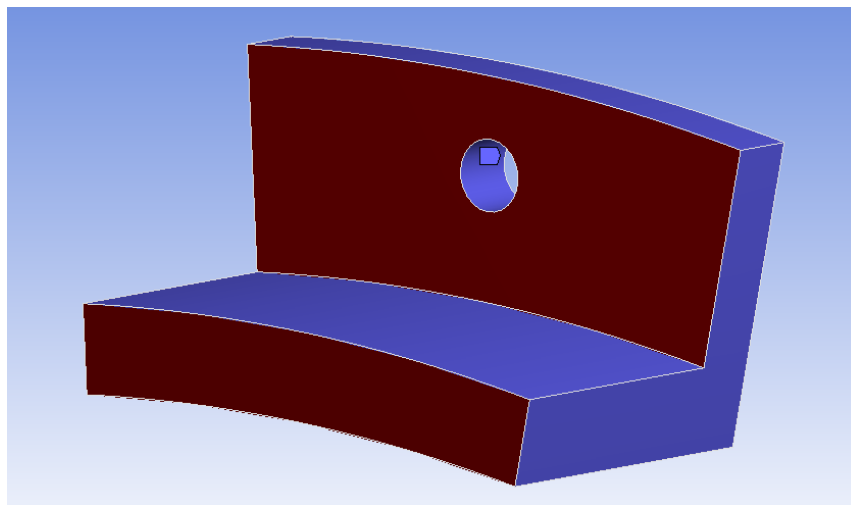


Figure 3.13 The opposite multizone source surfaces painted in red of the flange

Edge sizing is applied to the sectional flanges, by dividing the bolt hole circle into 24. The outer arcs, the inner arcs, and the lateral edges are meshed by specifying the edge sizing with maximum element size as 1.8 mm. The divided contours in yellow are seen in Figure 3.14.

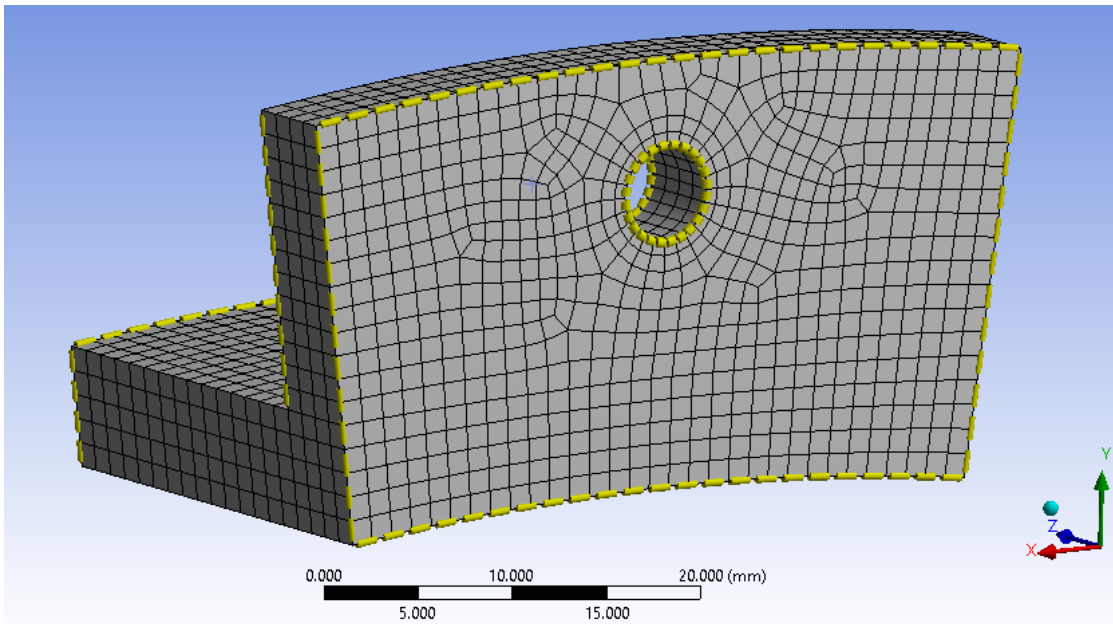


Figure 3.14 Edge sizing of the circular sector flange body with the mesh structure

### 3.1.4 Washer Geometry

The dimensions of the washer geometry are varied as the bolt size changes in the parametric analyses. By referring to [24], the washer thickness is taken as  $0.2d$ , the inner hole diameter of the washer is  $1.1d$  and the outer washer diameter is taken as  $2d$  where  $d$  is nominal bolt thread pitch diameter.

The trial analyses before the main study have revealed that the convergence problems occur between flange-washer contact when the washer is meshed with hexahedral elements without the mid-side nodes. After making troubleshooting operations, the problematic node was found on the washer contact interface. Therefore, the hexahedral elements containing mid-side nodes are used only in the washers to resolve the convergence problem.

In order to ensure that the hexahedral elements are located smoothly on the washers, the inner and the outer edges of the washers are divided into 24 equal segments in meshing by applying the edge sizing as shown in Figure 3.15.

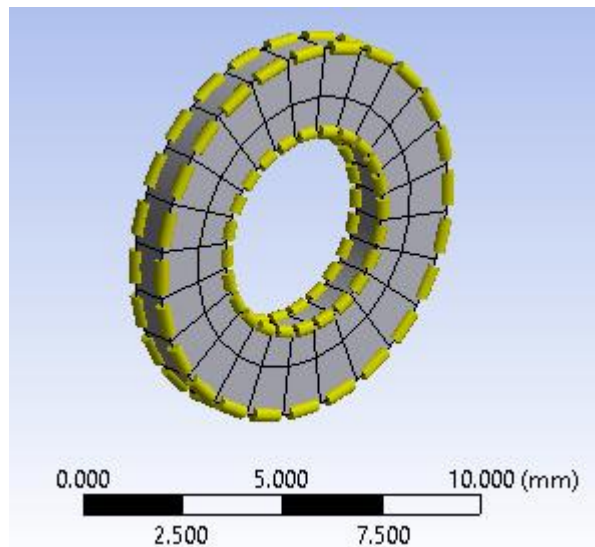


Figure 3.15 Edge sizing of the washer

### 3.1.5 Mesh Quality

A mesh metric called “element quality” is an indicator of the quality of the mesh distribution in ANSYS [7]. The element quality value is the ratio of the real element volume to the perfect element volume formed by the edge length of that element. A value of “1” indicates a perfect cube for a hexahedral element while “0” means zero volume [11]. Generally, the finer the mesh size is, the higher the mesh quality is. In this study, the average mesh quality of the final finite element analysis model with nominal parameter values is 0.977 indicating very high quality meshed structure model.

### 3.2 Material and Contact Details

The materials for all the parts and the specifications are listed in Table 3.2 and Table 3.3. Material properties used in the FE analysis are taken from ANSYS Engineering Data library [7].

Table 3.2 Material properties used in the analysis model [7]

<b>MATERIAL PROPERTIES</b>		
<b>Material</b>	<b>Young's Modulus (E), GPa</b>	<b>Poisson's Ratio (<math>\nu</math>)</b>
<b>Structural Steel</b>	200	0.3
<b>Aluminum Alloy</b>	71	0.33

Table 3.3 Materials of the components in analysis model

<b>MATERIALS OF THE PARTS</b>	
<b>Flange-1</b>	Aluminum Alloy
<b>Flange-2</b>	Aluminum Alloy
<b>Bolt-Nut Body</b>	Structural Steel
<b>Washer-1</b>	Structural Steel
<b>Washer-2</b>	Structural Steel

In the analysis model, two contact types are used. The first type is the frictional contact with the specific friction coefficient depending on the materials of the contact pairs. In Figure 3.16, the contacts 1, 2, 3, 4, and 5 are of this type. The latter type is the frictionless contact. In this contact type, the parts in contact act as frictionless supports against each other. The frictionless contact is used between the bolt body, including the threaded and the shank portions together, and the hole surfaces of the other parts through which the bolt body passes. It should be noted that although there are no permanent contacts between the bolt body and the other parts all the time since the holes are slightly bigger than the bolt diameter, the frictionless contacts are used in order to prevent probable interferences of the contact parts. All of the designated contact pairs shown in Figure 3.16 are presented with the part names, contact types, and the friction coefficients in Table 3.4.

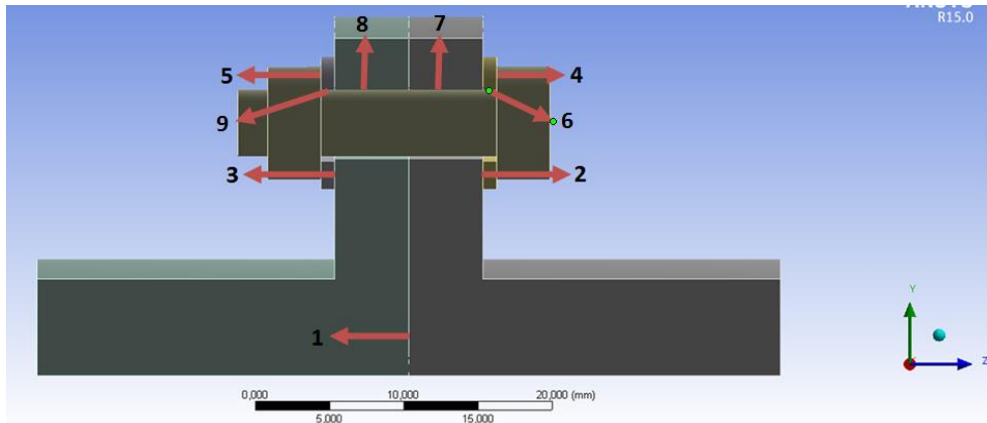


Figure 3.16 Representations of the contacts on the cross-sectional bolted flange connection view

Table 3.4 Contact details of the analysis model according to Figure 3.16

CONTACT DETAILS				
Contact No.	Contact Part-1	Contact Part-2	Contact Type	Static Friction Coefficient [26]
1	Flange-1	Flange-2	Frictional	1.20
2	Washer-1	Flange-1	Frictional	0.61
3	Flange-2	Washer-2	Frictional	0.61
4	Bolt-Nut	Washer-1	Frictional	0.74
5	Washer-2	Bolt-Nut	Frictional	0.74
6	Bolt-Nut	Washer-1	Frictionless	N/A
7	Bolt-Nut	Flange-1	Frictionless	N/A
8	Bolt-Nut	Flange-2	Frictionless	N/A
9	Bolt-Nut	Washer-2	Frictionless	N/A

All remaining settings related with the contacts such as penetration tolerance, contact stiffness, etc. are taken as the default settings of ANSYS in program controlled mode [7]. The contact formulation algorithm is Augmented Lagrange method while Gauss integration point is used as the contact detection method. The penetration tolerance in each contact is determined by the software.

### 3.3 Load and Boundary Conditions

The loading applied to flange-2 as the axial external force and the boundary conditions of the model are seen in Figure 3.17. There is a fixed support, in which all degree of freedoms are fixed, applied on the opposite surface on flange-1. The surface of flange-

2 in Figure 3.17, on which the force is applied, is fixed in radial and tangential directions. The lateral surfaces designated with 1 and 2 in Figure 3.18 for both flange-1 and flange-2 are constrained in the tangential direction. In flange-1 and flange-2, the surfaces of 3 and 4 are free surfaces. The terms,  $u_r$ ,  $u_\theta$  beyond each surface in figures indicate the boundary conditions of the related surfaces.

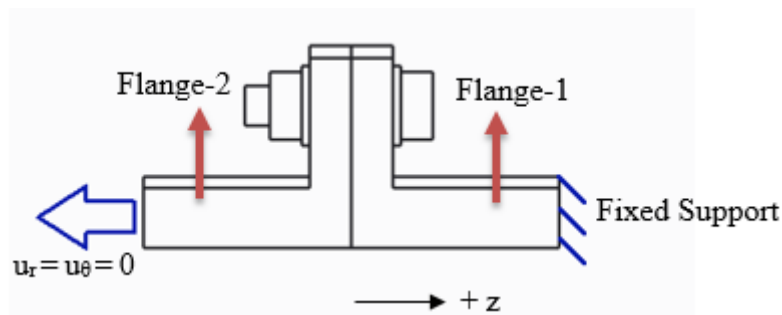


Figure 3.17 Load and boundary conditions; the fixed end on the right and the external force applied on the left

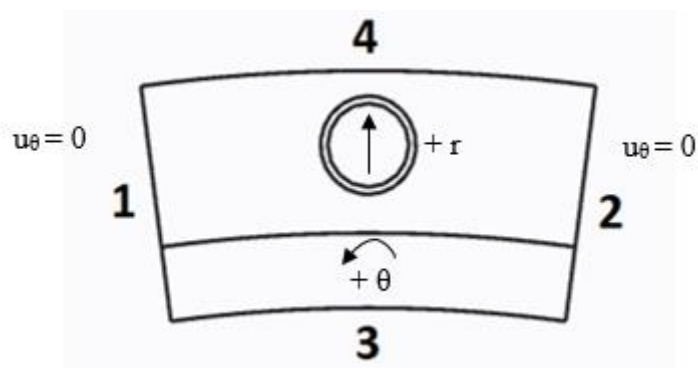


Figure 3.18 Load and boundary conditions: the designated lateral surfaces of the analysis geometry

### 3.4 Analysis Properties

The bolted flange connection loading in normal service conditions takes place in two successive steps. Firstly, all of the bolts are tightened with the required amount of torque to apply the bolt preload. Secondly, the loading conditions occur on the connection once the service begins. Therefore, the finite element analysis of bolted

flange connection must be performed in two steps as well. In the first step, the bolt pretension is applied and the axial external force is applied in the second step.

No thermal load or temperature changes have been previously specified in this study. However, if there were such a need in analysis, the number of solution steps could be increased from two to three or the thermal condition could be applied simultaneously with axial external load in two steps.

The FEM software makes several analysis settings available for user in order to control the analysis details. One of them is the auto time stepping option, which is a beneficial tool especially for nonlinear analyses [11]. In this option for the sub-steps of each step, “program controlled” mode has been selected in which the minimum number of sub-steps is one whereas the maximum is ten sub-steps for the nonlinear static structural analysis. In this mode, the software decides itself to divide the solution step into sub-steps within the stated limits depending on the convergence of the solution.

Initial analyses were performed including geometric nonlinearity, but the results showed that the maximum deformation value is rather small in comparison to the dimensions of the geometry. Hence, small deflection is assumed and the remaining analyses are performed utilizing small deflection assumption.

The nonlinear finite element analysis setup is solved by Newton-Raphson solution method as a default setting of the software.

### **3.5 Finite Element Solution of the Bolted Flange Connection**

In order to evade getting misleading results in the ANN training, finite element analysis of the bolted flange connection is evaluated by means of the average stress in a pre-defined contour in the flange instead of using the maximum stress values caused by the singularities or the stress concentrations. As observed in the preparatory analyses, high stress regions appear in the threaded and the shank portions for the bolt-nut single body while high stress area is observed on the matching faces of the flanges

close to the bolt holes. Figures 3.19 and 3.20 show the stress distributions in the flange and the bolt-nut body. The present study considers only the flange stress and the bolt load since the washers bear relatively low stresses. Figure 3.19 presents the most critical Von-Mises stress region in flange-1, which is around the bolt hole.

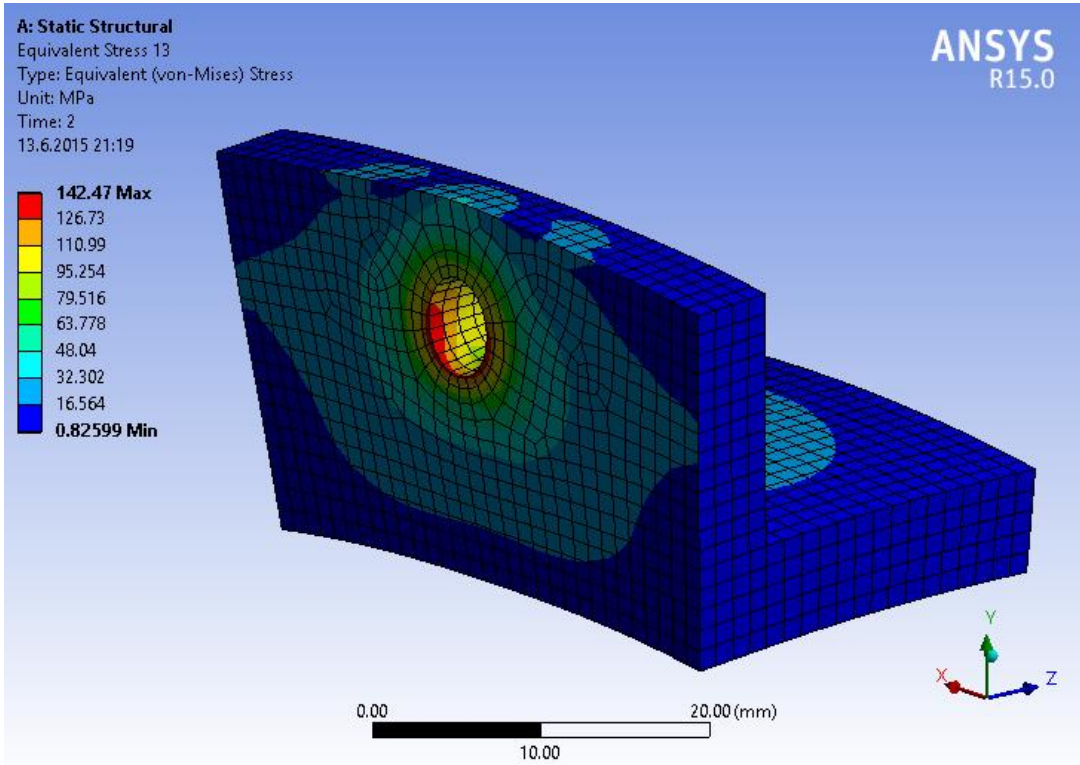


Figure 3.19 Equivalent Von Mises stress distribution in flange-1 with the maximum stress of 142.47 MPa

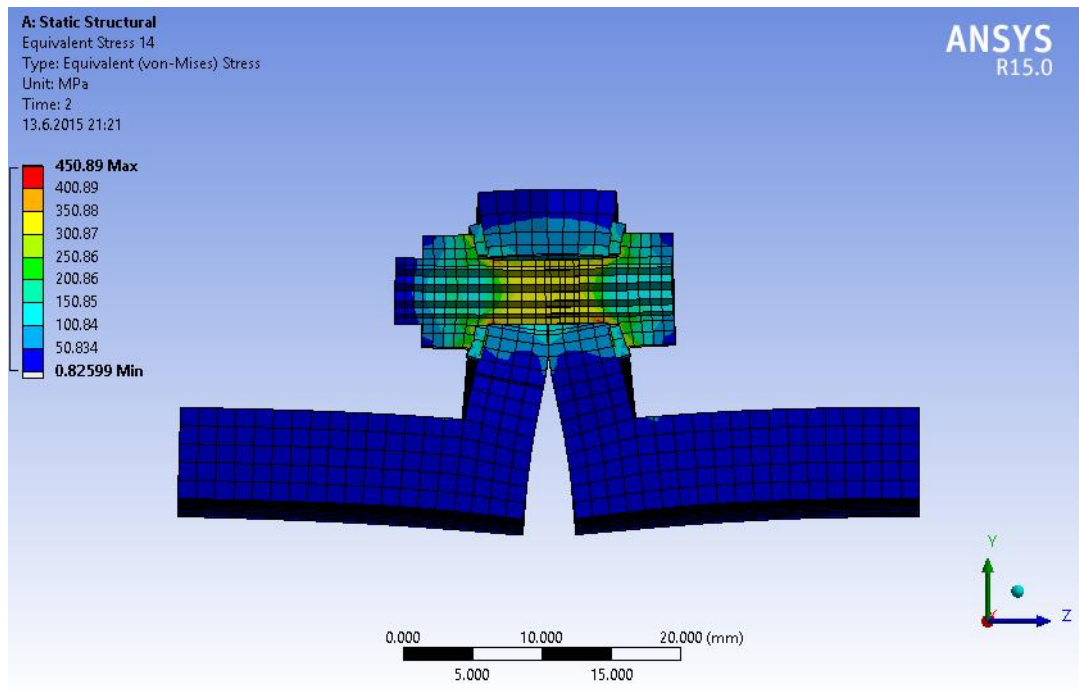


Figure 3.20 Equivalent Von Mises stress distribution inside the bolt with the maximum stress of 450.89 MPa (81X scaled, deformed body view)

There are two dominant stress sources effective on the high-stress region of the flange. The first source is the compression effect due to the bolt pretension. In Figure 3.21, z-axis stress tensor component distribution map in the cross-sectional view of the flange is given. The z-axis compressive normal stress is more effective than z-axis tensile normal stress in the final state after bolt pretension and external tensile force is applied. The portion of the flange compressed under the bolt head and the nut should be considered carefully. The second critical stress source is the tension existing on the flange surfaces in contact with the other flange and with the washer due to the bending moment formed by the axial external force. Figure 3.22 and 3.23 present the radial stress distribution maps. The critical radial stress region is observed around the bolt hole. The tensile normal radial stress is critical on the inner surface in contact with the other flange and the compressive stress is critical on the outer surface in contact with the washer. The equivalent stress in the flange is calculated by using Von Mises stress in the FE analysis.

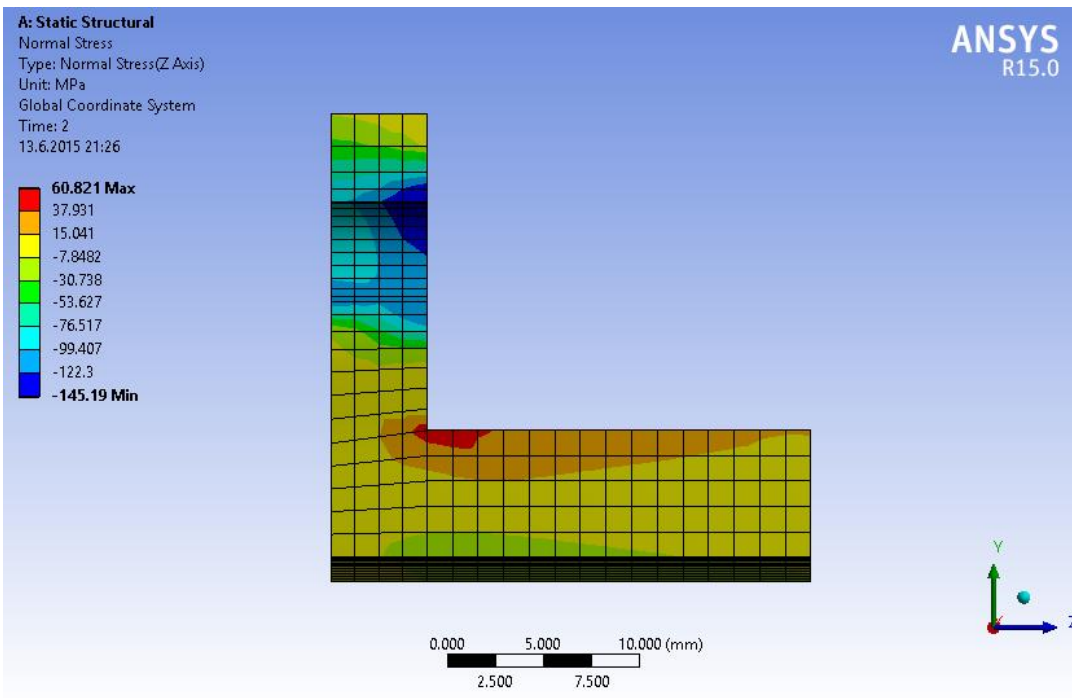


Figure 3.21 Z-axis (axial) normal stress distribution map in flange-1 cross section under bolt pretension and axial external tensile force (undeformed body view)

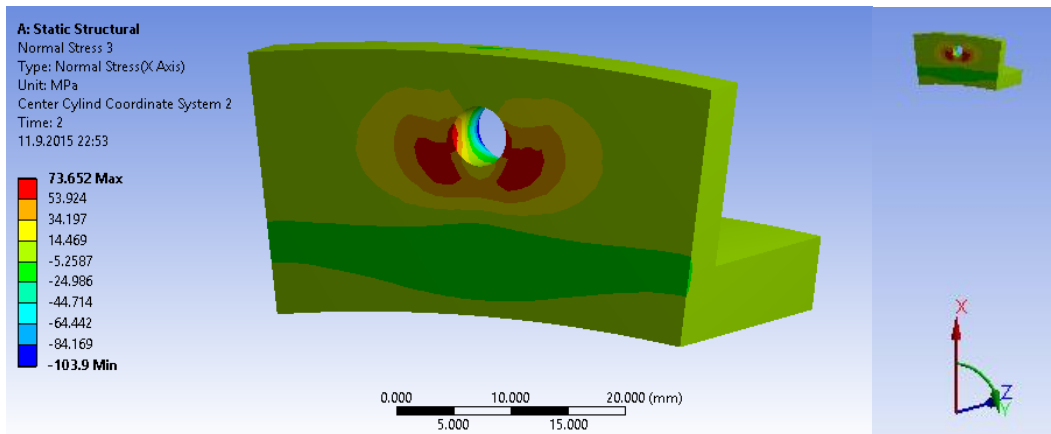


Figure 3.22 Radial-axis (x) normal stress distribution map in flange-1 under bolt pretension and axial external tensile force (undeformed body view)

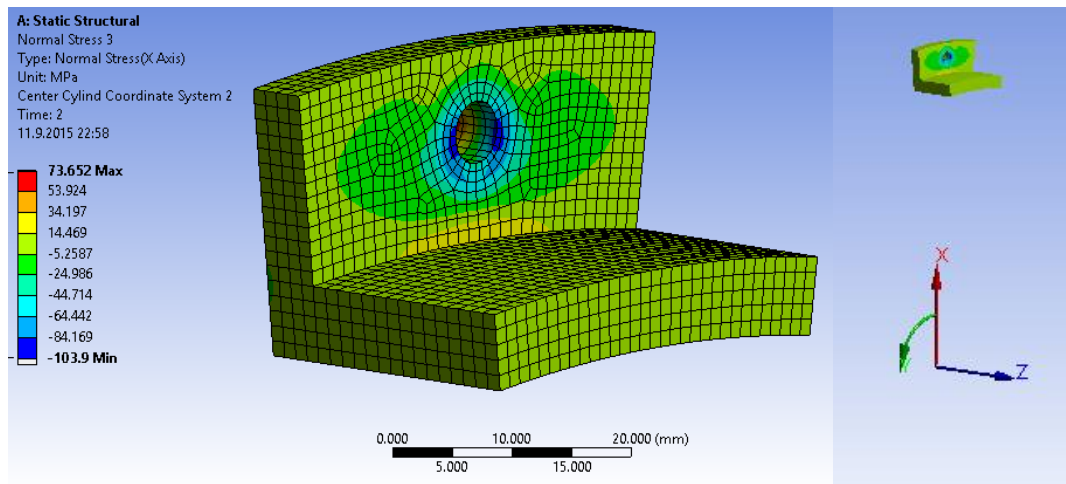


Figure 3.23 Radial-axis (x) normal stress distribution map in flange-1 under bolt pretension and axial external tensile force, the opposite view of Figure 3.22 (undeformed body view)

After deciding on the use of Von Mises equivalent stress for the evaluation of the structural integrity of the flange, the critical stress calculation point/region should be identified. One should realize that the selection of the flange stress location is critical since the output collection operation is automated. It can be claimed that using the maximum stress point value in the flange could be a solution. However, the maximum stress usually occurs in irrelevant, sharp edges or corners of geometry due to stress concentration effect. Using fixed data collection coordinates is also not a trustful solution since the analysis geometry changes during parametric study. When all aspects are considered, the idea of collecting the stress results in the flange from several specially defined points within the critical, high-stress region is turned out to be an applicable solution. In this respect, an average stress value of the high-stress region is obtained and the stress fluctuation risk is minimized. It should be noted that the data collection points have to vary simultaneously with the change of the flange geometry. Hence, the maximum flange stress is averaged across twelve data points on an imaginary circle whose pitch circle diameter varies with respect to the bolt size and location at the same time. If “d” is equal to the nominal bolt pitch diameter, the diameter of the imaginary data collection circle is formulated to be  $1.75d$ . In Figure 3.24, the data collection points are given. It should also be remembered that the flange stress is gathered from flange-1 because both parts are symmetric as well as having

almost symmetrical loads and boundary conditions. The contact status between flange-1 and flange-2 in the end of the analysis can be observed in Figure 3.25 in which the dark orange and the light orange painted regions imply the contacting surfaces of flange-1 and flange-2. Apparently, the smallest diameter inside the sticking and sliding region is about  $1.75d$  as seen in Figure 3.25. In theoretical solution method, the flange stress is calculated by taking an effective diameter inside the contact region, in which equal stress distribution is assumed inside the effective diameter for an axial load [4]. On the other hand, as one can realize by considering Figure 3.26, taking smaller stress collection circle causes the average stress results to increase greatly. For those reasons, the stress data collection circle is selected to be the one with the largest diameter, which is also inside the direct contact region.

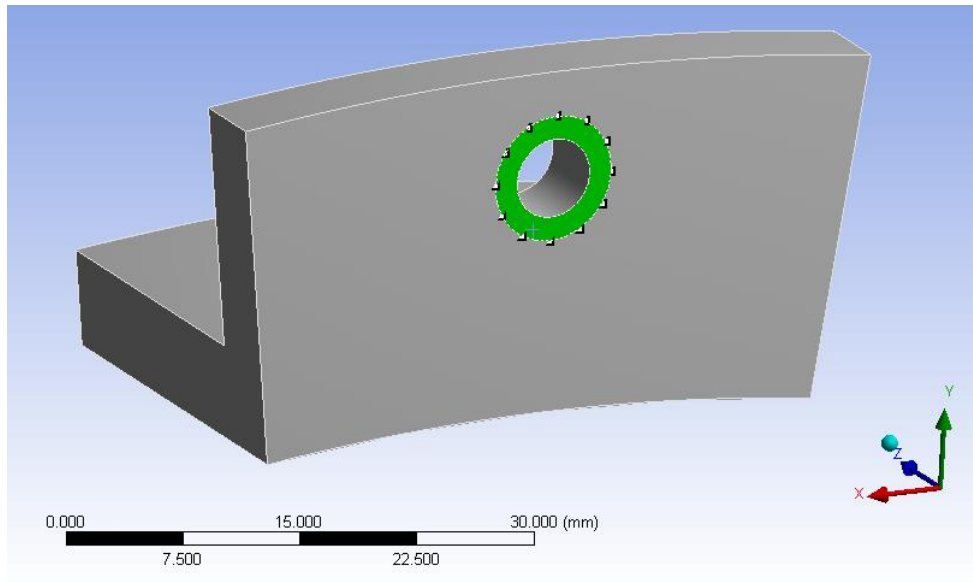


Figure 3.24 Equivalent Von Mises stress collection points on an imaginary circle of 1.75d in the flange geometry

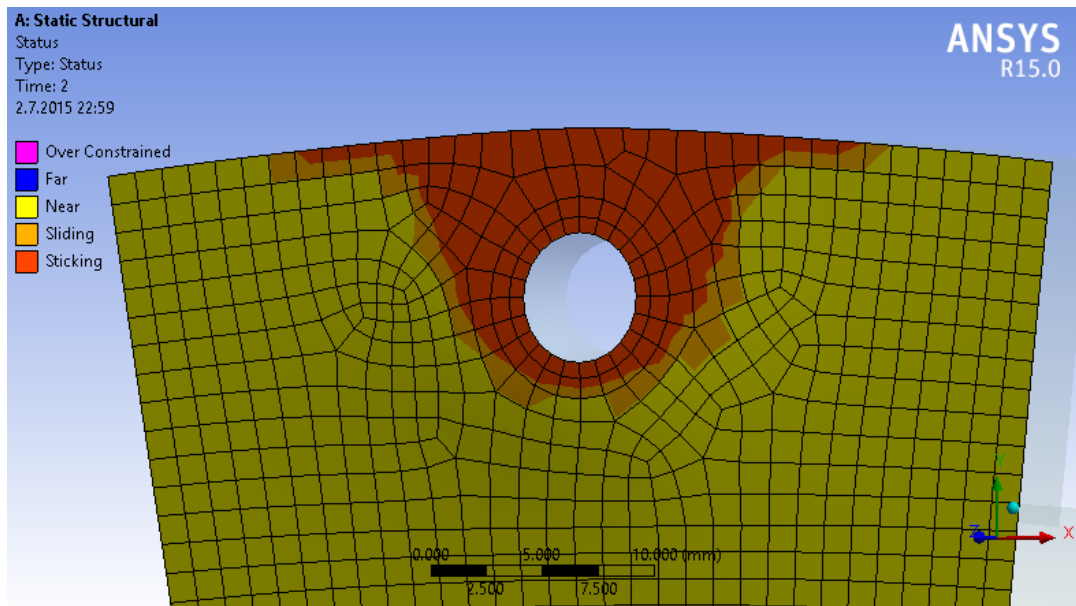


Figure 3.25 The contact status map for the contact between flange-1 and flange-2

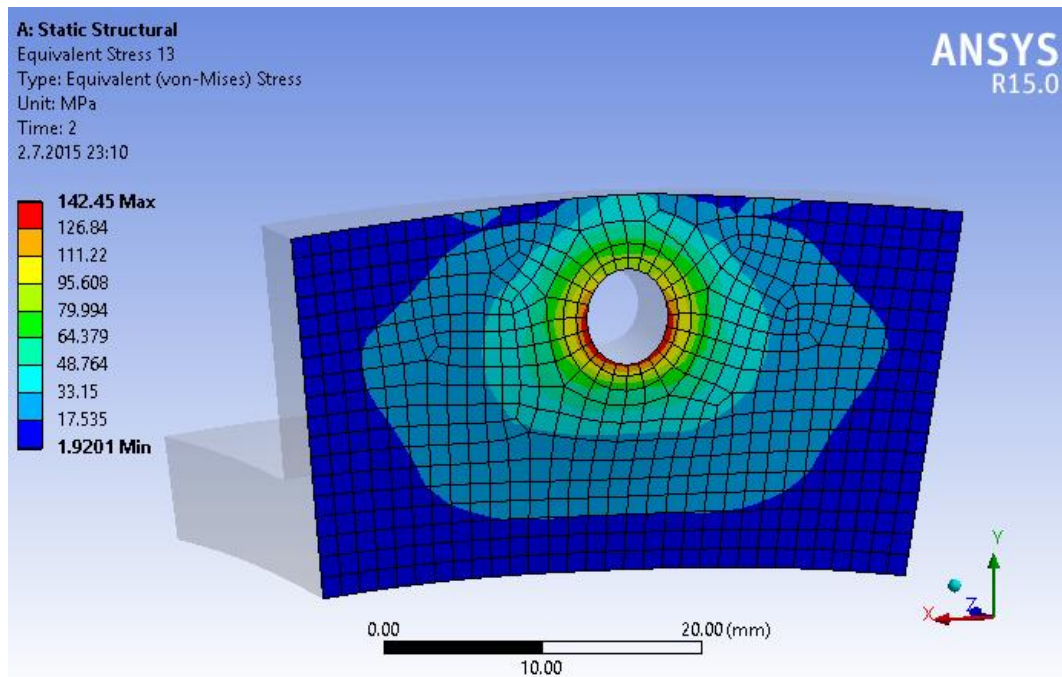


Figure 3.26 Equivalent Von Mises stress map for the contact surface between flange-1 and flange-2

For the same reason, the bolt stress result is calculated by dividing the reaction force occurring inside the shank portion of the bolt-nut body by the cross-sectional area of the bolt. As one can see in Figure 3.27, the heavily dominating component of the force reaction vector that occurs inside the bolt body is parallel to the bolt's internal axis (global z-axis). To exemplify, for the nominal arrangement of bolted flange FEM analysis model, z-component of the bolt force reaction ( $F_z$ ), is 5832.4 [N] whereas the x-component ( $F_x$ ) is 0.05 N and y-component ( $F_y$ ) is 1.17 N. Therefore, only the axial force reaction component is significant and this component of the reaction force is used to calculate the bolt stress. Subsequently, the bolt force reaction value is divided by the cross sectional area to calculate the bolt stress. Shigley [19] suggests using a tensile-stress area ( $A_t$ ) with the average of the pitch diameter ( $d_p$ ) (Equation 3.2) and the minor diameter ( $d_m$ ) (Equation 3.3). In this study, four different bolt diameters are used. Hence, four corresponding tensile-stress area values, tabulated in Table 3.5, are used during the bolt stress calculation in Equation 3.4.

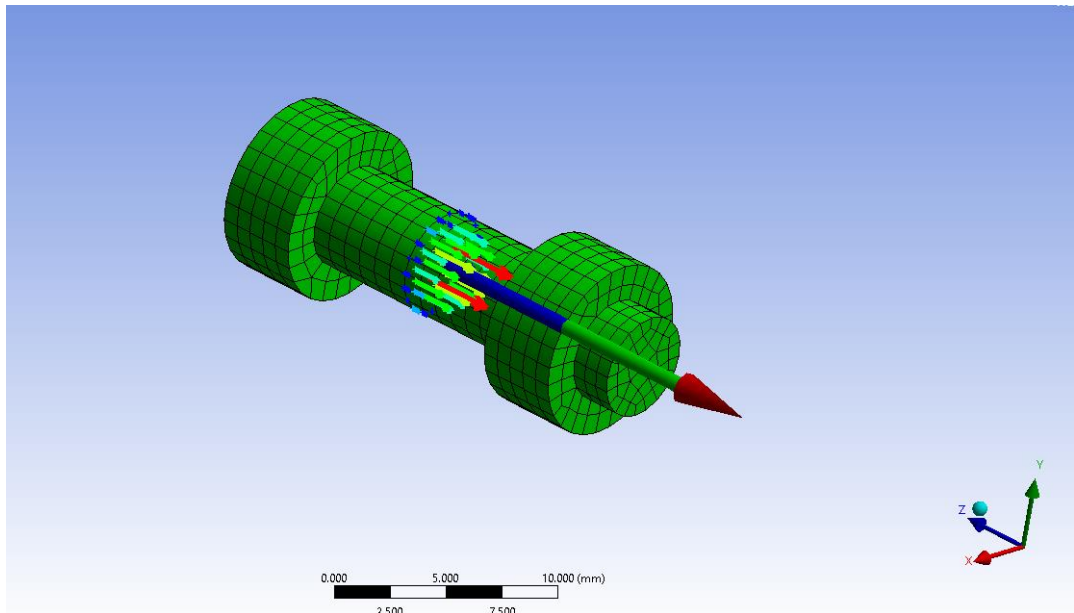


Figure 3.27 Resultant force reaction of 5832.4 N that occurs inside the bolt body when crossed orthogonally by a plane

$$d_m = d - 1.226869p \quad (3.2)$$

$$d_p = d - 0.649519p \quad (3.3)$$

$$\sigma_b = \frac{F_z}{A_t} \quad (3.4)$$

Table 3.5 The corresponding tensile stress area values for each bolt type

<b>BOLT TENSILE STRESS AREAS</b>		
<b>Nominal Bolt Diameter (d), mm</b>	<b>Pitch (p), mm</b>	<b>Tensile Stress Area (A<sub>t</sub>), mm<sup>2</sup></b>
4	0.7	8.78
4.166 (UNC-6)	0.79	9.03
4.83 (UNC-8)	0.79	11.29
5	0.8	14.2

### 3.6 Case Studies

One can be sure of the reliability of all the setting decisions made in the final model. In order to compare the analysis options and prove that the final analysis model bears

trustworthy force reaction and stress results, a few critical settings are examined by means of test analyses given in this section.

One should remember that the intention of the study is to use computational sources as efficiently as possible without compromising accuracy. Therefore, the elapsed time periods of all case studies are also measured. All of the test analyses for the case studies are performed in a computer which has Intel i7-3630QM 2.4 GHz CPU (with quad cores) and 8GB RAM memory. During the analyses, parallel processing with four cores are also employed.

### **3.6.1 Comparison of Mesh Sizes**

Mesh size is critical in finite element analysis because there is usually a compromise between the mesh size (consequently, accuracy of the results) and the computation time. Hence, the optimum mesh size for the parametric analysis must be determined so that the computational resources are used efficiently and reliable results are obtained as well. To illustrate, elapsed time for an analysis increases severely as the number of elements and the number of nodes used multiply in number. Thus, the mesh size determination process is essential to work efficiently. Table 3.6 presents five different analyses with different mesh sizes. The coarse-meshed analysis comprises 1582 elements and 2952 nodes while the numbers of the elements and the nodes increase until very-fine-meshed analysis in which there are 40471 elements and 50266 nodes. Five different analysis samples are examined in terms of the computational time requirement under the same conditions, the average Von Mises flange stress, the bolt force reaction occurring inside the bolt body. It should be noted that computational time, average Von Mises flange stress and the bolt force reaction are directly effective on the results of the ANN based flange tool and the computational power requirement of several parametric analysis to be run. When the average Von Mises flange stress values are considered, the second, third, and fifth cases are very close to each other numerically. By taking the flange stress obtained by very fine mesh (80.04 MPa) as the nominal value, the stress in the coarse mesh analysis is 3.0 % more than this value while the difference is -2.3 % for the fine mesh sizes. The numerical

variations between the cases of medium, medium-fine, and very fine mesh sizes are about 1 %, which makes three of the mesh sizes acceptable for the calculation of the average flange stress. Secondly, the nominal value of the bolt reaction force load can be taken in somewhere close to 5837 N. In this respect, the coarse meshed analysis, that is supposed to be the worst case among all, produces 0.4 % deviation from the nominal value. Accordingly, all of the mesh sizes are acceptable for the bolt load results. Lastly, the maximum total deformation value appears to be around 0.0468-0.0489 [mm]. In the medium-fine, fine, and very fine meshed analyses, the results are very close to each other (the maximum deviation is around 2 %). In the coarse and medium size meshed analyses, slightly higher deviation is obtained compared to the finest mesh case. Another point to be inspected is the average element qualities. The picture is the same as with the previous situation since the last three mesh size cases have very high element qualities. Last but not least, the elapsed time for each case hugely differs. It takes 14 seconds to finish an analysis in the coarse meshed model whereas the required time drastically increases to 293 seconds for the finest mesh case in the same computer. In the present study, after evaluating all aspects, the medium-fine mesh size with 11302 hexahedral elements and 15608 nodes is considered to be the optimum mesh size for all parametric analyses considering the reliability of the output and the computational power requirement.

Table 3.6 The comparison of five different mesh sizes in analyses

<b>COMPARISON OF MESH SIZES</b>							
<b>Mesh Size</b>	<b>The Numb. of Elements</b>	<b>The Numb. of Nodes</b>	<b>Avg. Elem. Quality</b>	<b>Elaps. Time, sec</b>	<b>Avg. Flange Stress, MPa</b>	<b>Bolt Reaction Force, N</b>	<b>Max. Total Deform. in Model, mm</b>
<b>Coarse mesh</b>	1582	2952	0.828	14	82.41	5814.36	0.0468
<b>Medium mesh</b>	4684	8470	0.894	29	79.14	5834.24	0.0469
<b>Medium-fine mesh</b>	11302	15608	0.977	71	79.69	5832.45	0.0483
<b>Fine mesh</b>	24261	30693	0.954	121	78.17	5829.73	0.0479
<b>Very fine mesh</b>	40471	50266	0.97	293	80.04	5837.26	0.0489

### 3.6.2 Comparison of Meshes with Linear and Quadratic Elements

A case study is performed to investigate the need for the mid-side nodes in meshing by conducting three separate analysis. The analysis with no mid-side node (linear elements) mesh in the finite element model, the analysis with mid-side nodes (quadratic elements) only in the washers (actual case), and the analysis with full of mid-side nodes in the finite element model are the three case studies. These results for the three case studies are given in Table 3.7. The first two columns in Table 3.7 give the two major output results of the parametric analysis with respect to the mesh types. The elapsed time for the completion of single analysis is listed in the third column. Lastly, the number of nodes in each analysis model is given in the fourth column. One should pay attention that all meshing options in this case study give almost the same average Von Mises flange stress and the bolt reaction. The maximum deviation obtained in the average flange stress is 0.57 % between the full mid-side nodes case and the finite element model without mid-side nodes. When the results of bolt reaction forces are checked, the difference is about 0.03 %, which is an insignificant deviation. Although the finite element model with full of mid-side nodes offers slightly better

approximation, utilization of the meshing with no mid-side nodes gives reliable results. In addition, if the analysis with full of mid-side nodes is compared with the analysis in which no mid-side nodes exist, the number of nodes contained is about almost four times and the time requirement is more than two times. Obviously, Table 3.7 proves that the use of meshes with full of elements containing mid-side nodes would be a waste of computational power since 0.57 percent stress deviation does not impose critical difference when the safety margin in the design is considered. As a result, the mesh type with only washer mid-side nodes is preferred in the FE analyses. As explained before, mid-side nodes are used in the finite element mesh of the washer to overcome the detected chronic convergence problems during initial analyses.

Table 3.7 The effect of mid-side nodes on the analysis results

<b>COMPARISON OF MESHES WITH AND WITHOUT MID-SIDE NODES</b>				
<b>Mesh Type</b>	<b>Avg. Flange Stress, MPa</b>	<b>Bolt Reaction Force, N</b>	<b>Elapsed Time, sec</b>	<b>The number of Nodes</b>
<b>Without mid-side nodes</b>	79.67	5833.05	44.00	14959
<b>With only washer mid-side nodes</b>	79.71	5832.24	50.00	15583
<b>With full of mid-side nodes</b>	80.13	5834.17	105.00	55909

### 3.6.3 Comparison of Small Deflection and Large Deflection Analysis

The next case study has been conducted to understand the effect and the necessity of the large deflection behavior in the parametric analyses. Table 3.8 gives the results of the analysis with small deflection and large deflection behavior. Apparently, all of the results including the average Von Mises flange stress, the bolt reaction force, and the maximum total deformation in model are almost exactly the same but the elapsed time to finish the analyses under the same computational power is 41% more in the analysis with the large deflection behavior. Therefore, based on the results of large and small deflection analysis, all of the analysis is conducted by assuming small deflection assumption in the rest of the study.

Table 3.8 The comparison of the large deflection behavior and the small deflection behavior in the analysis model

<b>COMPARISON OF LARGE DEFLECTION ON AND OFF</b>				
<b>Deflection Type</b>	<b>Avg. Flange Stress, MPa</b>	<b>Bolt Reaction Force, N</b>	<b>Max. Total Deformation, mm</b>	<b>Elapsed Time, sec</b>
<b>Large deflection off</b>	79.71	5832.24	0.0482	49.00
<b>Large deflection on</b>	79.72	5830.55	0.0482	69.00

### 3.6.4 Comparison of Effective Bolt and Nut Diameter on the Results

As explained before, the effective diameter of the hexagonal bolt head and the nut (the bolt head and the nut are assumed to have the same size hexagon) varies between 1.66d for M5 and 1.81d for M4 bolt thread sizes. It is seen that the average flange stress increases as the effective diameter decreases as seen in Table 3.9. Therefore, 1.7d is taken as the effective diameter for the bolt head and the nut since this size is within the limits and closer to the lower diameter limit (higher average flange stress). If 80.4 MPa stress (corresponding stress of 1.66d diameter) is taken as nominal, the deviation with 79.69 MPa (corresponding stress of 1.7d diameter) is only 0.87 % which is admissible.

Table 3.9 The comparison of the effect of effective bolt diameter size on the results

<b>COMPARISON OF THE EFFECTIVE BOLT AND NUT DIAMETER</b>		
<b>Effective Diameter Ratio</b>	<b>Bolt Reaction Force, N</b>	<b>Avg. Flange Stress, MPa</b>
<b>1.66d</b>	5829.92	80.4
<b>1.7d</b>	5832.45	79.69
<b>1.81d</b>	5837.81	77.94

## CHAPTER 4

### PARAMETERS CORRELATION STUDY

The problem of limited sources makes the user to judge the sensitivities of input parameters on output. In return, the number of intervals imposed for each input parameter is determined in a parametric study. In other words, the most effective input parameters should have more input values whereas less input points should be allocated for the weaker input parameters. The evaluation of the parametric sensitivities are evaluated with parameters correlation study.

#### 4.1 Theory

ANSYS Workbench [7] software has the toolbox named as DesignXplorer for some certain optimization objectives. The toolbox works on the basis of deterministic model [11]. On the contrary to probabilistic model, no randomness is allowed in deterministic approach and one always gets the same output for a specific input. Therefore, the toolbox can present accurate results depending on the quantity and quality of the input data.

DesignXplorer toolbox comprises of five different optimization tools aimed at separate purposes. One of the tools is “parameters correlation” which is heavily used in this study. Parameters correlation is served as a tool to reveal the relation between pre-defined parameters of the parametric study as its name suggests. The tool can be utilized to discover the effect of input parameters by analyzing the relative weights of the input parameters for each output parameter.

In a parameters correlation study, there are two commonly used linear correlation types: Pearson and Spearman correlations. The Pearson correlation has actually a full name of Pearson Product Moment Correlation and is also known as linear correlation. The technique employs an equation to relate two numerical data sets (variables) to

each other [34]. The result of this method gives the linear correlation between two data sets and it takes numerical values ranging from “-1” to “1” indicating negative and positive relations. Zero-value signifies the no-connection condition between two numerical sets in Pearson correlation [34]. Spearman’s rank correlation coefficient is one of the most commonly preferred nonparametric statistical technique [33] and it evaluates the strength of the correlation between two parameters by comparing with a monotonic function. In other words, if there is a perfectly monotonic increasing trend between parameters, the Spearman correlation result is “+1”. On the other hand, the relation between two parameters are perfect monotonic with inverse proportional behavior, the Spearman correlation result is “-1”. Zero value again indicates no relation between them [32]. The method is better in identifying non-linear, monotonic relationships and less restrictive in comparison to linear methods [11]. Hence, Spearman correlation method is selected in this study because of having non-linear analysis model. In both Pearson correlation and Spearman’s rank correlation techniques, the values changing from 0.5 to 1 are the sign of highly proportional relations while the values in between -0.5 to -1 denote strong inverse-proportional relations between two data sets [32, 34].

To express better, two data sets and their Spearman’s rank correlation is considered in Table 4.1. Set-1 and set-2 consist of three randomly selected elements. Rank-1 is created by giving corresponding numbers starting from 1 for the smallest element to 3 for the largest element in the increasing order considering the sequence of the elements’ numerical values. In the same way, rank of the set-2 is also formed (rank-2) in consideration to the element numerical value sequence. “ $d$ ” is the difference of rank-1 and rank-2. In the last column of Table 4.1 shows square of  $d$ . The Spearman’s rank correlation is represented by Equation 4.1, in which “ $n$ ” is the number of samples in each set ( $n = 3$  in this example) and “ $r$ ” is the correlation coefficient of set-1 and set-2.

Table 4.1 Sample problem data of Spearman's rank correlation

Set-1	Set-2	Rank-1	Rank-2	d	d <sup>2</sup>
7	4	2	1	1	1
6	15	1	3	-2	4
11	5	3	2	1	1

$$r = 1 - \left( \frac{6 \cdot \sum d^2}{n(n^2 - 1)} \right) \quad (4.1)$$

$$r = -0.5 \quad (4.2)$$

The results of the parametric study are exhibited in different forms by parameters correlation tool in ANSYS. The first type is correlation matrix. There are two options to exhibit the results of the correlation matrix. Correlation matrix with numerical values and its visual chart form expressing the same relation are the two options available. Correlation matrix explains linear correlation between each input-output pair. In matrix form, the values towards “1” indicate increasing linearity while the values approaching “-1” are interpreted as inversely linear relations. In other words, the coefficients in the correlation matrix are the indicators of the correlation direction and the grade. In the same way, the visual chart expresses the same relations with colors. In the second form, the same linear relationships are shown as bar or pie chart for each output parameter separately so that the global effects of input parameters on a specific output can be compared easily. In the sensitivities chart, correlation matrix is displayed for each output parameter separately.

## 4.2 Method

Development of bolted flange design tool is based on the FEM analysis database of 13500 analyses. If the total number of analyses is limited due to computational power, determination of the number of input values for each parameter is very crucial. If the number of input values for each parameter is increased, then total number of finite element analysis increases significantly because total number of analysis is obtained by the product of the number of input values of each parameter.

In this study, apart from the main parametric study to create the database, parametric analyses performed are to investigate the sensitivities of input parameters on the output and to compare them with each other to decide on the number of input values to be used for the main parametric analyses. In ANSYS Workbench under the “DesignXplorer” toolbox “Parameters Correlation” tool that exists is used for the purpose of determining the parameter sensitivities. The correlation strengths between the input and the output parameters are displayed both visually and numerically.

As stated in previous section, there are seven input parameters, five of which are geometric variables and the remaining ones are the loading variables. Without doubt, the loading variables have direct effect on the force and the stress results on the bolt and the flanges. However, the difficulty is to determine the sensitivities of the geometric variables due to the fact that the geometric variables do not have obvious linear effects on the output, rather they affect the equivalent flange and the equivalent bolt stiffness values. Since the theoretical approach for the calculation of the stiffness values are mostly based on the assumptions, the actual effects of the geometric input parameters on the output results are not clearly disclosed. Consequently, the parametric analysis study with parameters correlation is conducted for the geometric variables. Thus, the sensitivities of the geometric input variables on the output results are compared with each other to make a correct decision about the number of input intervals for each geometric design variable.

Parameters correlation study comprises certain steps. Firstly, the geometric variables of the bolted flange connection and the loading input containing the bolt pretension and the axial external force are defined with the nominal values. The parametric input values in each parametric set consisting of 100 FE analyses are specifically determined by ANSYS algorithms so that the selected input values are evenly distributed within the pre-defined lower and upper limits of the input parameters [11]. The sample generation algorithm prevents the overlaps of the input values while selecting the samples for correlations [11]. The values are transferred to ANSYS DesignModeler toolbox [7] to create 3D FEM analysis geometry. In the next step, the

created analysis geometry with respect to the selected sample points is sent to static structural FEM analysis. Here, the meshing operation of the parts is made consistent with the predefined meshing settings and the analysis is performed in the end. These steps are repeated in an automated way until one hundred analyses are finished to form a parametric set for the parameters correlation study. Once the parametric set is ready, parameters correlation study can be performed to understand the relation between the selected input parameters and the output. One can see the flowchart of the parameters correlation study procedure in Figure 4.1.

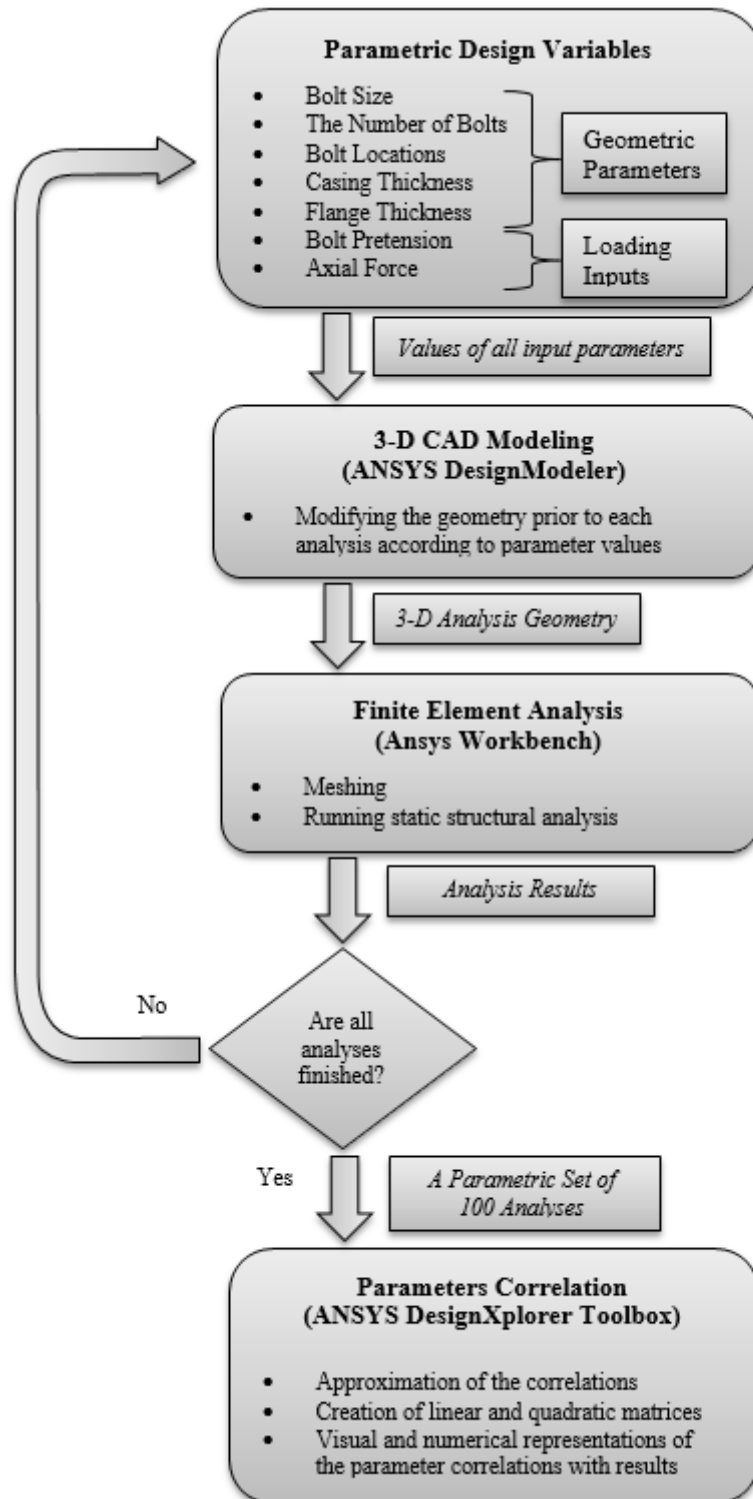


Figure 4.1 Flowchart of the parameters correlation study for a single parametric set

The parametric study consists of one main analysis set and additional eight more sets for the validation purpose, total of nine parametric analysis sets. Each of the analysis sets contains one hundred FEM analyses and each set is built up around nominal design values of the input. In each set, loading input variables, namely, axial external force applied from both end surfaces of the casing extensions and the bolt pretension are kept constant while all of five geometric input variables are assigned different values between the upper and the lower limits of the design variables in each analysis. All of the geometric input variables are seen in Figure 4.2, and Table 4.2 shows the nominal design values of seven inputs as well as the upper and lower limits of all. The nominal input values for the sample bolted flange design are specified by considering a medium-size aircraft engine as mentioned in the beginning of the study [23]. Parameter B (the number of bolts) is determined to be in between the one less and one more of the nominal value. For the variables D (casing thickness), E (flange thickness), upper and lower bounds are determined to be approximately ten percent more and ten percent less than the nominal values. In other words, these variables are located in twenty-percent bands. Parameter A (bolt size) is also thought to be in a twenty percent band as well. The nominal diameter, A, is 4.83 mm (0.19 inch) since the standard bolt sizes (either metric or inch) are used in this study. It should be noted that the variables A and B have discrete values whereas the others are continuous parameters. The upper and lower bounds of the parameter C (bolt location distance) are naturally determined by the geometry itself. That is, inner and outer radii of the flange geometry, parameter D (casing thickness), the washer diameter (directly dependent on the bolt size, A) establish the limits. Finally, the loading variable of axial force per bolt is settled in limits of -20 % and +20 % around its nominal value. One should realize that axial force variable indicates loading for only single bolt. Therefore, the number of bolts used (parameter B) changes regardless of the axial load per each bolt. In other words, the value of axial load per each bolt does not depend on the number of total bolts. The second loading input variable, bolt pretension, is taken with the limits located -30 % and +30 % around the nominal value.

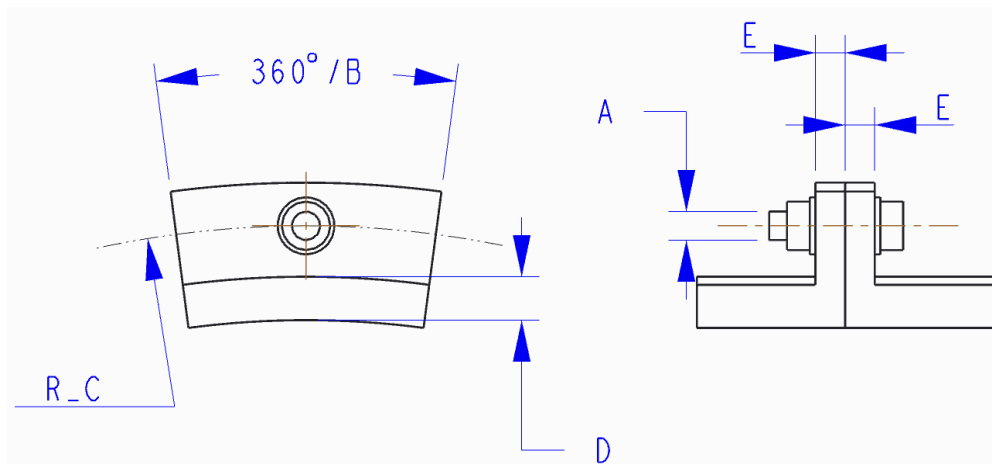


Figure 4.2 The geometric input parameters of the analysis model

Table 4.2 The nominal values, upper and lower limits of all input parameters

Input Variable	Explanation	Nominal	Lower	Upper
<b>A</b>	Bolt Size	4.83 mm	4 mm	5 mm
<b>B</b>	The Number of Bolts	24 pcs	23 pcs	25 pcs
<b>C</b>	Bolt Location	167.75	164.5 mm	168.9 mm
<b>D</b>	Casing Thickness	6.6 mm	5.9 mm	7.3 mm
<b>E</b>	Flange Thickness	5 mm	4.5 mm	5.5 mm
<b>Axial Force per Bolt Pretension</b>	-	1280 N	1024 N	1536 N
	-	5702 N	3991 N	7413 N

Normally, the parameters correlation results are analyzed for single set of one-hundred analyses by keeping the axial force and the bolt pretension constant. To be on the safe side, the axial force and bolt pretension parameters are also intended to be crossed with their three different values (nominal, upper limit, and lower limit values of each) so that the effect of having different constant loading values on the geometric parameter correlation study could also be investigated. The main analysis set with nominal loading values is listed in the first row of Table 4.3. Eight supplementary parametric sets are also listed with the loading input parameters in Table 4.3. The expected result is to obtain approximately the same correlation strengths of the geometric parameters on the output parameters regardless of the loading conditions in all the sets.

Table 4.3 Bolt pretension and axial force values for each analysis set

<b>Design Analysis Set Number</b>	<b>Bolt Pretension, N</b>	<b>Axial Force per Bolt, N</b>
1	5702	1280
2	3991	1024
3	7413	1536
4	3991	1280
5	7413	1280
6	5702	1024
7	7413	1024
8	5702	1536
9	3991	1536

The static structural finite element analyses, which are allocated for parameters correlation, are evaluated by two main output results. The first one is the equivalent force reaction that occurs in the bolt body (threaded and shank portions are assumed to be single, continuous feature). The second output is the average Von- Mises flange stress. In the parameters correlation study, the output results considered for the evaluation of the correlation are the same as before.

### 4.3 Results of Parameters Correlations

Parameters correlation charts are set up after the completion of the first parametric set with one hundred analyses. Additionally, it is also aimed to examine whether any change occurs in the relative weights of five geometric parameters by trying distinct combinations of the constant axial force and the bolt pretension values in each different set with eight extra sets. It should be noted that one of the analyses with a special geometric parameters configuration in all parametric sets failed to converge. Hence, the graphs of all sets are constructed on the ninety-nine design points, and Spearman correlation technique is employed in all correlation analysis.

The graph given in Figure 4.3 is the correlation matrix visual chart which belongs to parametric set-1 in Table 4.3. In this visual correlation matrix, the correlations

between design parameters are represented with the colors indicating the strength levels. The red color means the highest proportional correlation of “1” between two variables while the blue color is the indicator for the highest inversely proportional relation between two parameters. The combination of any parameter with itself is always designated with the full red color, which means the direct relation of a parameter with itself. The rest of the colors are expressed in the color map of Figure 4.3. The visual correlation chart is useful to show the effect of the input parameters on the results at a glance. The locations of the parameters in the charts are not related with the importance level and are defined by the software. The same parameters are located in both the row and the column in the same sequence. According to Figure 4.3, the most effective input variable is the bolt location distance from the center axis (parameter C) with a strong linear correlation for the bolt force reaction result. The bolt size used (parameter A) has a weak, increasing effect whereas the casing thickness (parameter D) and the flange thickness (parameter E) display weak decreasing effect on the bolt reaction force. When the second output result, the average equivalent flange stress, is considered, the parameters A and C are remarkable. As the bolt size (parameter A) enlarges, the average flange stress diminishes. On the other hand, the increase in the bolt location distance (parameter C) increases the average flange stress. The number of bolts (parameter B) seems to have almost no effect on the results. However, one should pay attention that the changes in the number of bolts does not affect the corresponding portion of the axial external force applied to the whole flange. The axial force applied to the circular sector flange model is constant in the parameters correlation study. In other words, the change in the number of bolts used in the fully circular flange assembly only changes the angle of the flange sector arc. Table 4.4 is the numerical representation of the same linear correlation matrix. The correlation weight more than 0.5 or less than -0.5 are painted in red color in Table 4.4. If the correlations of the parameters with themselves or the correlations of the output parameters with each other are omitted, the remaining red cells are the critical ones designated with bold letters.

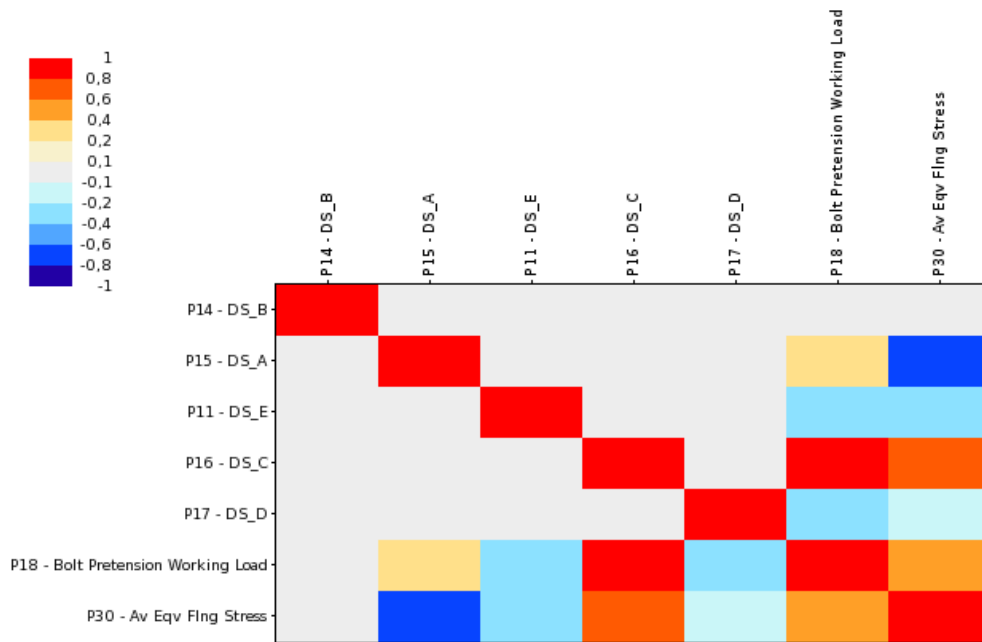


Figure 4.3 Visual chart of the correlation matrix of parametric set-1

Table 4.4 The correlation matrix of parametric set-1

<b>CORRELATION MATRIX (LINEAR)</b>							
<b>Parameters</b>	<b>B</b>	<b>A</b>	<b>E</b>	<b>C</b>	<b>D</b>	<b>Bolt Load</b>	<b>Avg. Flng. Stress</b>
<b>B</b>	1.000	-0.010	-0.009	0.003	0.018	0.089	-0.009
<b>A</b>	-0.010	1.000	0.001	0.012	-0.008	0.261	<b>-0.667</b>
<b>E</b>	-0.009	0.001	1.000	-0.010	-0.006	-0.316	-0.363
<b>C</b>	0.003	0.012	-0.010	1.000	0.004	<b>0.855</b>	<b>0.603</b>
<b>D</b>	0.018	-0.008	-0.006	0.004	1.000	-0.297	-0.143
<b>Bolt Load</b>	0.089	0.261	-0.316	<b>0.855</b>	-0.297	1.000	0.502
<b>Avg. Flng. Stress</b>	-0.009	<b>-0.667</b>	-0.363	<b>0.603</b>	-0.143	0.502	1.000

The correlation matrix results can also be evaluated by considering the sensitivities chart in Figure 4.4 since the sensitivities chart is another representation type of the correlation matrix in order to display the global sensitivities of output parameters [11]. The dominant design parameters on the output parameters explained above are clearly seen in the sensitivities chart.

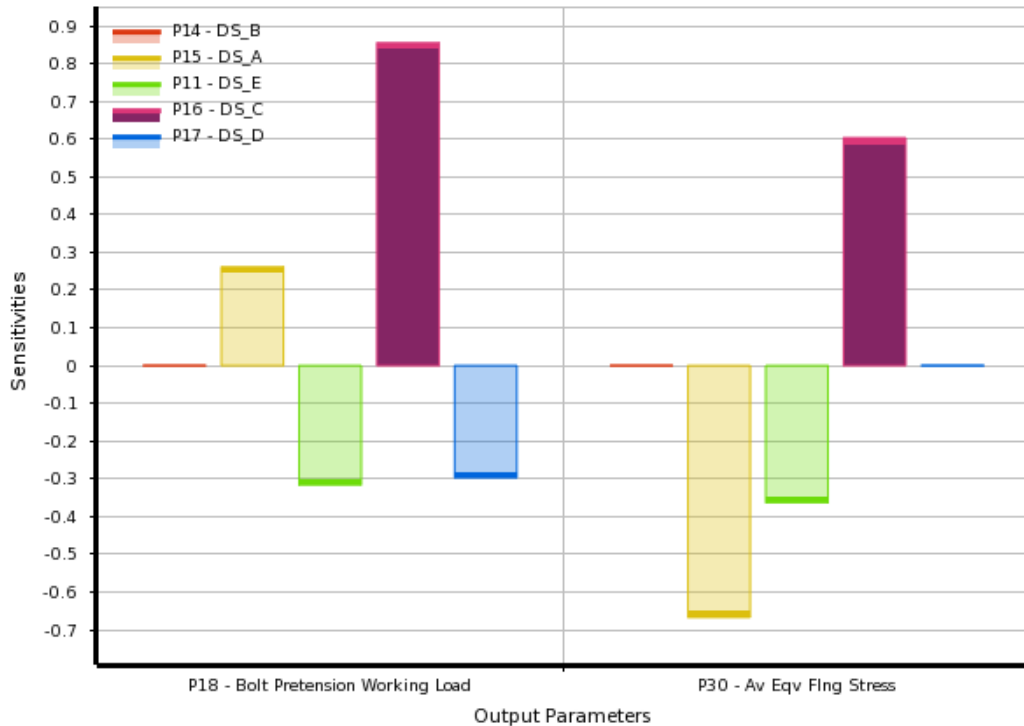


Figure 4.4 The sensitivities chart of parametric set-1

When the results of the correlation study for the main parametric set are examined, parameter C stands out as the most critical factor for the bolt load output. Parameters E and D exhibit relatively low relations on the bolt load. Parameter A has a slightly lower correlation with bolt load. Parameter B has almost no effect on the bolt load. On the other hand, parameters A and C together seem to have noteworthy effects on the average flange stress result. Parameter E comes in the third place in terms its effect on the average flange stress. Parameters B and D do not have profound effect on the average flange stress.

The results considered in Figures 4.3, 4.4 and Table 4.4 present that the bolt location (parameter C) has a very strong proportional impact on the bolt reaction force as well as on the average Von Mises flange stress. Therefore, parameter C is accepted to be the most critical geometric parameter in this study. Bolt size (parameter A) is the second crucial geometric parameter since it has strong inversely proportional effect on the average Von Mises flange stress output. The flange thickness (parameter E) is slightly more effective than the casing thickness (parameter D) on the output by

considering the coefficients. Finally, the number of bolts (parameter B) has almost no effect on the output when the first column of the correlation matrix is considered. One should pay attention that a portion of total axial external force is applied constantly to the structure throughout the parameters correlation study. Therefore, the change of the number of bolts affects only the angle of the circular sector while the applied force is always constant in this study. This is why parameter B looks ineffective here. In the final bolted flange design tool, the change in parameter B is going to directly affect the corresponding axial force on the sectional analysis geometry.

In the final step of the parameters correlation study, the significance of the geometric parameters are found to be in the following order:  $C > A > E > D > B$ .

The results of the parameters correlation study with a parametric set of 100 analyses are checked by repeating the study for the same parameters with a set of 200 analyses. It is seen that the parameters correlation study with 200 FE analyses gives almost the same correlation coefficients. Therefore, the importance levels of the geometric input parameters are sorted in the same order.

The number of values of the parameters to be used in building the ANN model are determined by considering the outcome of the parameters correlation study. Table 4.5 shows the number of input values for each design variable to be used in the parametric analysis as design points. Two load variables and one geometric parameter (parameter C, bolt location) are the most effective parameters on the output. Therefore, five design points are allocated to them. For the geometric parameters E, D, B, three design points are allocated as seen in Table 4.5. In the final parametric set, there are 13500 separate FE analyses when all of the input parameters are combined with each other.

Table 4.5 The input values for the input parameters to be used in the main parametric study

<b>Input Variable</b>	<b>Explanation</b>	<b># of Inputs</b>	<b>Input 1</b>	<b>Input 2</b>	<b>Input 3</b>	<b>Input 4</b>	<b>Input 5</b>
<b>A</b>	Bolt Size	<b>4</b>	4	4.2	4.826	5	-
<b>B</b>	The Number of Bolts	<b>3</b>	23	24	25	-	-
<b>C</b>	Bolt Location	<b>5</b>	164.5	165.6	166.7	167.75	168.9
<b>D</b>	Casing Thickness	<b>3</b>	5.9	6.6	7.3	-	-
<b>E</b>	Flange Thickness	<b>3</b>	4.5	5	5.5	-	-
<b>Axial Force per Bolt</b>	-	<b>5</b>	1024	1152	1280	1408	1536
<b>Bolt Pretension</b>	-	<b>5</b>	3991	4846.5	5702	6557.5	7413

The significance of the geometric input parameters and the corresponding input values are established in consideration to the correlation results of the first parametric set. The remaining eight parametric sets are also analyzed to verify the significance sequence of the geometric input parameters and reveal the effect of loading changes on the geometric input correlations. Table 4.6 lists the geometric input parameter correlations of each parametric set. It can be seen that the determined the sequence of the significance levels does not differ although there exist minor changes in the correlation values. Keeping the bolt pretension constant, the axial force increases in the order of parametric sets 6, 1, and 8 (constant bolt pretension of 5702 N); 2, 4, and 9 (constant bolt pretension of 4562 N); and 7, 5, and 3 (constant bolt pretension of 6842 N) as Table 4.3 shows. Similarly, keeping the axial force constant, the bolt pretension increases in the order of parametric sets 2, 6, and 7 (constant axial force of 1024 N); 4, 1, and 5 (constant axial force of 1280 N); and 9, 8, and 3 (constant axial force of 1536 N). When the parametric set results are compared with each other, it is judged that the increase in the axial force with constant bolt pretension intensifies the effect of parameter C on average flange stress.

Table 4.6 The correlation values for the remaining parametric sets as well as the main parametric set in reference to Table 4.3

<b>CORRELATION MATRIX RESULTS OF THE PARAMETRIC SETS</b>					
<b>Parameters</b>	<b>Bolt Load</b>	<b>Av. Flng. Stress</b>	<b>Parameters</b>	<b>Bolt Load</b>	<b>Av. Flng. Stress</b>
<b>Set 1</b>			<b>Set 6</b>		
<b>A</b>	0.26	-0.67	<b>A</b>	0.26	-0.72
<b>B</b>	0.09	-0.01	<b>B</b>	0.11	-0.02
<b>C</b>	0.86	0.60	<b>C</b>	0.86	0.49
<b>D</b>	-0.30	-0.14	<b>D</b>	-0.34	-0.18
<b>E</b>	-0.32	-0.36	<b>E</b>	-0.27	-0.35
<b>Set 2</b>			<b>Set 7</b>		
<b>A</b>	0.27	-0.59	<b>A</b>	0.18	-0.70
<b>B</b>	0.09	0.00	<b>B</b>	0.17	-0.01
<b>C</b>	0.86	0.66	<b>C</b>	0.86	0.55
<b>D</b>	-0.31	-0.18	<b>D</b>	-0.28	-0.12
<b>E</b>	-0.30	-0.38	<b>E</b>	-0.29	-0.40
<b>Set 3</b>			<b>Set 8</b>		
<b>A</b>	0.26	-0.68	<b>A</b>	0.26	-0.55
<b>B</b>	0.09	-0.02	<b>B</b>	0.08	0.01
<b>C</b>	0.85	0.59	<b>C</b>	0.86	0.68
<b>D</b>	-0.30	-0.12	<b>D</b>	-0.30	-0.19
<b>E</b>	-0.32	-0.38	<b>E</b>	-0.29	-0.39
<b>Set 4</b>			<b>Set 9</b>		
<b>A</b>	0.26	-0.46	<b>A</b>	0.26	-0.41
<b>B</b>	0.09	0.02	<b>B</b>	0.08	0.01
<b>C</b>	0.84	0.71	<b>C</b>	0.88	0.75
<b>D</b>	-0.30	-0.23	<b>D</b>	-0.30	-0.26
<b>E</b>	-0.25	-0.37	<b>E</b>	-0.24	-0.39
<b>Set 5</b>					
<b>A</b>	0.22	-0.72			
<b>B</b>	0.11	-0.02			
<b>C</b>	0.87	0.55			
<b>D</b>	-0.29	-0.12			
<b>E</b>	-0.30	-0.37			

## CHAPTER 5

### ARTIFICIAL NEURAL NETWORK APPROXIMATION

#### 5.1 Theory

Artificial neural networks are the computational structures with several computational cells to solve especially complex, non-linear or stochastic problems by employing simple, self-organizing algorithm. The artificial neural network (ANN) mechanism works on the principles of the biological nerve system (neural network) of human [29]. The characteristic properties are the capabilities of organizing, generalizing, classifying, and learning data [30].

The dynamic structure of the network is formed by a group of processing units called neurons, in which each neuron has connections with all of the neurons located in the previous and next layers with different weights defined in the training [18]. Figure 5.1 represents an ANN network structure. In this network, there are three input parameters taken from the input layer terminals and two output parameters sent through the output layer terminals. The hidden layer is formed by four processing neurons. Therefore, the structure of the ANN in Figure 5.1 is nominated as 3:4:2 architecture. Since the input and output layers can only transmit the data, the capability of an ANN is adjusted with the number of hidden layers and the number of neurons in each layer and this is a trial and error method [30]. Each neuron in a layer has connections with all the neurons located in the previous and the next layers. The strength of a connection between a specific neuron pair is known as “weight”. The weights are defined in the training operation.

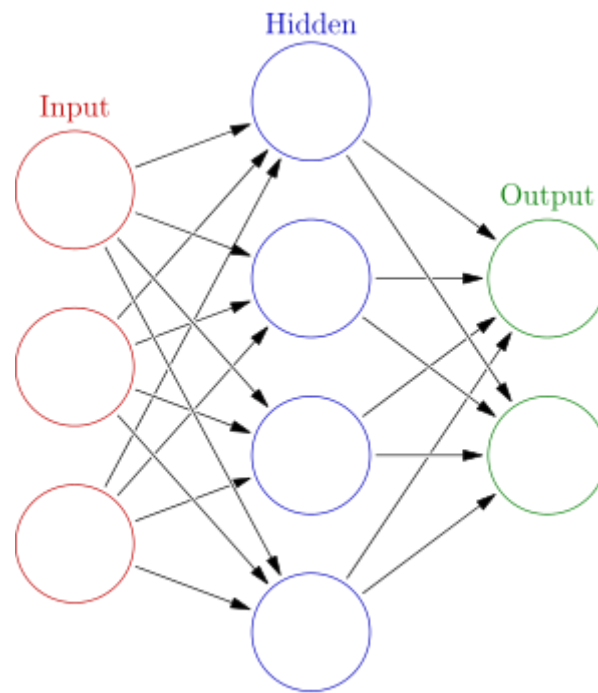


Figure 5.1 The structure of a sample ANN with three input and two output parameters

The training of artificial neural network operation is carried out in six phases which consist of creating the network, configuring the network, initializing the weights and biases, training the network, validating the network, and using the network in sequence [22].

In the neural network toolbox of Matlab, there are four main neural network tools. The first tool is “function fitting”. In this tool, it is possible to train neural networks in different architectures in order to fit any kind of function. “Pattern recognition” tool is the next one in neural network toolbox, which is employed for detecting object and classifying the input data based on intended data properties. Another tool in the toolbox is “data clustering”. Data clustering is used to group data by considering similarities. The fourth tool is “time series analysis”, in which a neural network with a dynamic behavior is employed to forecast the future activities by looking at the past data. In this study, the function fitting tool is employed for approximation.

The backpropagation method trains ANNs utilizing the calculated errors of output layers to find the hidden-layer errors by propagating back [31]. Levenberg-Marquardt (LM) algorithm is extensively-used backpropagation neural network training method which offers the speed of Gauss-Newton method and the stability of the steepest descent method in minimizing the sum squared errors of the targets and the output results of the trained network [28]. Neural network toolbox of Matlab [8] recommends Levenberg-Marquardt backpropagation method to be preferred as a first-choice since it is the fastest algorithm in the toolbox [22].

In LM algorithm,  $\mathbf{w}$  is the weight vector of the network,  $\mathbf{e}$  is the error vector between the output and the target points.  $F(\mathbf{w})$  is the performance function, which is mean squared error or the sum squared error.  $\mu$  is known as learning rate. The incremental changes in weights are determined by  $\mu$ . In each iteration of the ANN training, the performance function  $F(\mathbf{w})$  is compared with the previous performance value. Depending on the performance comparison,  $\mu$  is increased or decreased accordingly. Once the value of  $\mu$  is revised, then the incremental weights and the weights are revised. The iterations go on until the desired performance is reached.

The process taking place inside a simple neuron is expressed in Figure 5.2 where  $i$  is a scalar input,  $b$  is bias scalar,  $f$  is the specified transfer function, and  $a$  is the output of the neuron. As seen in Figure 5.2 and expressed in Equation 5.1, the input is multiplied with the corresponding weight  $w$  and then summed up with the bias  $b$ . In the next step, processed in a transfer function (TF) to give the neuron output  $a$  [22]. There are commonly used transfer functions in ANN, namely linear and tan-sigmoid transfer functions. The linear transfer functions can give any results and they are mostly employed in the output layers. On the other hand, the tan-sigmoid is hyperbolic tangent sigmoid TF and it can only give values from “-1” to “1”. Tan-sigmoid functions are generally used in hidden layers in function fitting [22].

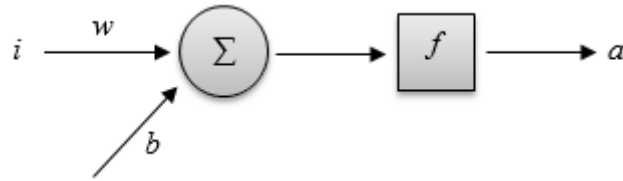


Figure 5.2 The mathematical process in a simple neuron

$$a = f(w \cdot i + b) \quad (5.1)$$

The artificial neural networks can be adapted to find solution for wide range of problems including function fitting, pattern recognition, data-mining, prediction, detection, clustering, etc. Moreover, the problems can be non-analytical, non-linear, stochastic, non-stationary, etc. Another major advantage of the artificial neural network is the capability of solving complicated problems without serious requirement of specially programming for a specific problem. The ANN methodology eliminates the need of having heavy mathematical background of a problem. Thus, the methodology can be utilized by everyone instead of by only experts in that area [29].

## 5.2 The Artificial Neural Network Generation Process

Having a successfully trained ANN is heavily related with having sufficient data points in the supplied database. For this purpose, a parametric database of 13500 design points (analyses) are employed. The parametric set of 13500 analyses are divided into 25 equal sets in order to manage the analysis better. In the end of the analyses, there are 25 parametric sets with the tabulated results in the form of spreadsheet. Each set consists of 540 separate FE analyses. All of the design points succeeded in converging to a solution.

After the completion of all analyses, the solution results are post processed for ANN training. Firstly, twenty five spreadsheets in ANSYS are exported to Microsoft Excel [27] by hand. Each analysis set containing input and output values is placed to distinct sheets in the file. A script is prepared to collect the spreadsheets from Excel and concatenate the twenty five separate matrices into a single matrix.

Although there is no failing design points in this parametric study, the script comprises a control loop to check the results of each analysis. This operation is achieved by an algorithm filtering the zero-results coming from the parametric analyses. Figures 5.3 and 5.4 show the failed-analysis samples with zero and empty output results in both ANSYS parametric study results and exported MS Excel result spreadsheet. The failed analysis results are eliminated, if there is any, prior to the training of the ANN. In the next step, the united matrix with 13500 design points are divided into two final matrices, namely the ANN training input and the ANN training target (output). The script has been arranged in a parametric way such that even if the number of parametric sets or the number of total analyses are modified, the script conducts preprocessing, training of the ANN with the defined settings, and presents the finalized network to be used whenever necessary.

1	Name	P11 - DS_E	P14 - DS_B	P15 - DS_A	P16 - DS_C	P17 - DS_D	P18 - Bolt Pretension Working Load	P30 - Av Eqv Flng Stress
2	Units	mm	mm	mm	mm	N	Pa	
42	DP 39	4.7246	25.001	4.8906	166.75	6.6528	5825.9	7.6118E+07
43	DP 40	4.7246	25.001	4.8906	166.75	6.6528	5825.9	7.6118E+07
44	DP 41	4.5436	25.136	4.9342	166.16	6.2208	5835	7.6865E+07
45	DP 42	4.9989	24.861	4.5416	167.19	6.0697	0	0
46	DP 43	4.6403	25.853	4.1862	169.45	6.2411	5889.7	1.1013E+08
47	DP 44	4.6953	25.165	4.4461	165.18	6.5989	5793.2	8.0969E+07

Figure 5.3 The failed analysis row encircled by red frame in a parametric study page in ANSYS

DP 40	4.724581509	25.00092675	4.890554593	166.750564	6.652812415	5825.9	87.69250611	76117929.75
DP 41	4.543557052	25.13605918	4.934158487	166.1571712	6.22075082	5835	89.40501602	76865164.82
DP 42	4.998873081	24.86126672	4.541575796	167.1867677	6.069739921	0	0	0
DP 43	4.640202180	25.85205530	4.180100651	169.4355133	6.241151793	5889.7	121.7273743	110130037.1
DP 44	4.695339343	25.16520779	4.446051032	165.1801747	6.59889425	5793.2	93.09152595	80969236.37
DP 45	4.581603952	23.42487677	4.102336661	167.3509166	6.088070293	5835	120.1721672	102336564.8

Figure 5.4 The failed analysis row encircled by red frame in a MS Excel exported results spreadsheet

Training of ANN is another important step in the development of the bolted flange connection design tool. The success of the developed tool is primarily dependent on the training performance of the ANN.

It should be noted that more complicated problems can be solved better as the neuron number increases. However in this case, there is a risk of overfitting with the higher number of neurons as well as increased computational time. Hence, the selection of correct number of neurons in the training is a trial and error process for each specific problem. Therefore, in this study, several networks are setup to reach the optimal arrangement of the ANN structure. Finally, the neuron number has been chosen to be 14 for the ANN training since the best performance is obtained with this layout. The training structure of the ANN is presented in Figure 5.5. The transfer function of the neurons in the hidden layer is tan-sigmoid. Output layer neurons employ the linear transfer functions. The seven input parameters are taken into the toolbox, processed in the 14 artificial neurons located in the hidden layer, and transferred to two output neurons in the end. In other words, the architecture of the ANN is 7:14:2. Although it seems that the structure consists of four layers with separate output layer and output terminals in Figure 5.5, these two parts are assumed as a single layer since each neuron in output layer is directly connected to the corresponding output terminal.

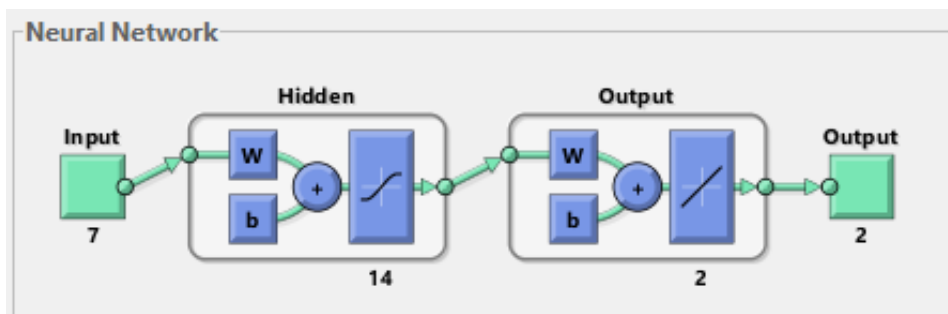


Figure 5.5 The neural network training structure with seven input parameters and two output parameters

For the training operation, the supplied data is divided into three normally. They are the training set, validation set, and the test set. The following values are used as default for the division of the data [8]:

- 70 % for training
- 15 % for validation

- 15 % for testing.

The training set is used for only in training of the weights and biases between the neurons. Validation set is not employed in training but utilized for the validation purpose in the end of every training iteration to terminate the training process. Test set is completely unconnected with the training operation. The test samples are employed in order to check the performance of the finalized network. It should be noted that the validation and test sets are not processed in the training operation. In this study, the complete database of 13500 samples are divided into three sets as follows:

- 90 % for training
- 5 % for validation
- 5 % for testing.

In the construction of the ANN, the samples are assigned to each set randomly according to the percentages. In the training process, the performance criterion is taken as the mean squared error. In calculation of the mean squared error, the importance of all targets are equal to each other as a default setting. Therefore, the elements in error matrix arising from both bolt force reaction output and flange stress output are taken into account equally in calculation of mean squared error. The error weighting values can be adjusted as desired [22]. Epoch limit is one of the training termination criteria in which the training of ANN is stopped when the number of iterations exceeds a specified limit. For the training progress, epoch limit is set to 5000 iterations. After this limit, the training is terminated without considering the performance. Another termination criterion is the number of validation checks for iterations. In this study, validation check limit is adjusted to 300 iterations which means that if the mean squared error is not decreased for 300 successive iterations, the training operation is finalized.

### 5.3 Results of the Artificial Neural Network

In the end of all training efforts, the best trained ANN has a performance of 2.55 mean squared error. Mean squared error performance implies the mean square of the deviations between the trained ANN output values and the target output values for the same design points. One can understand the meaning of mean squared error for this study better if the nominal output values are considered. The bolt force reaction results alter in a range of 4000-8000 N approximately. When compared to these values, 2.55 is a highly promising mean squared error which is relatively very small numerical value for the network. The training is completed because of reaching the validation check limit and total training is carried out in 3993 iterations.

Figure 5.6 shows the dramatical performance improvement of the ANN. In the very beginning of the training, the mean squared error performance values of the training, validation, and test sets are very high, but the performance improves rapidly within the approximately 300 iterations. After 300 iterations, the performances improve quite slowly. Finally, the mean square errors for the training, validation, and test sets are obtained as 2.55, 1.41, and 5.77 respectively when the ANN formation process is terminated. The training is finished in 3993 iterations and the training operation did not improve within the last 300 iterations. Figure 5.7 shows the termination of the training process in which the vertical axis shows the number of successive validation fails and the horizontal axis indicates the total number of iterations in the end of the training. As seen in Figure 5.7, after approximately 1100 iterations, the performance of the training does not improve for approximately 200 iterations. After this point, the performance increases again. Since successive performance improvement fails are less than 300 iterations, the training is not terminated here. On the other hand, after approximately 3600 iterations, there are 300 successive training improvement fails in the final portion of the training iterations and the training is accordingly terminated.

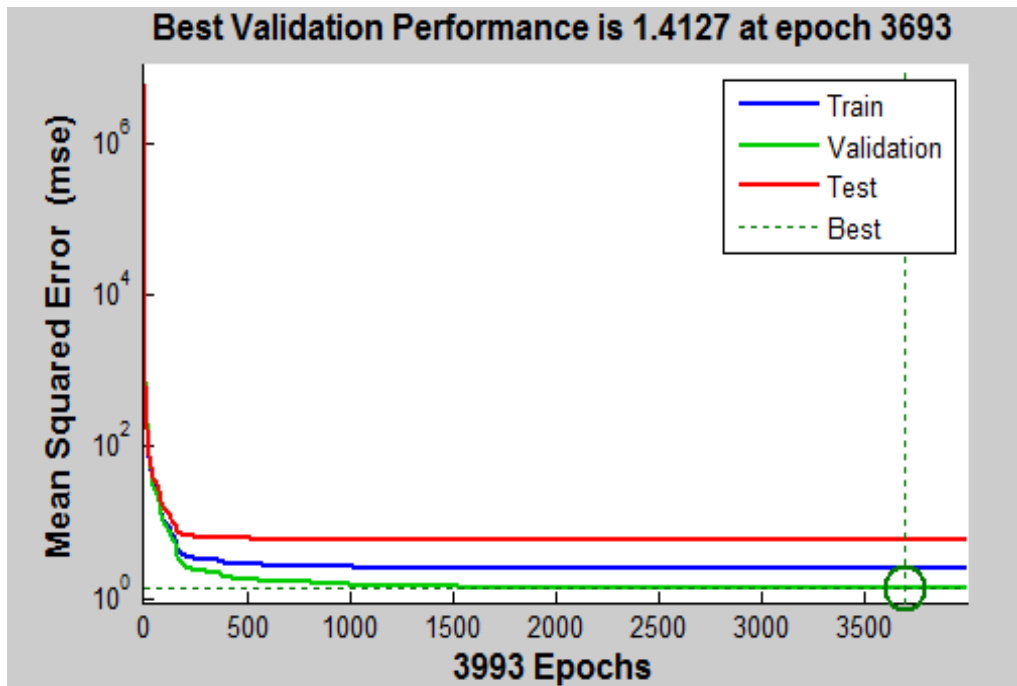


Figure 5.6 The performance improvement of the ANN along with the training iterations

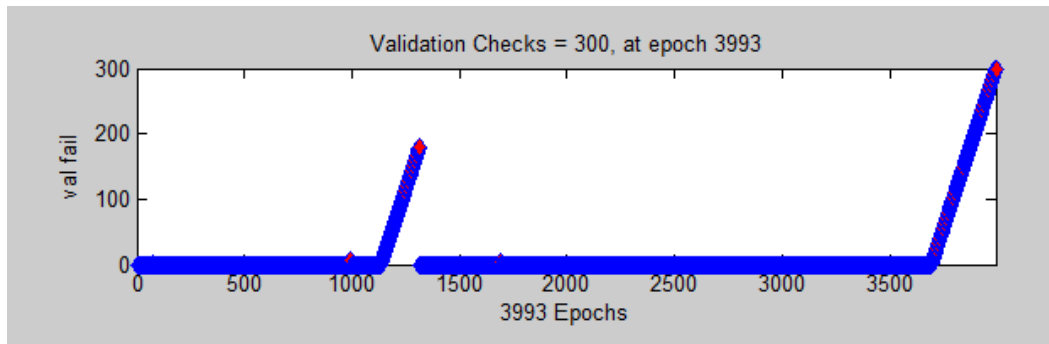


Figure 5.7 Termination of the ANN training due to validation check limit

The linear regression plot of the training database target relative to the ANN output is an indicator of the training quality. In Figure 5.8, the vertical axis shows the finalized ANN output results for all design points while the horizontal axis shows the target results coming from the parametric FEA database. The dashed line with 45 degree slope implies perfect target output matching in regression. The blue line, on the other hand, is the regression line for the finalized ANN results. It is observed that the blue line and the dashed line almost exactly match meaning that the ANN training is quite

successful as desired. As a result, the dashed is blocked by the blue fit line in Figure 5.8.

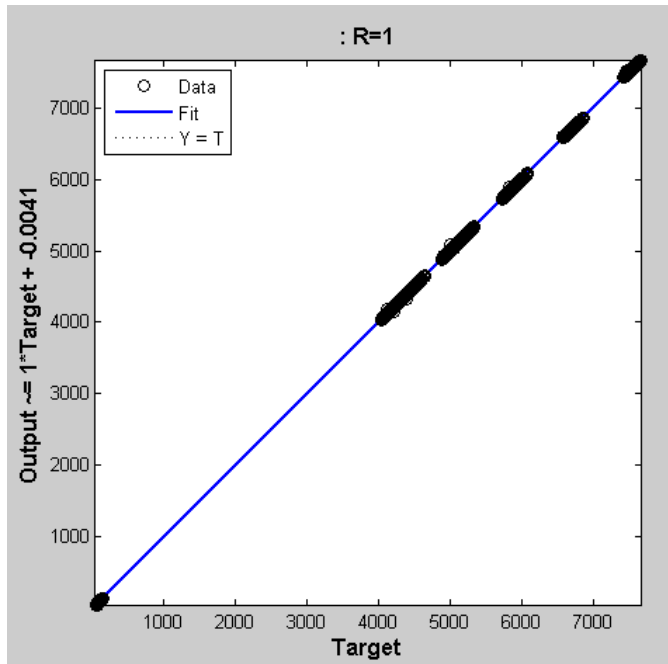


Figure 5.8 The regression plot to evaluate the ANN performance (the vertical axis stands for the training output results and the horizontal axis is for target results)

The successfully trained ANN is stored as a function in order to produce instant results. The desired structural analysis solution of the bolted flange connection can be obtained by supplying the seven input values of the design parameters in the correct order to the stored ANN function. The ANN function then calculates the two output values instantly.

## CHAPTER 6

### RESULTS AND EVALUATION

The established bolted flange design tool based on the trained neural network is assessed to verify the performance in distinct cases before the actual use. The best results that the bolted flange design tool can give is the exact FEM solution since the tool is created based on FEM analysis database. Therefore, the tool is tested against direct FEM solutions in the first place. Secondly, the comparison with theoretical approach is also done.

The instant results can be taken from the bolted flange design tool by supplying the desired input values in the correct order. The tool is stored under the Matlab workspace with a function named “net”. A sample input command is below:

```
net([4.5;24;167.75;6.6;5;1500;5000])
```

where the input matrix inside “net” function contains the geometrical parameters (A, B, C, D, E) and the loading parameters (the bolt pretension, the axial external force) respectively with the proper set of units.

When this command is run in the Matlab workspace, the software gives the following output:

```
ans =  
  
1.0e+003 *  
5.2383  
0.0847
```

where the 5238.3 is the bolt reaction force in N and 84.7 is the equivalent Von Mises flange stress in MPa.

### 6.1 Comparison with Finite Element Analysis

The trained network has already been tested in the end of the training operation automatically by Matlab [8]; however, the tool can be tested against direct FEM solutions to check the accuracy of the approximation for different cases.

The test analyses are examined in three categories. The first set contains ten design points selected randomly from the training points. Table 6.1 presents the ten test points with the values of the parameters.

Table 6.1 Test set-1, (the samples are selected from the training points)

	<b>A, mm</b>	<b>B, pcs</b>	<b>C, mm</b>	<b>D, mm</b>	<b>E, mm</b>	<b>Axial Force per Bolt, N</b>	<b>Bolt Pretension, N</b>
<b>1</b>	4.20	25.00	166.70	7.30	5.50	1152.00	5702.00
<b>2</b>	4.20	23.00	167.75	6.60	4.50	1024.00	4846.50
<b>3</b>	4.83	24.00	168.90	6.60	5.00	1408.00	4846.50
<b>4</b>	5.00	24.00	165.60	5.90	4.50	1280.00	6557.50
<b>5</b>	4.20	24.00	164.50	5.90	4.50	1152.00	3991.00
<b>6</b>	5.00	23.00	164.50	5.90	5.50	1280.00	7413.00
<b>7</b>	5.00	25.00	165.60	6.60	5.50	1280.00	3991.00
<b>8</b>	4.20	23.00	165.60	5.90	4.50	1024.00	3991.00
<b>9</b>	4.00	23.00	166.70	6.60	5.00	1408.00	3991.00
<b>10</b>	4.00	25.00	165.60	7.30	5.00	1536.00	7413.00

The ANN results for set-1 are given in Table 6.2. Table 6.2 shows that the bolted flange design tool is able to give very accurate output values when the input values are selected from the training points. If the FEM analysis output is taken as the correct value, then the maximum percent error for the bolt force reaction is %0.040 while the maximum absolute error is %1.5 for the average flange stress.

Table 6.2 The results of test set-1, (the samples are selected from the training points)

<b>FEM Force, N</b>	<b>FEM Stress, MPa</b>	<b>ANN Force, N</b>	<b>ANN Stress, MPa</b>	<b>Error % (Force)</b>	<b>Error % (Stress)</b>
5755.37	78.36	5756.30	78.41	-0.016	-0.059
4936.89	84.60	4936.79	84.60	0.002	-0.002
5126.58	80.68	5128.24	81.06	-0.032	-0.473
6661.07	84.25	6660.48	84.28	0.009	-0.039
4117.73	67.11	4117.52	67.60	0.005	-0.734
7458.21	80.99	7459.07	79.78	-0.012	1.485
4157.66	49.09	4156.02	49.22	0.040	-0.275
4097.88	68.96	4098.45	69.41	-0.014	-0.656
4205.97	75.33	4205.88	74.97	0.002	0.478
7483.91	107.85	7484.19	109.26	-0.004	-1.309

Although the bolted flange design tool can give results with low error percentages, the most critical capability expected from the tool is to predict the non-linear analysis relations in between the training points to successfully create a continuous domain. Therefore, in the second set, given in Table 6.3, ten design points are randomly selected by choosing the parameter values between the training points. Such a set truly shows the performance of the approximation.

Table 6.3 Test set-2, (the samples are in between the training points)

	<b>A, mm</b>	<b>B, pcs</b>	<b>C, mm</b>	<b>D, mm</b>	<b>E, mm</b>	<b>Axial Force per Bolt, N</b>	<b>Bolt Pretension, N</b>
<b>1</b>	4.00	23.00	166.90	6.90	5.30	1400.00	4150.00
<b>2</b>	5.00	25.00	165.00	6.00	5.30	1400.00	4150.00
<b>3</b>	4.20	25.00	167.00	6.20	4.55	1500.00	6800.00
<b>4</b>	4.83	24.00	168.70	7.20	4.80	1500.00	6800.00
<b>5</b>	5.00	24.00	168.50	7.00	4.70	1100.00	5200.00
<b>6</b>	4.00	23.00	167.75	5.90	4.55	1000.00	5200.00
<b>7</b>	4.83	23.00	168.00	6.80	4.90	1300.00	6500.00
<b>8</b>	4.20	24.00	164.70	6.30	5.20	1300.00	6500.00
<b>9</b>	4.00	25.00	165.10	7.00	4.60	1220.00	4000.00
<b>10</b>	5.00	25.00	166.00	6.00	5.30	1220.00	4000.00

The percent errors for all test samples for the test set 2 are given in Table 6.4. From Table 6.4 it is seen that the maximum absolute bolt force reaction error is %0.061 and the maximum error in the average Von Mises flange stress is about %2.5. Although the maximum error for the test cases slightly increased, the error ranges for the set-2 results are similar in comparison to set-1. Therefore, the error levels are admissible to verify the bolted flange design tool performance inside the parametric training limits.

Table 6.4 The results of test set-2, (the samples are in between the training points)

<b>FEM Force, N</b>	<b>FEM Stress, MPa</b>	<b>ANN Force, N</b>	<b>ANN Stress, MPa</b>	<b>Error % (Force)</b>	<b>Error % (Stress)</b>
4325.40	72.41	4326.40	70.58	-0.023	2.536
4363.24	55.38	4364.13	55.44	-0.020	-0.098
6951.65	117.36	6951.00	116.45	0.009	0.775
6966.41	98.55	6966.40	98.67	0.000	-0.126
5317.04	73.14	5317.37	72.54	-0.006	0.812
5281.53	93.96	5281.60	94.93	-0.001	-1.031
6608.52	90.47	6608.74	89.99	-0.003	0.526
6551.61	90.26	6555.62	89.29	-0.061	1.085
4120.35	66.37	4119.45	66.79	0.022	-0.628
4181.85	54.36	4181.89	54.48	-0.001	-0.205

In the last case, ten data points are selected randomly by choosing the test points outside the training limits. In other words, extrapolation performance of the design tool is tested with the set-3 given in Table 6.5. In Table 6.5, each line is a different analysis point, and the painted elements indicate the parameter values outside the training limits.

Table 6.5 Test set-3, (extrapolation, the painted cells indicate the values outside the training limits)

	<b>A, mm</b>	<b>B, pcs</b>	<b>C, mm</b>	<b>D, mm</b>	<b>E, mm</b>	<b>Axial Force per Bolt, N</b>	<b>Bolt Pretension, N</b>
<b>1</b>	3.50	24.00	166.70	6.00	4.50	1600	4000
<b>2</b>	5.49	21.00	167.00	5.50	4.20	1000	5000
<b>3</b>	3.50	28.00	164.00	6.60	4.50	1280	3991
<b>4</b>	5.49	26.00	166.00	4.00	6.00	1200	8000
<b>5</b>	3.50	20.00	169.20	7.80	4.20	1000	3000
<b>6</b>	5.20	20.00	163.80	5.00	4.20	900	8500
<b>7</b>	3.50	22.00	169.20	4.50	4.60	900	8500
<b>8</b>	3.50	25.00	168.00	8.50	5.80	1200	3000
<b>9</b>	3.50	23.00	169.20	7.80	4.00	1000	3500
<b>10</b>	3.50	21.00	169.20	7.70	4.20	1000	3500

The results for set-3 are presented in Table 6.6. As one can easily see in Table 6.6, the extrapolation performance of ANN is not as good as the interpolation performance as expected. It is seen that the error percentages have grown up in almost all samples of set-3. For the bolt force, maximum percent error is about %1.1 which could be acceptable in a design study. However, the maximum average flange stress error is about %10.2. Therefore, the design tool should be used with caution outside the training limits.

Table 6.6 The results of test set-3 (extrapolation)

<b>FEM Force, N</b>	<b>FEM Stress, MPa</b>	<b>ANN Force, N</b>	<b>ANN Stress, MPa</b>	<b>Error % (Force)</b>	<b>Error % (Stress)</b>
4325.92	109.13	4373.85	110.16	-1.108	-0.944
5083.00	59.95	5141.71	66.06	-1.155	-10.192
4100.03	76.11	4117.21	76.32	-0.419	-0.279
8033.62	74.92	8075.43	81.29	-0.520	-8.499
3155.85	79.88	3191.93	87.83	-1.143	-9.947
8503.36	98.56	8507.05	96.77	-0.043	1.815
8532.79	163.02	8549.18	172.05	-0.192	-5.534
3137.11	52.24	3162.32	54.00	-0.803	-3.385
3640.31	89.96	3666.85	97.49	-0.729	-8.373
3626.72	86.28	3657.06	94.16	-0.837	-9.131

## 6.2 Comparison with Theoretical Approach

In this section, an analysis with the specified input parameters is conducted to compare the theoretical approach of ESDU [4] and the parametric FEM based bolted flange design tool.

A selected sample bolted flange configuration has been solved by the theoretical approach of ESDU, direct FEA solution, and by the bolted flange design tool and their results are compared.

In the ESDU approach, the structure is classified as thin feet and thick feet flanges by considering the total thickness of the matching flange extensions [4]. The key point in

the theoretical analysis of the bolted flange is to obtain the equivalent stiffness constants under real service conditions. ESDU utilizes modification coefficients to obtain the real stiffness values of the parts acting with the bolt and acting with the flanges. Once the stiffness constants are calculated, the bolt stress or the required bolt pretension for a safe design is found by taking the prying effect into account. In the development of the bolted flange design tool, ESDU approach is considered as one of the main references since it is a commonly used method in this field.

In theoretical calculations, the solution of the example problem 1 in ESDU [4] is followed step by step by imposing the dimensions of the bolted flange geometry studied in the present thesis. The problem geometry is presented in Figure 6.1.

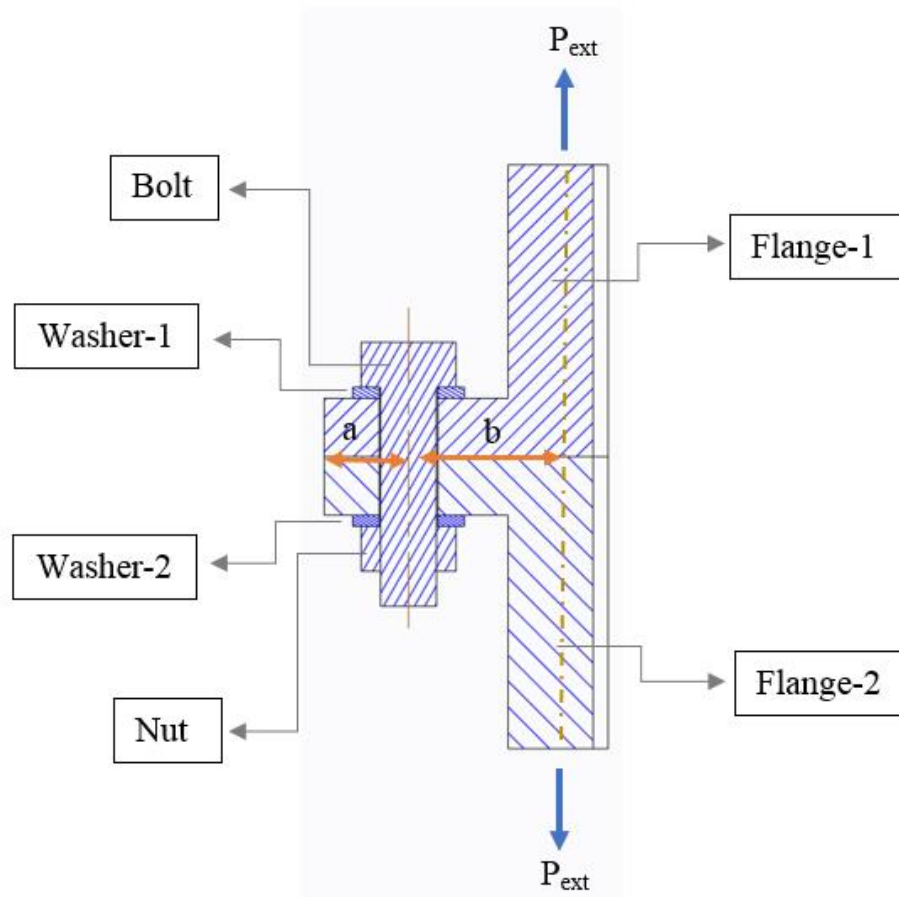


Figure 6.1 The schematic drawing of the thin feet bolted flange connection by ESDU [4]

The details of the new bolted flange joint are:

- $A(\text{bolt size}) = M4 (4 \text{ mm})$
- $B (\text{the number of bolts}) = 24 (\text{not applicable here})$
- $C (\text{bolt location}) = 167.75 \text{ mm}$
- $D (\text{casing thicknesses}) = 6.6 \text{ mm}$
- $E (\text{flange thicknesses}) = 5 \text{ mm}$
- $t_{bh} (\text{bolt head and nut thicknesses}) = 3.2 \text{ mm}$
- $p(\text{pitch of the bolt thread}) = 0.7 \text{ mm}$
- $d_{min} (\text{bolt thread minor diameter}) = 3.2 \text{ mm}$
- $P_t (\text{Bolt pretension}) = 4000 \text{ N}$
- $P_{ext} (\text{Axial external force}) = 1500 \text{ N}$
- $t_w (\text{washer thickness}) = 0.8 \text{ mm}$
- $d_w (\text{washer outer diameter}) = 8 \text{ mm}$
- $d_{wi} (\text{washer and flange inner (hole) diameter}) = 4.4 \text{ mm}$
- $d_{bh} (\text{bolt head effective diameter}) = 6.8 \text{ mm}$
- $R_{out} (\text{flange outer radius}) = 175 \text{ mm}$
- $R_{in} (\text{flange inner radius}) = 151.9 \text{ mm}$
- $E_b (\text{Young's modulus of bolt}) = 200 \text{ GPa}$
- $E_f (\text{Young's modulus of flanges}) = 71 \text{ GPa}$
- $E_w (\text{Young's modulus of washers}) = 200 \text{ GPa}$
- $a (\text{the distance from bolt center to outer flange surface}) = 7.25 \text{ mm}$
- $b (\text{the distance from bolt center to inner flange surface}) = 12.55 \text{ mm}$

The ESDU calculation steps [4] can be followed step by step below. The process starts with the calculation of equivalent stiffness of the bolt group according to Equation 6.1. The bolt group stiffness is formed by the effective bolt thread stiffness ( $k_{th}$ ), effective bolt shank stiffness ( $k_{sh}$ ), the washers' stiffness ( $k_w$ ), the stiffness of the flange-1 acting with the bolt group ( $k_{fb1}$ ), and the stiffness of the flange-2 acting with the bolt group ( $k_{fb2}$ ). A portion of the flange pair thicknesses are assumed to act with

the bolt group since the external force is transferred to bolt group through these regions. The flange located close to bolt head is named as flange-1 and the flange closer to the nut is called as flange-2. ESDU suggests to assume that  $\frac{1}{4}$  thickness of the total flange-1 thickness acts with the bolt group and the remaining  $\frac{3}{4}$  of the flange-1 thickness acts with the flange group while calculating the effective stiffness values. In the same way, the stiffness contributions to bolt group by flange-2 is taken as  $\frac{1}{5}$  of the total flange-2 thickness based on the experience of ESDU.

$$(k'_b)^{-1} = (k_{th})^{-1} + (k_{sh})^{-1} + (k_w)^{-1} + (k_{fb1})^{-1} + (k_{fb2})^{-1} \quad (6.1)$$

The shank portion of the bolt is equal to the sum of the thicknesses of the flanges and the washers:

$$l_{sh} = 2 \cdot E + 2 \cdot t_w \quad (6.2)$$

$$l_{sh} = 11.6 \text{ mm} \quad (6.3)$$

A portion of the flexible bolt head acts as part of the shank. Therefore, the effective bolt shank length ( $l'_{sh}$ ) is calculated as given in Equation 6.4. This effect is represented by the shank increase coefficient ( $x_{sh}$ ). The coefficient is taken as 0.2 as suggested by ESDU [4].

$$l'_{sh} = l_{sh} + x_{sh} \cdot t_{bh} \quad (6.4)$$

$$l'_{sh} = 12.24 \text{ mm} \quad (6.5)$$

The effective bolt shank stiffness is calculated with the cross-sectional area of the shank by considering Equation 6.6:

$$k_{sh} = E_b \cdot (\pi \cdot A^2 / 4) / l'_{sh} \quad (6.6)$$

$$k_{sh} = 205.333 \cdot 10^6 \text{ N/m} \quad (6.7)$$

In order to calculate the stiffness of the threaded section of the bolt, the effective length of the threaded portion of the bolt is calculated first. Since the threaded portion of the bolt is assumed to begin with the nut engagement, the threaded portion length inside the flange hole is taken as zero so  $l_{th}$  is “0” in Equation 6.8. The stiffness contribution by the bolt thread inside the nut is considered with the thread engagement coefficient ( $x_{pt}$ ) by multiplying it with the thread pitch ( $p$ ) in Equation 6.8. The third term on right hand side in Equation 6.8 represents the effective length term of the nut contributing to the stiffness of the threaded portion via the nut coefficient ( $x_{nu}$ ). ESDU [4] suggests  $x_{pt}$  to be taken as 1 and  $x_{nu}$  to be taken as 2 for the standard nut.

$$l'_{th} = l_{th} + x_{pt} \cdot p + x_{nu} \cdot A \quad (6.8)$$

$$l'_{th} = 8.7 \text{ mm} \quad (6.9)$$

The effective diameter of the threaded portion of the bolt ( $d'_{th}$ ) is also needed and it is calculated by taking an average value between the minimum diameter of the threaded portion of the bolt ( $d_{min}$ ) and the nominal bolt diameter ( $A$ ) with the typical thread diameter coefficient ( $x_{th}$ ) of 0.3 multiplying the difference as suggested by ESDU [4].

$$d'_{th} = d_{min} + x_{th} \cdot (A - d_{min}) \quad (6.10)$$

$$d'_{th} = 3.44 \text{ mm} \quad (6.11)$$

The effective stiffness of the threaded portion of the bolt is calculated by Equation 6.12:

$$k_{th} = E_b \cdot (\pi \cdot d'_{th}{}^2 / 4) / l'_{th} \quad (6.12)$$

$$k_{th} = 213.657 \cdot 10^6 \text{ N/m} \quad (6.13)$$

It should be noted that the washers in assembly are identical. Therefore, the total stiffness of both washer can be calculated by calculating the stiffness of single washer and then dividing the stiffness by two since the two identical washers are in serial spring model. The washer stiffness term ( $k_w$ ) accounts for total washer stiffness in Equation 6.16. For the calculation of the washer effective outer diameter ( $d'_w$ ), the average of the washer outer diameter and bolt head-nut effective diameter is taken by referring to ESDU [4]:

$$d'_w = (d_w + d_{bh})/2 \quad (6.14)$$

$$d'_w = 7.4 \text{ mm} \quad (6.15)$$

$$k_w = E_w \cdot (\pi \cdot (d'_w - d_{wi})^2/4)/(t_w \cdot 2) \quad (6.16)$$

$$k_w = 3.475 \cdot 10^9 \text{ N/m} \quad (6.17)$$

The contribution of the flange to the stiffness of the bolt group can be calculated by adding the active thicknesses of flange-1 and flange-2 since they are made up of the same material. The total thickness of flange-1 and flange-2 acting with the bolt group is indicated by  $t_{fb}$  and  $k_{fb}$  stands for the combined flange stiffness acting with the bolt group. The external load is transferred to the joint via the flanges, a small portion of the flanges under both bolt head and nut is compressed more. Therefore, these small portions are assumed to act with the bolt group. ESDU [4] takes these portions as 1/4 of flange-1 thickness and 1/5 of flange-2. On the other hand, the change of the selected flange portions does not affect significantly the effective bolt group stiffness. In the calculation of the effective area, the same diameters in Equation 6.16 are used.

$$t_{fb} = (1/4 + 1/5) \cdot E \quad (6.18)$$

$$t_{fb} = 2.25 \text{ mm} \quad (6.19)$$

$$k_{fb} = E_f \cdot (\pi \cdot (d'_w - d_{wi})^2/4)/t_{fb} \quad (6.20)$$

$$k_{fb} = 1.837 \cdot 10^9 \text{ N/m} \quad (6.21)$$

The effective bolt stiffness is now calculated by Equation 6.1.

$$k'_b = 96.314 \cdot 10^6 \frac{\text{N}}{\text{m}} \quad (6.22)$$

In order to calculate the effective flange stiffness, it is critical to determine the effective contact area. For this purpose, ESDU [4] offers a chart to determine the effective area of the flanges. To utilize the chart, two different ratios are calculated in Equations 6.27 and 6.28.  $l'_f$  is the equivalent flange thickness given by Equation 6.23 including the washer thicknesses.

$$l'_f = 2 \cdot (E + t_w) \quad (6.23)$$

$$l'_f = 11.6 \text{ mm} \quad (6.24)$$

The effective diameter of the practical working area can be calculated in a few different ways. As suggested by ESDU [4], twice the distance from the bolt center to the outer end of the flange is used here.

$$D_f = 2 \cdot (R_{out} - C) \quad (6.25)$$

$$D_f = 14.5 \text{ mm} \quad (6.26)$$

Now, we can determine the ratios to use the chart and by using these ratios the equation for the effective flange area is calculated by Equation 6.29 with the constant value 1.27 read from the chart. The chart can be seen in Appendix C.

$$D_f/d'_w = 1.959 \quad (6.27)$$

$$l'_f/d'_w = 1.568 \quad (6.28)$$

$$\frac{A_f}{\left(\frac{\pi}{4}\right) \cdot ((d'_w)^2 - (d_{wi})^2)} = 1.27 \quad (6.29)$$

$$A_f = 3.531 \cdot 10^{-5} m^2 \quad (6.30)$$

The effective flange stiffness,  $k'_f$ , is calculated by Equation 6.31 and the numerical result is in Equation 6.32.

$$k'_f = E_f \cdot (A_f) / \left(\left(\frac{3}{4} + \frac{4}{5}\right) \cdot E\right) \quad (6.31)$$

$$k'_f = 323.485 \times 10^6 \text{ N/m} \quad (6.32)$$

To summarize, by following each calculation step in the ESDU example [4], and taking the same modification coefficients, equivalent stiffness of the bolt group (the structure acting with bolt) and the equivalent stiffness of the flange group (the structure acting with two flanges) are found as:

- $k'_b = 96.314 \times 10^6 \text{ N/m}$
- $k'_f = 323.485 \times 10^6 \text{ N/m}$

At this stage of the solution, the possibility of separation must be checked. In case of separation, the prying effect drastically increase the load carried by the bolt group.  $P_{as}$  is the critical externally applied load to separate the flanges from each other.  $P_{as}$  value can be calculated by Equation 6.33. In case of separation, the bolt load including prying effect has to exceed  $P_{as}$ . Separation control can be made by calculating the bolt load with prying effect in Equation 6.35. As specified above, the distance from bolt center to outer flange surface (a) is 7.25 mm and the distance from bolt center to flange inner surface (b) is 12.35 mm.

$$P_{as} = P_t \cdot \frac{k'_b + k'_f}{k'_f} \quad (6.33)$$

$$P_{as} = 5190.95 \text{ N} \quad (6.34)$$

$$P_b = P_{ext} \cdot \left(1 + \frac{b}{a}\right) \quad (6.35)$$

$$P_b = 4096.55 \text{ N} \quad (6.36)$$

As seen in Equation 6.36, the bolt load with prying effect is less than the critical value for separation. As a result, the load carried by the bolt group is calculated without considering the prying effect. The portion of the external load carried by the bolt is calculated by considering the stiffness ratio of the bolt and the flange groups.  $P_t$  is bolt pretension value in Equation 6.36. The bolt load is calculated as:

$$P_b = P_t + P_{ext} \cdot \frac{k'_b}{k'_f + k'_b} \quad (6.37)$$

$$P_b = 4344.14 \text{ N} \quad (6.38)$$

The same problem is modeled in ANSYS and finite element analysis of the bolted flange connection involving contact is performed. The bolt force reaction is obtained as 4306.4 N as seen in Figure 6.2.

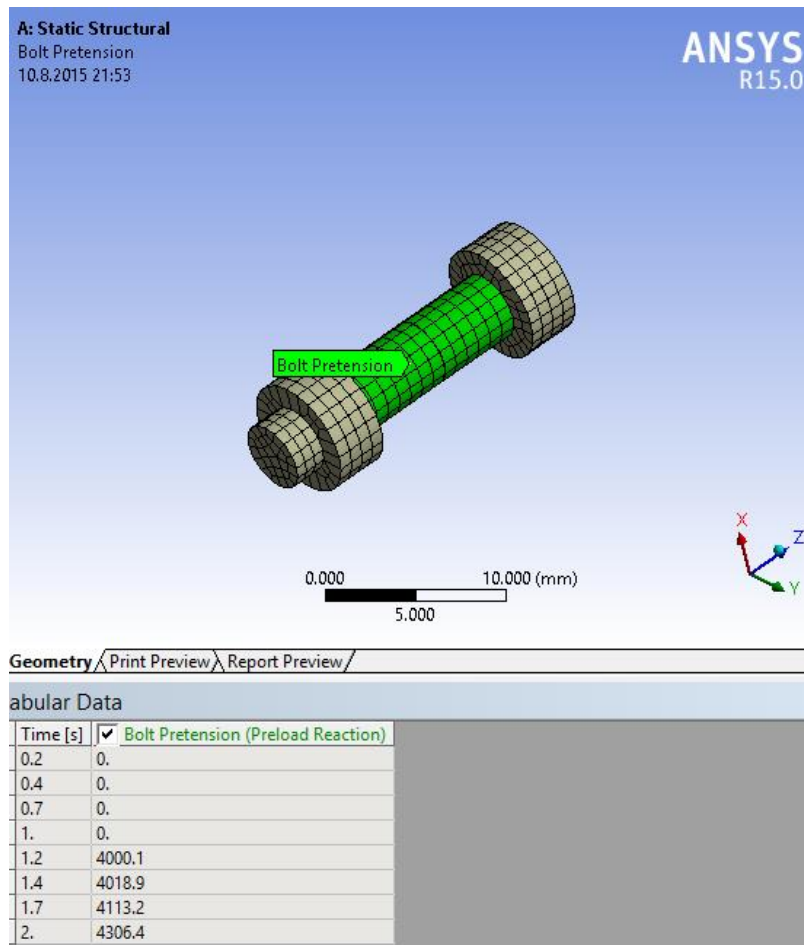


Figure 6.2 Bolt load result in the end of the FEM analysis

Lastly, ANN based bolted flange design tool is used for the same problem by supplying the same input, and the bolt force reaction is determined as 4309.9 N.

The same problem with the same dimensions, except bolt location (parameter  $C$ ), can be solved for the case in which separation occurs under the bolt head. Bolt location parameter is taken as larger value in Equation 6.39 than previous one to increase prying effect. For the same purpose, the axial external load and the bolt pretension input values are changed so that the external load exceeds the critical separation load. Two load sets are considered for the sample problem with separation. The first loading set is formed by:

$$C = 168.9 \text{ mm} \quad (6.39)$$

$$P_t = 1000 \text{ N} \quad (6.40)$$

$$P_{ext} = 1500 \text{ N} \quad (6.41)$$

The stiffness values are the same for both groups as before. Therefore, the critical separation load is calculated in Equation 6.42 with the same stiffness values as in Equation 6.33.

$$P_{as} = 1297.7 \text{ N} \quad (6.42)$$

Due to having larger external force than the critical load, the separation under bolt head is assumed. “a” and “b” values are calculated again with respect to new “C” value in Equations 6.43 and 6.44.

$$a = R_{out} - C \quad (6.43)$$

$$b = C - R_{in} - D/2 \quad (6.44)$$

$$a = 6.1 \text{ mm} \quad (6.45)$$

$$b = 13.7 \text{ mm} \quad (6.46)$$

The bolt reaction force is now calculated by considering the separation with Equation 6.35.

$$P_b = 4868.9 \text{ N} \quad (6.47)$$

However, FEM solution gives the bolt reaction force of 2789.8 N and the developed bolted flange design tool gives 2332.7 N for the same problem.

In the second load set for the separation, the bolt pretension ( $P_t$ ) and the axial external force ( $P_{ext}$ ) are taken as 3000 N and 4500 N. By taking all other parameters are the same as in the first case of separation problem and following the same steps, the bolt load is found in Equation 6.48.

$$P_b = 14606.6 \text{ N} \quad (6.48)$$

The result from ANSYS for the same input parameters is 8461.6 N and the tool gives 10745.8 N.

All the results taken from theoretical, FEM, and developed tool solutions are compared for the sample problems with and without separation in Table 6.7. In the calculation of the error percentages for the tool solution and theoretical solution, ANSYS results are taken as nominal values.

Table 6.7 The results of the sample problems with and without separation solved by theoretical approach, FEA, and the developed tool

	ANSYS	Developed Tool	Theoretical Approach	Tool Error %	Theoretical Error %
<b>Bolt force reaction (N) in problem without separation</b>					
P <sub>t</sub> =4000 N P <sub>ext</sub> =1500 N	4306.4	4309.9	4344.1	0.0813	0.875
<b>Bolt force reaction (N) in problems with separation</b>					
P <sub>t</sub> =1000 N P <sub>ext</sub> =1500 N	2789.8	2332.7	4868.9	-16.4	74.5
P <sub>t</sub> =3000 N P <sub>ext</sub> =4500 N	8461.6	10745.8	14606.6	27.0	72.6

The theoretical approach, direct FEM solution, and the design tool all give results with small deviations with respect to each other in case of no separation under the bolt head. Therefore, it can be concluded that the tool is in a good agreement with both the theory and the direct FEM solution if no separation occurs under the bolt head. As seen in Table 6.7 three methods give similar results. The maximum error is 0.875

percent by the theoretical approach result. On the other hand, the solutions obtained from theoretical method are too different than the solutions from the others for the sample problems with separation. One should realize that developed bolted flange design tool extrapolates the results in the separation problems since the bolt pretension in the first case and the axial external force in the second case are out of ANN training limits. Nevertheless, theoretical approach results far worse than the tool results with 74.5 % and 72.6 % deviations in separation problems. As a results, developed bolted flange design tool exhibits better performance than theoretical method in overall evaluation.

## CHAPTER 7

### CONCLUSION AND FUTURE WORKS

#### 7.1 Conclusion

In this study, an ANN based bolted flange design tool is developed. ANN based design tool is established utilizing the non-linear finite element analysis database with contact and frictional nonlinearities. The tool is designed for the design and analysis of the bolted flange connection of a medium scale aircraft engine under axial load. Since the developed tool utilizes artificial neural network approximation of the database formed by non-linear finite element analysis involving contact, the structural analysis of the bolted flange joint can be made very fast with high accuracy with the developed tool.

The development procedure of the ANN based design tool requires the determination of input parameters to be used in parametric analysis. The geometric variables used in the design tool are defined to be the bolt size, the number of bolts, bolt location, casing thickness, and flange thickness with upper and lower limit input limits while the load variables are the axial external force and the bolt pretension. Parameters correlation study is conducted to determine the sensitivities of the input parameters on the output and to decide on the number of intervals for each variable in the upper and the lower range of the design variables. For the training of the ANN, a parametric study with 13500 non-linear FE analyses is conducted to form a FEA solution database. The FEA database comprises the combination of all input parameter values with each other. In the final step, the created FEA database is trained to setup an artificial neural network to establish the bolted flange design tool. ANN based design tool gives two output. The first one is the force reaction in the bolt body and the second one is the average Von Mises stress in the flange. The trained ANN based bolted flange design tool gives

parametric analysis results instantly within a continuous input domain within the upper and lower limits of each design variable.

The developed bolted flange design tool is verified via two case studies. In the first one, the tool is tested against the commercial FEA software for three separate conditions: the test points the same with the training points, the test points between the training points (interpolation), and the test points outside the limits of training points (extrapolation). The analysis results show that the tool delivers successful results with very low deviation from the direct FEA solutions when the test points are within the training limits. When the test points are outside the limits of the training points, the performance of the tool drops, as expected. However, in the overall, the ANN based bolted flange design tool performs very well in approximating the non-linear behavior of the bolted flange analysis results obtained by FEM. Utilization of the tool eliminates time requirements in FEA.

In the second case study the bolted flange design tool output is compared with the results of the theoretical approach [4] for the same problems of the cases with and without separation. The results showed that the theoretical approach and the bolted flange design tool are consistent with each other for the bolt reaction force until the separation of flange. As both case studies suggest, the developed ANN based bolted flange design tool can be used as a reliable structural analysis method inside the training domain. On the other hand, theoretical approach gives too inaccurate results in comparison to FEM solution when the separation under the bolt head occurs. Although the developed tool is tested with extrapolation outside the training limits, it gives closer results to FEM results when compared with the theoretical results in separation problem. If the tool is trained further for larger limits including the input parameters causing separation, it can give quite reliable results as FEM solutions. Therefore, theoretical approach has a limited applicability in structural analysis of bolted flange connection. Moreover, ESDU approach focusses on the bolt force and the bolt stress rather than flange stress. However, developed tool can give solution for both bolt and flange in structural analysis by taking power of FEA.

It is also concluded that the ANN based flange design tool can be used as the fast solver in conjunction with an optimizer to achieve weight reduction in the aircraft engine flange. In the optimization process, ANN based design tool serves as very accurate approximate model replacing the non-linear finite element solver. Thus, with the ANN based solver, flange optimization can be performed very fast compared to employing non-linear FE based solver in each design iteration in the optimization process.

The study conducted here not only demonstrates the successful use of the ANN as the bolted flange design tool, but also shows promise for the applicability of this methodology to different non-linear structural problems.

## **7.2 Future Works**

The study intends to offer a new approach to axisymmetric circular bolted flange connections. The developed methodology is applied for the bolted flange connection exposed to axial external force. However, this approach is not only limited with single load condition but also any loading type or the combinations can be integrated into the tool. Moreover, it is possible to broaden the scope of the tool by enlarging the parametric input limits and increasing the number of the parameters. In order to improve the extent and the abilities of the bolted flange connection tool, the finite element analysis database can be systematically enriched by adding more analyses. Obviously, the larger the training database, the better the artificial neural network. By including different loading types and enlarging the input database, the developed tool can be used for larger scope of bolted flange problems. Moreover, in the near future a graphical user interface is going to be created for the ease of use of the bolted flange design tool. The developed tool with a graphical user interface can be utilized as an optimization tool to reduce bolted flange connection weight in design.



## REFERENCES

- [1] Demirkan, O., Olceroglu, E., Basdogan, I., & Özgüven, H. N., 2013, “A New Design Approach for Rapid Evaluation of Structural Modifications Using Neural Networks”, *Journal of Mechanical Design*, 135(2), 021004.
- [2] Kim, J., Yoon, J.-C., & Kang, B.-S., 2007, “Finite element analysis and modeling of structure with bolted joints”, *Applied Mathematical Modelling*, 31(5), 895–911.
- [3] Haidar, N., Obeed, S., & Jawad, M., 2011, “Mathematical representation of bolted-joint stiffness: A new suggested model”, *Journal of Mechanical Science and Technology*, 25(11), 2827–2834.
- [4] The Institution of Mechanical Engineers., 2012, “Analysis of pretensioned bolted joints subject to tensile (separating) forces”, (978 0 85679 527 5).
- [5] ASME, 2004, “2004 ASME Boiler and Pressure Vessel Code, Section VIII, Division I”, New York: American Society of Mechanical Engineers.
- [6] Coro, A., 2004, “Flange-Designer : A New Flange Design Methodology Based on Finite Element Analysis”, In *International Ansys Conference*. Retrieved from <http://www.ansys.com/staticassets/ANSYS/staticassets/resourcelibrary/confpaper/2004-Int-ANSYS-Conf-107.PDF>
- [7] ANSYS Workbench Version: 15.0.7, 2014
- [8] MATLAB Version: 7.11.0.584, 2010
- [9] Deng, L., & Ghosn, M., 2001, “Pseudoforce Method for Nonlinear Analysis and Reanalysis of Structural Systems”, *Journal of Structural Engineering*, 127(5), 570.
- [10] Kren, L., 2001, “Don't get bent out of shape when FEA is nonlinear”, *Machine Design*, (18).
- [11] ANSYS Help, 2014, “ANSYS 14.5 Help”, Washington, DC: Author. Retrieved from ANSYS Workbench 14.5 Help Directory
- [12] Wang, E., Nelson, T., & Rauch, R., 2004, “Back to Elements - Tetrahedra vs. Hexahedra (p. 16)”, 2004 International ANSYS Conference. Retrieved from <http://www.ansys.com/staticassets/ANSYS/staticassets/resourcelibrary/confpaper/2004-Int-ANSYS-Conf-9.PDF>

- [13] Zienkiewicz, O. C., & Morgan, K., 2006, "Finite Elements & Approximation", New York, NY: Dover Publications, Chap. 5.
- [14] Cook, R. D., Malkus, D. S., Plesha, M. E., & Witt, R. J., 2001, "Concepts and Applications of Finite Element Analysis", Hoboken, NJ: John Wiley & Sons, Chap. 6.
- [15] Cook, R. D., Malkus, D. S., Plesha, M. E., Witt, R. J., 2001, "Concepts and Applications of Finite Element Analysis, 4th Edition", Wiley. ISBN: 9780471356059
- [16] Heinstein, M.W., Attaway, S.W., Swegle, J.W., & Mello, F.J., 1993, "A general-purpose contact detection algorithm for nonlinear structural analysis codes", New Mexico: Sandia National Laboratories. Print. SAND92-2141.
- [17] "An Augmented Lagrangian Formulation for the Finite Element Solution of Contact Problems", 1986, California: University of California at Berkeley. Print. AD-A166 649.
- [18] Muliana, A., Steward, R., Haj-Ali, R. M. & Saxena, A., 2002, "Artificial Neural Network and Finite Element Modeling of Nanoindentation Tests", Metallurgical and Materials Transactions A.
- [19] Budynas, R. G., Nisbett, J. K., 2008, "Shigley's Mechanical Engineering Design (8th ed.)", New York, NY: McGraw-Hill, Chap. 8.
- [20] Schaaf, M., Bartonicek, J., 2003, "Calculation of Bolted Flange Connections of Floating and Metal-To-Metal Contact Type", Proceedings of PVP2003.
- [21] Azim, R., 2013, "An Analytical Investigation On Bolt Tension Of A Flanged Steel Pipe Joint Subjected to Bending Moments", International Journal of Engineering and Applied Sciences, 2(3), 71-81.
- [22] MATLAB Help, 2010, "MATLAB 2010 Help", DC: Author. Retrieved from MATLAB 2010 Help Directory
- [23] TEI, Inc. <http://www.tei.com.tr>
- [24] Metric Fasteners (n.d.). Retrieved April 12, 2015, from <http://www.metrication.com/engineering/fastener.html>
- [25] Multistandard Components Corp., 2000, "Full Thread Hexagon Head Screws", Retrieved April 12, 2015, from <http://www.metricmcc.com/catalog/ch1/1-2.pdf>

- [26] “Reference Tables -- Coefficient of Friction”, 2015, April 4. Retrieved from <http://www.engineershandbook.com/Tables/frictioncoefficients.htm>
- [27] Microsoft Excel Version: 15.0.4701.1001, 2013.
- [28] Suratgar, A. A., Tavakoli, M. B., & Hoseinabadi, A., 2007, "Modified Levenberg-Marquardt Method for Neural Networks Training", *International Journal of Computer, Control, Quantum and Information Engineering*, 1(6), 1719-1721.
- [29] Graupe, D. (2013). “Principles of Artificial Neural Networks (3rd Edition)”. Singapore: World Scientific Publishing Company
- [30] Gomes, H. M., & Awruch, A. M., 2004, “Comparison of response surface and neural network with other methods for structural reliability analysis”, *Structural Safety*, 2649-67.
- [31] Petrini, M., 2012, “Improvements to The Backpropagation Algorithm”, *Annals of The University of Petrosani Economics*, 12(4), 185-192.
- [32] Corder, G.W., & Foreman, D.I., 2014, “Nonparametric Statistics: A Step-by-Step Approach”, Wiley, ISBN 978-1118840313
- [33] Borkowf, C. B., 2000, “A new nonparametric method for variance estimation and confidence interval construction for Spearman's rank correlation”, *Computational Statistics and Data Analysis*, 34219-241.
- [34] Wall Emerson, R., 2015, Causation and Pearson's Correlation Coefficient, *Journal of Visual Impairment & Blindness*, 36(3), 242-244.
- [35] Yildirim, A., Akay, A., Gulasik, H., Coker, D., Gurses, E., & Kayran, A. (2015). Development of Bolted Flange Design Tool Based on Finite Element Analysis and Artificial Neural Network. Manuscript submitted for publication.
- [36] Yildirim, A., Akay, A., Gulasik, H., Coker, D., Gurses, E., & Kayran, A. (2015). Parameters Correlation Study to Investigate the Effects of Geometric Variables on the Safety of Bolted Flange Connections. Manuscript in preparation.



## APPENDIX A

### INSTRUCTIONS TO PREPARE ARTIFICIAL NEURAL NETWORK FOR THE BOLTED FLANGE DESIGN TOOL

The aim of this section is to explain concisely how to setup an artificial neural network for static analysis of the bolted flange connection in order to expand the developed bolted flange design tool for broader parametric input limits or establishing completely new artificial neural network (ANN) for different analysis cases.

To begin with, the parametric finite element analyses containing the desired number of analyses and the desired parametric input values, must be completed before starting to generate the ANN. In order to give parametric input sets, the input values can be modified and sorted as desired in Microsoft Excel. Then the data is simply copied and pasted to the Parameters Set window in ANSYS.

After the completion of the parametric study in ANSYS Workbench [ANSYS Workbench Version: 15.0.7, 2014], “Parameter Set” is opened by double clicking in the project schematic window as shown in Figure A.1. In the beginning of the parametric solution process, the input lines are filled by the user and the related solution cells are empty. After the parametric study, the solution cells in each line of the design points are updated by the software.

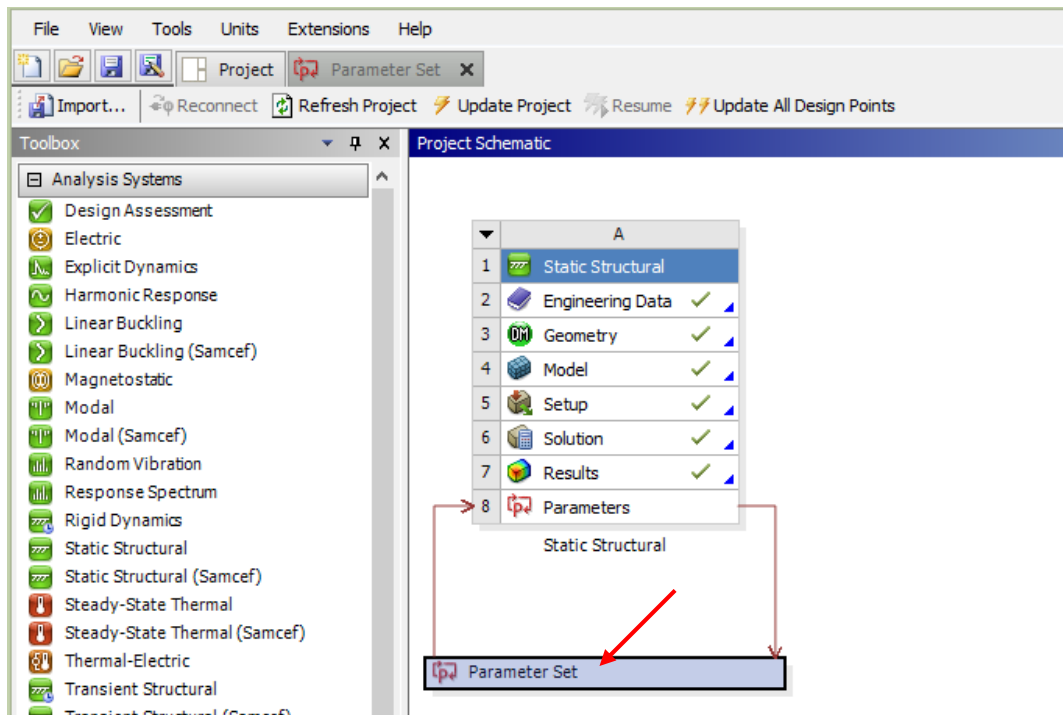


Figure A.1 ANSYS Workbench project schematic window for static structural analysis

In the parameter set window, both the parametric input values and the output parameter results are listed as in the form of spreadsheet in which every row stands for a separate analysis. “DP #” located in the first cell of each row means design point number of that specific analysis. The data listed in the form of spreadsheet must be transformed into different format in which the data can be easily read and modified whenever necessary. The data of the parametric study can be exported in csv (comma separated value) format by right clicking on anywhere in the spreadsheet window and selecting “export” as seen in Figure A.2. By specifying the file name, the data is stored in csv format.

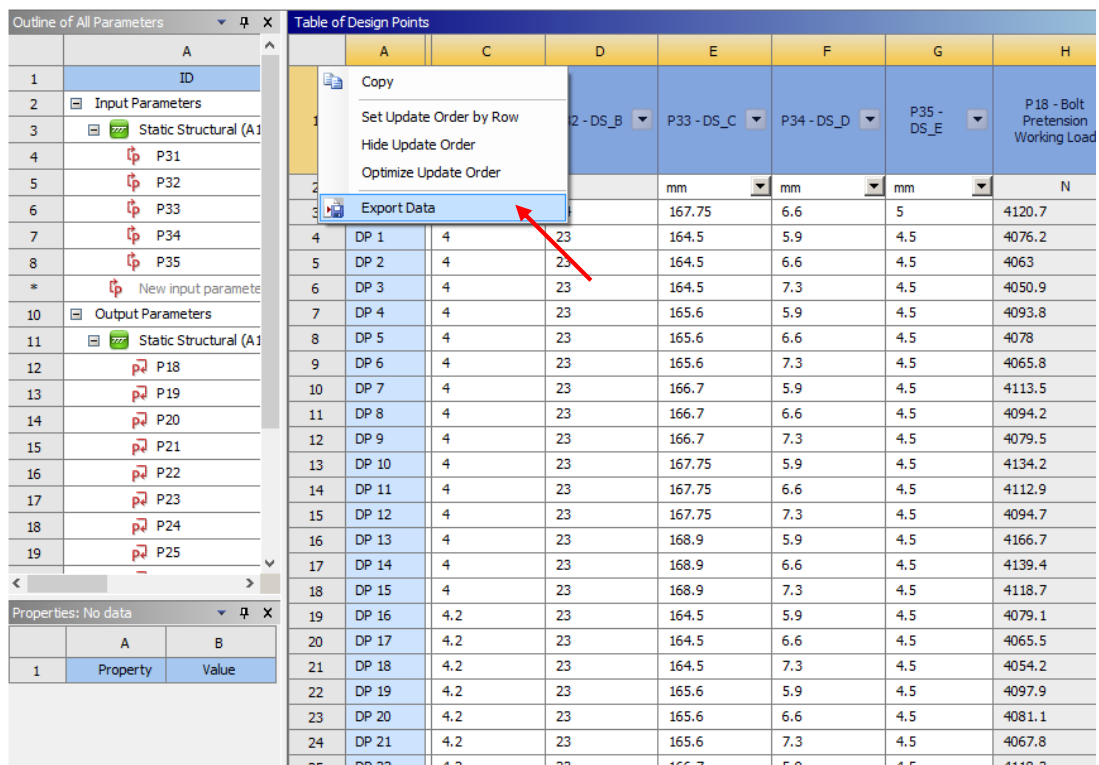


Figure A.2 Exporting the parametric study results

The exported data contains both all the input values and all the related output values. One may be curious about the necessity of collecting the input which has been already provided by the user. The update order of each analysis may change depending on the software settings in a parametric study. Therefore, the process of collecting the input and the output together prevents obtaining incorrectly matched input-output pairs. In this respect, even if the user changes the design point solution orders, the solution sets are addressed to the right input lines.

The newly created csv file is imported into Microsoft Excel [Microsoft Excel Version: 15.0.4701.1001, 2013]. Since the csv file contains a lot of numerical values in a complicated order, importing the data requires special attention in Excel. This operation can be done by the utilization of “Text Import Wizard” placed under “Data” tab of the software as Figure A.3 exhibits. At this point, user should select the previously created csv result file.

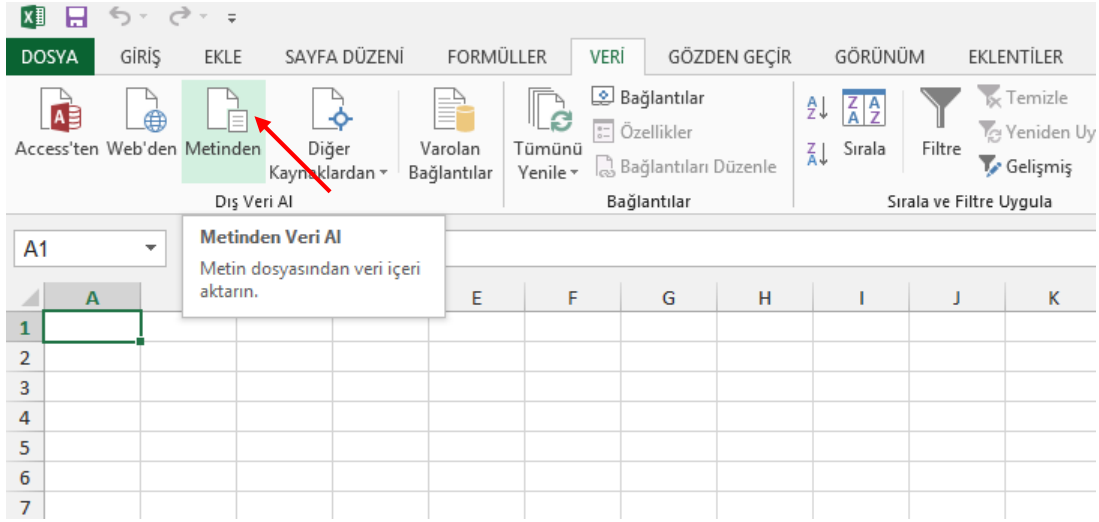


Figure A.3 Data import from a text file

Once the csv file of interest is pointed, the software launches import wizard window as one can see in Figure A.4. “Delimited” option must be chosen here in order to split rows and columns. As observed in Figure A.4, lower segment of the wizard window presents how the data is split into rows. Finally, “Next” is chosen.

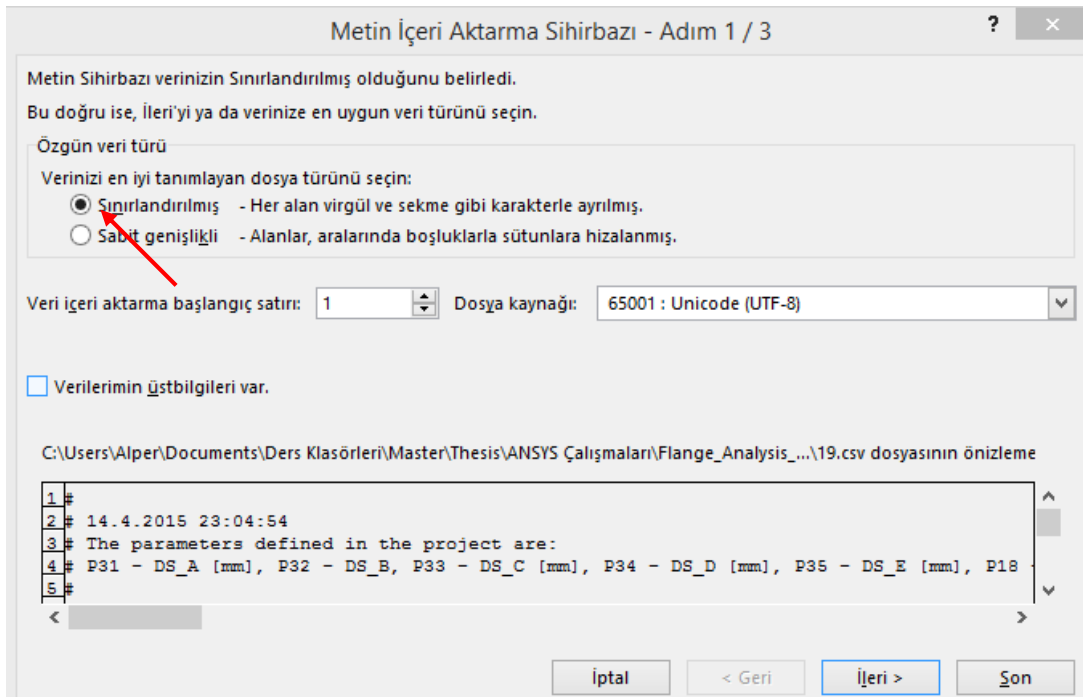


Figure A.4 Data import wizard window and row separation

The following page shown in Figure A.5 presents the separator options for columns. The only selected option should be “Comma” in this study. The lower segment of the page exhibits the resultant columns to check.

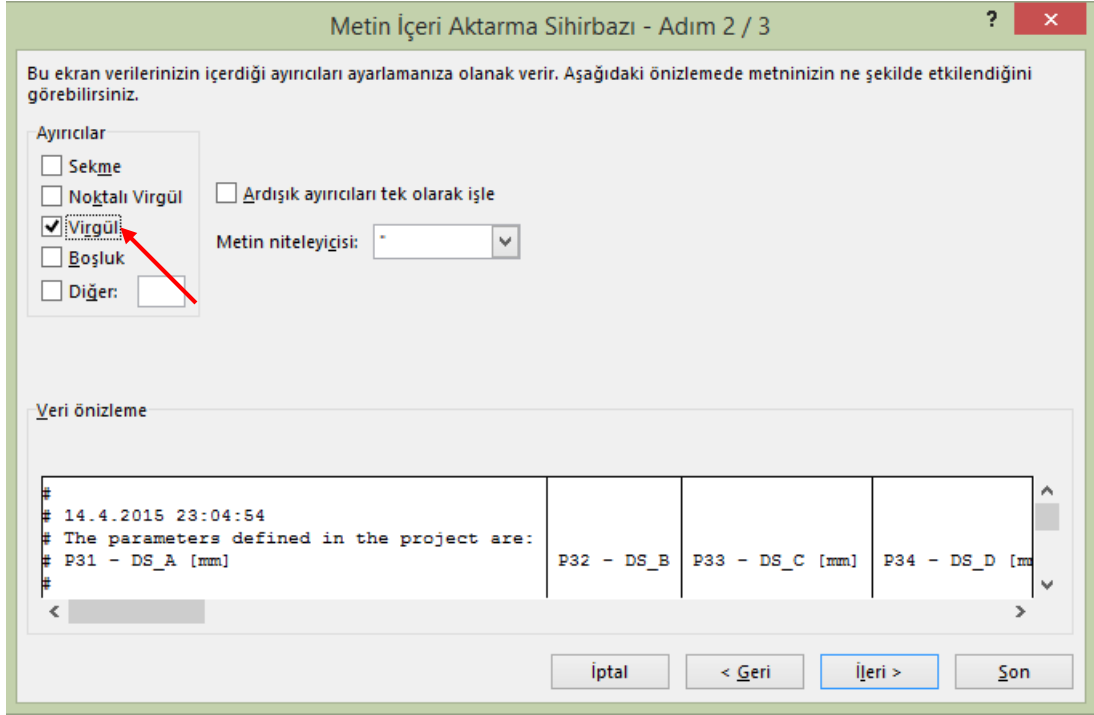


Figure A.5 Column separation options

In the next step, the data type options are specified. In this study, the user should keep this preference in “General” as seen in Figure A.6. Finally, user presses the “Finish” button and specifies the data starting cell in Excel spreadsheet.

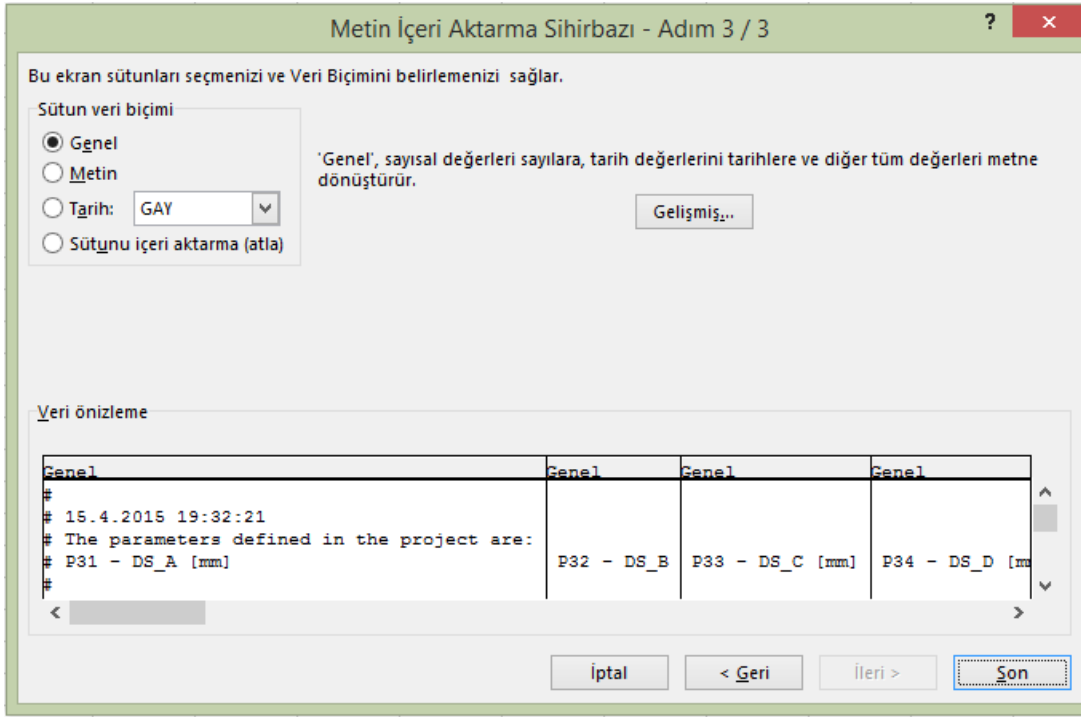


Figure A.6 Data type selection and finalizing

The data is successfully transferred into Excel at the end of the previous steps. In order to collect the input and output parameters correctly, all unnecessary rows and columns are manually erased by the user in the spreadsheet. The erased cells contain information such as date, legend, etc. In the simplified form, there must be only the values of the input and the output in the correct order for data collection operation later. Figure A.7 presents the initial form of the imported csv data into the Excel spreadsheet.

1	#					
2	# 15.4.2015 19:32:21					
3	# The parameters defined in the project are:					
4	# P31 - DS_A [mm]	P32 - DS_B	P33 - DS_C [mm]	P34 - DS_D [mm]	P35 - DS_E [mm]	P18 - Bolt Pretension Working Load [N]
5	#					
6	# The following header line defines the name of the columns by reference to the parameters.					
7	Name	P31	P32	P33	P34	P35
8	DP 0	4.83	24	167.75	6.6	5
9	DP 1	4	23	164.5	5.9	4.5
10	DP 2	4	23	164.5	6.6	4.5
11	DP 3	4	23	164.5	7.3	4.5
12	DP 4	4	23	165.6	5.9	4.5
13	DP 5	4	23	165.6	6.6	4.5
14	DP 6	4	23	165.6	7.3	4.5
15	DP 7	4	23	166.7	5.9	4.5
16	DP 8	4	23	166.7	6.6	4.5
17	DP 9	4	23	166.7	7.3	4.5
18	DP 10	4	23	167.75	5.9	4.5
19	DP 11	4	23	167.75	6.6	4.5
20	DP 12	4	23	167.75	7.3	4.5
21	DP 13	4	23	168.9	5.9	4.5
22	DP 14	4	23	168.9	6.6	4.5
23	DP 15	4	23	168.9	7.3	4.5

Figure A.7 The initial form of the imported data

Figure A.8 shows the simplified final version of the data with Excel filename “alldata”. In the final version of the spreadsheet, five input parameters and two output parameters are listed in each column. Every row stands for a specific analysis. Therefore, the number of rows and the number of analyses in parametric study must be equal to each other.

	A	B	C	D	E	F	G
1	4	23	164.5	5.9	4.5	7503.775644	120725798.7
2	4	23	164.5	6.6	4.5	7489.854169	115511195.6
3	4	23	164.5	7.3	4.5	7477.663604	112404719.3
4	4	23	165.6	5.9	4.5	7525.270619	125206043.6
5	4	23	165.6	6.6	4.5	7508.25267	121016334.4
6	4	23	165.6	7.3	4.5	7492.341633	116789684.3
7	4	23	166.7	5.9	4.5	7546.366616	130881367.6
8	4	23	166.7	6.6	4.5	7526.495516	127039375.9
9	4	23	166.7	7.3	4.5	7509.274131	122139600.9
10	4	23	167.75	5.9	4.5	7567.886905	136306898.5
11	4	23	167.75	6.6	4.5	7546.466211	131681785
12	4	23	167.75	7.3	4.5	7527.281775	128263873.8
13	4	23	168.9	5.9	4.5	7601.357383	144541160.5
14	4	23	168.9	6.6	4.5	7574.009312	140113429.7
15	4	23	168.9	7.3	4.5	7552.173587	136779648.1
16	4.2	23	164.5	5.9	4.5	7508.295518	113737060.3
17	4.2	23	164.5	6.6	4.5	7492.819018	111416224.5
18	4.2	23	164.5	7.3	4.5	7481.390153	106514726.2
19	4.2	23	165.6	5.9	4.5	7528.942551	120017198.9
20	4.2	23	165.6	6.6	4.5	7511.691449	116835598.5
21	4.2	23	165.6	7.3	4.5	7495.614845	112432996.5
22	4.2	23	166.7	5.9	4.5	7552.855351	126170193.4
23	4.2	23	166.7	6.6	4.5	7533.046513	121450293.5
24	4.2	23	166.7	7.3	4.5	7514.288349	118195183.1

Figure A.8 The final version of the imported data

The example conducted in this study comprises five geometric input parameters, two loading (the bolt pretension and the axial external force) input parameters, and two output parameters (the bolt force reaction in N and the flange stress in MPa). Table A.1 lists input parameters with the upper and lower limit values. The parametric analysis database is created with these limits and the ANN is trained with these limits as well. Table A.2 presents the parametric input values for each variable. All of the parametric input values of the variables are crossed with each other to obtain the FEA database covering all combinations. In this respect, a set of 540 ( $4 \times 3 \times 5 \times 3 \times 3 = 540$ ) design points exists when all geometric input values are crossed. In the same way, the number of the loading input combinations is equal to 25 ( $5 \times 5 = 25$ ). As a result, there are 13500 ( $540 \times 25 = 13500$ ) design points in the FEA database in total.

Table A.1 Limits of the input parameters for parametric analyses and ANN training

Input Variable	Explanation	Nominal Value	Lower Bound	Upper Bound
A	Bolt Size	4.83 mm	4 mm	5 mm
B	The Number of Bolts	24 pcs	23 pcs	25 pcs
C	Bolt Location	167.75 mm	164.5 mm	168.9 mm
D	Casing Thickness	6.6 mm	5.9 mm	7.3 mm
E	Flange Thickness	5 mm	4.5 mm	5.5 mm
Axial Force per Bolt	-	1280 N	1024 N	1536 N
Bolt Pretension	-	5702 N	3991 N	7413 N

Table A.2 The parametric input values for each variable in the parametric analyses

Input Variable	Explanation	# of Inputs	Input 1	Input 2	Input 3	Input 4	Input 5
A	Bolt Size	4	4	4.2	4.826	5	-
B	The Number of Bolts	3	23	24	25	-	-
C	Bolt Location	5	164.5	165.6	166.7	167.75	168.9
D	Casing Thickness	3	5.9	6.6	7.3	-	-
E	Flange Thickness	3	4.5	5	5.5	-	-
Axial Force per Bolt	-	5	1024	1152	1280	1408	1536
Bolt Pretension	-	5	3991	4846.5	5702	6557.5	7413

In the parametric study conducted in this example, two loading parameters are not listed in the rows shown in Figure A.8 because the single parametric study has been divided with respect to each loading parameter combination. In the solution of the present example, there are 25 parametric sets, each of which contains 540 analyses (the number is equal to the geometric input combinations). At this point, the results of each parametric set corresponding to loading parameter combinations are listed in different sheets of the Excel file. In other words, each sheet in the file is formed with the 540 analysis (five geometric input values and two output values for each) as seen in Figure A.8. Since the corresponding loading parameter combination values of each

parametric set is known, all combinations of the seven input parameters are listed separately in another Excel file which are combined in Matlab later on. Figure A.9 displays the values of two loading parameters for 25 parametric sets in the form of Excel spreadsheet with the name of “loading”. If the user has more than one parametric analysis sets with different loading parameters, then a similar loading input file must be prepared.

	A	B	C	D
1	1024.00	3991.00		
2	1152.00	3991.00		
3	1280.00	3991.00		
4	1408.00	3991.00		
5	1536.00	3991.00		
6	1024.00	4846.50		
7	1152.00	4846.50		
8	1280.00	4846.50		
9	1408.00	4846.50		
10	1536.00	4846.50		
11	1024.00	5702.00		
12	1152.00	5702.00		
13	1280.00	5702.00		
14	1408.00	5702.00		
15	1536.00	5702.00		
16	1024.00	6557.50		
17	1152.00	6557.50		
18	1280.00	6557.50		
19	1408.00	6557.50		
20	1536.00	6557.50		
21	1024.00	7413.00		
22	1152.00	7413.00		
23	1280.00	7413.00		
24	1408.00	7413.00		
25	1536.00	7413.00		

Figure A.9 Loading input for each of the 25 parametric sets

In the next step, all of the created input and output data should be collected with the help of the script prepared in Matlab [MATLAB Version: 7.11.0.584, 2010]. Running the generated script is the last step for generating the artificial neural network to approximate the FE analyses. The script that generates the artificial neural network is given in Appendix B.

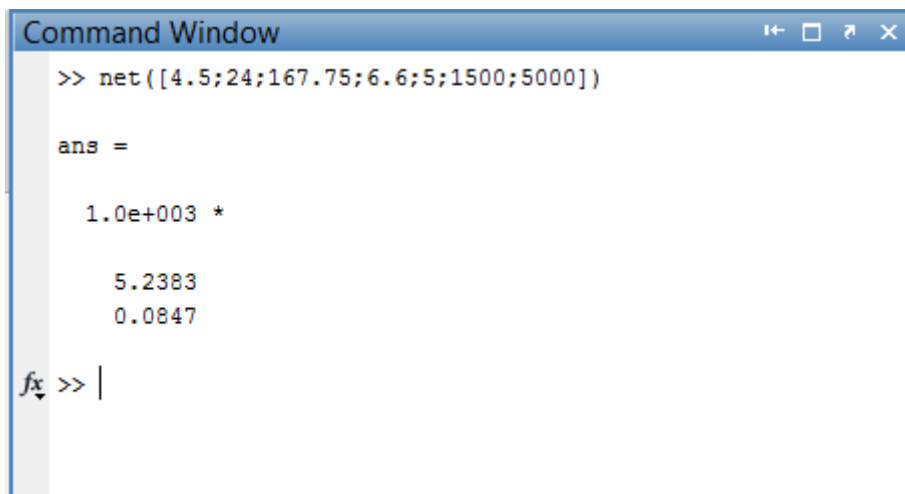
The script is a Matlab m-file and it comprises a few separate functional parts explained below.

- In the first part, the loading data from the created Excel files is collected into “loading” matrix and the number of loading combinations is determined since the number loading combinations are equal to the number of parametric sets.
- In a loop, each separate sheet of “alldata” file is taken to temporary matrix and then combined in “alldata” matrix. Consequently, 25 sheets of the parametric results are transformed into a single matrix. The loop counter limit is equal to the number of loading parameter combinations.
- In the next part, “alldata” matrix is divided into two matrices where “a” is for geometric parameter input and “b” is for output.
- The next loop adds the “loading” matrix to “a” matrix in order to form the complete input matrix “a” with both the geometric and the loading parameters.
- Before starting to create the ANN, failed FE analyses must be checked in order not to utilize null analysis results. ANSYS Workbench parametric study gives “0” values for all output cells of that specific analysis in the result spreadsheet whenever an analysis fails. Therefore, there is a control loop in the script which counts the number of failed analysis in the “error\_count” variable. In the control loop, there is an if-else statement that checks whether there is “0” results in output matrix “b”. If there exist, the failed analysis result is eliminated and “error\_count” is increased by one. If not, the non-zero line of “a” and “b” matrices are copied to “A” and “B” matrices. In the end of the loop, the matrices “A” and “B” with no failed analyses are transposed into new “A” and “B” matrices in order to supply to “Neural Network” toolbox in the correct form.
- The rest of the script automatically conducts the artificial neural network operation and gives performance statistics in the end.
- Once the ANN is created with the name of “net”, the software is able to give instant output for any input given in the correct order. The ANN structure is stored under the function with the name of “net”. A sample input command to

be entered in Matlab workspace must be in the following form as seen in Figure A.10:

- `net([4.5;24;167.75;6.6;5;1500;5000])`

where the input matrix inside “net” function contains the geometrical parameters (A, B, C, D, E) and the loading parameters (the axial external force, the bolt pretension) respectively with the units stated before.



```
Command Window
>> net([4.5;24;167.75;6.6;5;1500;5000])

ans =

    1.0e+003 *
         5.2383
         0.0847

fx >> |
```

Figure A.10 Giving input and taking output after training ANN in Matlab workspace

- When this command is run in the Matlab Workspace, the software gives the following output:

```
ans =
1.0e+003 *
5.2383
0.0847
```

where the 5238.3 is the bolt reaction force in N and 84.7 is the equivalent Von Mises flange stress in MPa.

## APPENDIX B

### THE ARTIFICIAL NEURAL NETWORK SETUP SCRIPT

```
%Alper YILDIRIM

%Artificial Neural Network Code to Approximate Bolted Flange Connection
%Analyses

clear all
clc

%Collecting inputs

loading=xlsread('loading.xlsx'); %Axial force and bolt pretension input
%parameters of each parameteric set is collected here.

num_load=size(loading,1); %Total number of loading variables combination
%(equals to analysis sets)

alldata=[]; %"alldata" matrix is defined as an empty matrix.

%Taking ANSYS resultant datasheets into system

for i=1:1:num_load; %the number of loadin input combinations which is equal
%to the number of parametric data sets.

    num_sheet=sprintf('Sayfa%d',i)

    %Each sheet of "alldata.xlsx" contains the five geometric input
    %parameters and two output parameters of a parameteric set. Since there are
    %25 parametric sets, 25 sheets exist in this file as well
    temp=xlsread('alldata.xlsx',num_sheet);

    alldata=[alldata;temp]; %Uniting results of all analysis datasheets
    %in single matrix in Matlab

end

%Defining the numbers of parameters

num_geo=size(temp,1); %Total number of geometric variables combination

num_analy=num_load*num_geo; %Total number of all variables combination
num_par=7; %Total number of input parameters

%Defining the initial input and output matrices of ANN
%"a" matrix is ANN training input matrix and "b" is corresponding ANN
%target matrix. In this step The first five columns consisting of geometric
```

```



```

```

        error_count=error_count+1; %The number of failed analyses are
%stored here.

        error_set(error_count)=j+((i-1)*num_geo); %Failed analysis data
%is kept to be reviewed later.

    end

end

xlswrite('alldata_united.xlsx',alldata); %The final "alldata" matrix is
%stored in an Excel file as reserve.

B(:,2)=B(:,2)/1e6; %the flange stress is converted in MPa unit before
%training of ANN.

%Taking transpose for the neural network tool
A=transpose(A);
B=transpose(B);

%After this point, ANN training auto created code begins.

% Solve an Input-Output Fitting problem with a Neural Network
% Script generated by NFTOOL
% Created Sat Apr 18 14:51:39 PKT 2015
%
% This script assumes these variables are defined:
%
%   A - input data.
%   B - target data.

inputs = A;
targets = B;

% Create a Fitting Network
hiddenLayerSize = 14; %The number of neurons is defined here.
net = fitnet(hiddenLayerSize);

% Choose Input and Output Pre/Post-Processing Functions
% For a list of all processing functions type: help nnprocess
net.inputs{1}.processFcns = {'removeconstantrows','mapminmax'};
net.outputs{2}.processFcns = {'removeconstantrows','mapminmax'};

% Setup Division of Data for Training, Validation, Testing
% For a list of all data division functions type: help nndivide
net.divideFcn = 'dividerand'; % Divide data randomly
net.divideMode = 'sample'; % Divide up every sample

%The percentages of training, validation, and test sets are specified here.
net.divideParam.trainRatio = 90/100;
net.divideParam.valRatio = 5/100;
net.divideParam.testRatio = 5/100;

```

```

% For help on training function 'trainlm' type: help trainlm
% For a list of all training functions type: help nntrain
net.trainFcn = 'trainlm'; % Levenberg-Marquardt

% Choose a Performance Function
% For a list of all performance functions type: help nnperformance
net.performFcn = 'mse'; % Mean squared error
net.trainParam.max_fail = 300;
net.trainParam.epochs = 5000;

% Choose Plot Functions
% For a list of all plot functions type: help nnplot
net.plotFcns = {'plotperform','plottrainstate','ploterrhist', ...
    'plotregression','plotfit'};

% Train the Network
[net,tr] = train(net,inputs,targets);

% Test the Network
outputs = net(inputs);
errors = gsubtract(targets,outputs);
performance = perform(net,targets,outputs)

% Recalculate Training, Validation and Test Performance
trainTargets = targets .* tr.trainMask{1};
valTargets = targets .* tr.valMask{1};
testTargets = targets .* tr.testMask{1};
trainPerformance = perform(net,trainTargets,outputs)
valPerformance = perform(net,valTargets,outputs)
testPerformance = perform(net,testTargets,outputs)

% View the Network
view(net)

% Plots
% Uncomment these lines to enable various plots.
%figure, plotperform(tr)
%figure, plottrainstate(tr)
%figure, plotfit(net,inputs,targets)
%figure, plotregression(targets,outputs)
%figure, ploterrhist(errors)

%-----

```

## APPENDIX C

### SUPPLEMENTARY CHARTS

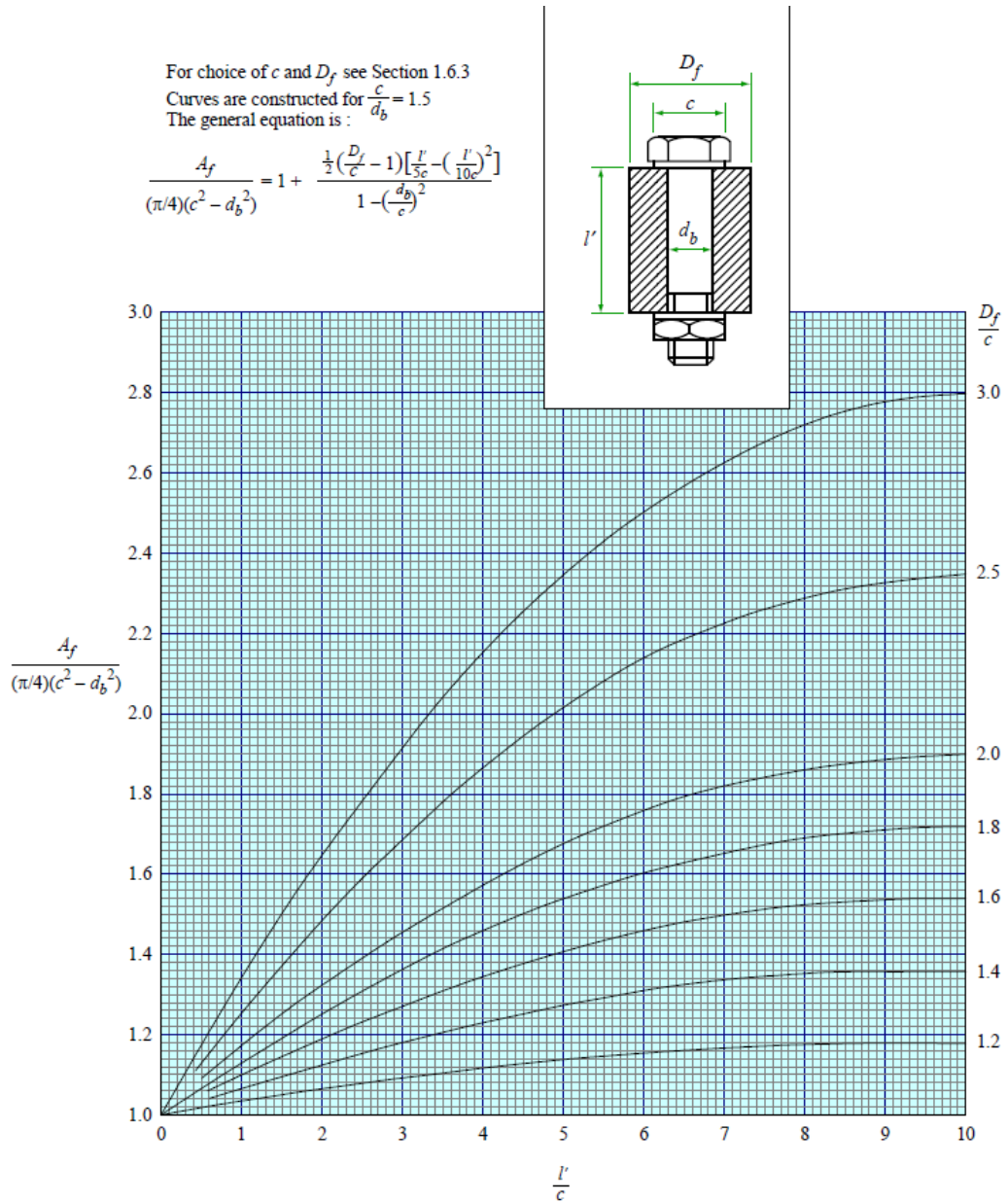


Figure C.11 The chart for variation in effective area of plates for axisymmetrically loaded joints (taken from ESDU [4])